

ELECTRICAL RESISTIVITY AND GROUND-PENETRATING  
RADAR AS TOOLS TO CHARACTERIZE GROUNDWATER-  
SURFACE WATER INTERACTION AT MIRROR LAKE, NH

---

A Thesis  
Submitted to the  
Temple University College Graduate Board

---

In Partial Fulfillment  
of the Requirements for the Degree  
Master of Science

---

By  
Natasha Mitchell  
August, 2008

---

Dr. Jonathan E. Nyquist, Advisor

---

Dr. Laura Toran

---

Dr. Allison Tumarkin-Deratzian

# TABLE OF CONTENTS

Section	Page
<b>ABSTRACT</b> .....	<b>iv</b>
<b>ACKNOWLEDGMENTS</b> .....	<b>v</b>
<b>DEDICATION</b> .....	<b>vii</b>
<b>LIST OF FIGURES</b> .....	<b>viii</b>
<b><u>CHAPTER</u></b>	
<b>1. INTRODUCTION AND BACKGROUND</b> .....	<b>1</b>
<b>2. STUDY SITE</b> .....	<b>5</b>
2.1 Study Site Overview .....	5
2.2 Study Site Hydrology and Geology.....	5
2.3 Road Salt Contamination at Mirror Lake.....	9
<b>3. METHODS</b> .....	<b>12</b>
3.1 Electrical Resistivity Survey Overview .....	12
3.2 Towed-Cable Surveys at Mirror Lake.....	17
3.3 Stationary-Cable (Lake-Bottom) Survey.....	19
3.4 Data Inversion .....	22
3.5 Inversion Error Analysis .....	24
3.6 Resistivity Test Box .....	27
3.7 Sediment Sampling .....	27
3.8 Ground Penetrating Radar.....	30
3.9 Seepage Meters .....	36
3.10 Bathymetry.....	38
3.11 Data Coordinates.....	38
<b>4. RESULTS AND DISCUSSION</b> .....	<b>40</b>
4.1 Introduction.....	40
4.2 Resistivity Survey Results Overview .....	40
4.3 Southwest Shore Resistivity and Seepage Results .....	51
4.3.1 Resistivity Values 1500 to 3000 $\Omega$ -m and Seepage Rates.....	52
4.3.2 Low (200 $\Omega$ -m) Resistivity and Low Seepage Rates.....	59
4.4 Eastern Shore Seepage and Resistivity .....	61
4.5 Northeast Inlet: Resistivity and Road Salt Contamination.....	62
4.6 Ground Penetrating Radar Surveys.....	64
<b>5. CONCLUSIONS</b> .....	<b>74</b>
5.1 Electrical Resistivity .....	74
5.2 Electrical Resistivity Field Techniques.....	74
5.3 Ground Penetrating Radar.....	75
5.4 Ground Penetrating Radar Field Techniques .....	76
5.5 Using Electrical Resistivity and Radar In Tandem .....	76

5.6 Position Data .....	76
5.7 Suggestions for Further Study .....	77
5.8 Implications for understanding groundwater-lake interaction.....	78
<b>REFERENCES.....</b>	<b>80</b>
<b>APPENDIX A, SOUTHWEST SHORE BATHYMETRY.....</b>	<b>84</b>
<b>APPENDIX B, DATA DISCS .....</b>	<b>85</b>

## ABSTRACT

The results of electrical resistivity surveys using both surface-towed and stationary (lake-bottom) cables at Mirror Lake, NH suggested that resistivity surveying can be useful for characterizing geologic heterogeneities that control groundwater-surface water interaction, as well as for imaging road salt contamination. In-situ measurements of seepage coincident with resistivity surveys suggested a relationship between resistivity values and seepage rates. Specifically, we observed that seepage rates were low (averaging -20 cm/day) at Mirror Lake where resistivity values were greater than or equal 3000  $\Omega$ -m and where they were less than or equal to 200  $\Omega$ - m. Low (200  $\Omega$ -m) resistivity values were indicative of organic matter deposits. High (3000  $\Omega$ -m) resistivity values were indicative of low porosity, poorly sorted till. Intermediate (~1500  $\Omega$ -m) resistivity values were observed in the regions where seepage rates were highest (averaging -80 cm/day). Core, modeling, and slug test data suggest that these intermediate resistivity values reflect well-sorted, higher-porosity glacial drift. Resistivity surveys of the suspected region of salt contamination revealed a plume-shaped feature of low resistivity. Low resistivity and higher chloride content were confirmed by laboratory analysis of pore fluid. The results of ground penetrating radar (GPR) surveys suggested that this technique can also identify geologic features that relate to seepage. GPR surveys identified the bounds of a blanket of organic matter that covers the bottom of Mirror Lake; previous work suggested that this organic matter controls seepage there. Radar also confirmed the results of previous work at Mirror Lake about the distribution of cobbles and boulders there. We conclude that the rapidly acquired towed-cable resistivity survey and ground-penetrating radar surveys can guide placement of higher-resolution, more time-consuming stationary cable surveys. The use of stationary cable resistivity surveys in the very near-shore environments (< 2 m from shore), which are generally inaccessible with a towed-cable survey and yield very low resolution GPR images, can guide seepage meter placement.

## ACKNOWLEDGMENTS

I owe thanks to many people and organizations for the roles they have played in the completion of this work. First, thank you to the National Science Foundation Hydrologic Sciences Program, who funded the project under Award No. 0609827. Thank you also to the Hubbard Brook Research Foundation for providing logistical support. Dr. Jonathan Nyquist, my advisor, took a leap of faith (no pun intended...well, kind of intended) when he took me on, a religion major. Thank you, Dr. Nyquist, for all you have taught me, and for making me laugh. Dr. Laura Toran, a committee member but as much my advisor as Dr. Nyquist, was a remarkably strong presence in the project; her keen scientific and editing eye shaped the work more than I could have imagined. Dr. Allison Tumarkin-Deratzian, also a committee member, had a steady voice and concise, thoughtful suggestions. Thank you, Dr. Allison, for letting me be your first thesis advisee. Matthew Heaney, who began the project a year before I arrived at Temple and in whose broad footprints I strove to walk, set a wonderful example. His intelligence, wisdom, and, most of all, his company added a sweetness to my time at Temple I could not have imagined. Roger Cutitta's warmth carried me gently through stretches of dark, rough waters; Billy Zacharatos' ability to make me blush without warning was an oasis. Jim Mikochik made me giggle at most unexpected moments, and Paul Freyer, Jason Mintz, Gary Stinchcomb and Hallie Meighan not only got me started on this road but were responsible for a suite of star-filled evenings. Steve Peterson, Eva Gladish, and Sam Galenty have been the most wonderful of friends; their presence became a fact of daily life and I will miss them deeply. Shelah Cox, unendingly courageous and steadfast, withstood the brunt of storms as the bow of a boat strikes through the waves of a hurricane. We would have sunk without her. Mike Whitson, wherever he is now, brought me to geology. I never could have seen where that journey would bring me, I only knew I wanted to take it. Dr. Max Tegmark had the most wonderful of twinkles; I always held on to the idea that the universe was infinitely rich, and he made me think I was right to do so. The memory of him leaning down, as we walked for commencement, looking me straight in the eye, and telling me not to lose my sparkle lives deep inside my heart. Rich Nourrie: of all the rafts I have held to, he was and is one of the warmest. As you wrote to me once, Rich, we are blessed by the connection we have. Jane, John Paul, Kate and Peter MacDuffie – I love you very much.

Thank you for all you have given me. And to Marjorie Adis: these words, as we have said, can be insufficient for what they address -- like saying the universe is big. I hesitate to say anything at all, for fear of making it smaller, or crushing what I am afraid is a fragile crystal. Only it's not fragile, and that's the sweetest part of all.

## **DEDICATION**

To Dr. Max Tegmark:  
who helped me believe in sparkles

and

To Marjorie Adis  
Who made them real.

## LIST OF FIGURES

Figure	Title	Page
1.	Figure 2-1. Study Site Overview.....	6
2.	Figure 2-2. Groundwater Flow at Mirror Lake .....	8
3.	Figure 2-3. Road Salt Contamination at Mirror Lake. ....	11
4.	Figure 3-1. Electrical Resistivity.....	13
5.	Figure 3-2. SuperSting R8 Marine Resistivity System. ....	15
6.	Figure 3-3. Survey and Cable Types.....	16
7.	Figure 3-4. Locations of Towed- and Stationary-Cable surveys at Mirror Lake .....	18
8.	Figure 3-5 Equipment used .....	20
9.	Figure 3-6. The Inversion Process.....	23
10.	Figure 3-7. Sample Inverted Resistivity Section with Error Assessment.....	26
11.	Figure 3-8. Resistivity Test Box. ....	28
12.	Figure 3-9. Sediment Core in Collection Tube. ....	29
13.	Figure 3-10. Sample Radargram. ....	32
14.	Figure 3-11. Radar Equipment in Boat. ....	34
15.	Figure 3-12. Location of Radar Surveys at Mirror Lake.....	35
16.	Figure 3-13. Seepage Meter. ....	37
17.	Figure 4-1. Towed-Cable Resistivity Survey Results .....	42
18.	Figure 4-2. Stationary Cable Resistivity Survey Results.....	46
19.	Figure 4-3. Towed- vs. Stationary-Cable Resistivity Values. ....	50
20.	Figure 4-4. Seepage Rate By Location Within Long Line Survey Area. ....	53
21.	Figure 4-5. Long Line Resistivity Survey and Seepage. ....	55
22.	Figure 4-6. Model of Effect of Variations in Porosity on Resistivity, with Different Values of $a$ and $m$ .....	58
23.	Figure 4-7. Coincidence of Resistivity Results with Sand and Gravel Deposit .....	60
24.	Figure 4-8. Zones of Low Resistivity Below 2 m depth in Northeast Inlet Area. ....	63
25.	Figure 4-9. Radargrams from Mirror Lake .....	66
26.	Figure 4-10. Extent of Gyttja Blanket as Inferred from Radargrams. ....	71
27.	Figure 4-11. Comparison of Old and New Map of Gyttja Blanket. ....	72

## CHAPTER 1 INTRODUCTION AND BACKGROUND

The goal of this study was to develop the use of electrical resistivity and ground-penetrating radar for the characterization of groundwater-surface water interaction. Characterizing and quantifying the interaction of groundwater with surface water across a watershed is a complex task; seepage rates (groundwater discharge to surface flow systems or surface flow recharge of the groundwater system), which are controlled by geologic heterogeneity, can vary by an order of magnitude or more over a distance of 1-2 meters. Characterizing seepage is therefore difficult in any setting. Finding, characterizing, and quantifying underwater seepage is all the more difficult because the groundwater-surface water interfaces lies beneath a column of water. These zones of exchange, however, represent important features of hydrologic systems. The temperature, solute content, and water-flow conditions of seepage zones make them crucially important to many aquatic species (Kalbus et al., 2006; Hayashi and Rosenberry, 2002; Brunke and Gonser, 1997; Asbury, 1990). Seepage can also be a significant source or sink of water to or from lakes and streams (Rosenberry, 2005; Lee, 1977; McBride and Pfannkuch, 1975). Watershed management is therefore partially contingent upon an understanding of the interaction of groundwater with surface water. The ability to model the effects of and treat a groundwater contaminant plume, for example, is dependent upon understanding how that plume is likely to interact with surface water (Shaban et al., 2005; Sophocleous, 2002; Ball et al., 2006; Cherkauer, 1991). Predicting the effects of pumping on aquifer recharge, flow of local surface water bodies, or salt-water intrusion is also contingent upon knowing how much water is supplied or lost to those bodies via groundwater-surface water exchange (Taylor, 1982; Taylor and Cherkauer, 1984; Cherkauer and Carlson, 1997; Snyder and Wightman, 2002; Shaban et al., 2005). Tools that can characterize and quantify the interaction between groundwater and surface water are therefore essential to watershed management strategies.

Researchers' efforts to quantify seepage have been, historically, limited to point measurement. Formal efforts to characterize seepage began in the 1940's with seepage meters, cylindrical drums that could be pressed into sediment to effectively seal the zone beneath the drum from the external

environment. Seepage was calculated by measuring the amount and rate at which water was discharged or recharged within that sealed zone, researchers measured seepage (Lee, 1977; Kalbus et al., 2006). Methods were also developed to calculate seepage based upon proxies such as hydraulic and temperature gradients. Hydraulic gradients, calculated via head measurements from wells within the region of interest, can suggest seepage locations, as can temperature gradients (potentially caused by the intrusion of groundwater which is of different temperature than the surface water to which it discharges). Hydraulic conductivity can also indicate zones of seepage; where lake-bottom sediment is particularly hydraulically conductive, as calculated from slug or pumping tests, high rates of seepage may exist. Flow analysis via dye or isotope tracing can also point to seepage (summarized by Kalbus et al., 2006). Though point techniques can measure seepage directly, they are limited in that they are labor and time intensive. Moreover, estimates of seepage will be over- or undervalued if spatial variation is not measured.

Geophysical surveying techniques, with which the researcher can rapidly characterize a large area, yield information about geologic heterogeneities. Because geologic heterogeneities can control seepage rates, geophysical characterization techniques offer a means of guiding point measurement of seepage. Electrical resistivity profiling, which responds to variations in porosity, saturation, pore fluid conductivity, and lithology, was one of the first geophysical methods tested (Taylor, 1982; Taylor and Cherkauer, 1984; Cherkauer, 1991; Cherkauer and Carlson, 1997). Taylor and Cherkauer (1984) and Cherkauer (1991) built upon earlier work by Archie (1942), using electrical resistivity to identify geologic heterogeneity in the sediment beneath Lake Michigan, and then drawing conclusions about likely seepage rates based upon that lithologic information. In particular, Taylor and Cherkauer (1984) showed that seepage rates at Lake Michigan varied with clay content. Because clay is electrically conductive, regions where sediment resistivity was low were indicative of regions with high clay content and therefore indicative of regions where seepage rates were likely to be low. Taylor and Cherkauer confirmed this relationship via seepage meter measurements, piezometer measurements, and by laboratory analysis of sediment permeability. The authors concluded that further investigation ought be pursued at a small, well-characterized lake to deepen understanding of the relationship between

electrical resistivity profiles, lithology, and seepage. Though several related surveys have been conducted in the 20+ years since (e.g., Cherkauer, 1991; Panthulu, et al., 2001; Snyder and Wightman, 2002; Manheim et al., 2004; Day-Lewis et al., 2005; Ball et al., 2006), no study explicitly addressing understanding of the relationship between resistivity, geologic heterogeneity and seepage rates had been published as of the spring of 2006.

The technology available for resistivity surveys has evolved markedly from what was available to Taylor and Cherkauer in the 1980's. Taylor and Cherkauer were limited to 1-dimensional resistivity profiles; today, 2-D resistivity profiles are standard. GPS coordinate positioning did not yet exist at the time of the Taylor and Cherkauer study; it was therefore difficult to link geophysical observations with ground truth data. Finally, the computing power available to control the collection, processing and inversion of apparent resistivity data has grown substantially more powerful since the 1980s.

The work presented in this thesis represents the second stage of a project meant to explore the relationship between resistivity, geologic heterogeneity and seepage in a means similar to that suggested by Taylor and Cherkauer in 1984, with the more powerful tools available 20 years later. The results of the first stage of that project were presented by Heaney et al. (2006) and Heaney (2007). That stage of the project focused on Lake Lacawac, a small, glacial lake in northeast Pennsylvania for which there were geologic and hydrologic data available. Heaney et al. (2006) used a resistivity survey system that allowed them to gather 2-D resistivity data, a GPS device to tie resistivity data directly to location, and computers and software which allowed them to rapidly process these data. That technology represented significant advance from the 1-D data gathered by Taylor and Cherkauer (1984), the strip charts used to record those data, and the limited ability to tie resistivity data to location. In short, Heaney et al. (2006) were not only able to follow up on the questions raised by the work of Cherkauer and Taylor (1984) at exactly the sort of site the authors had suggested, but they were able to do so with equipment which offered far greater resolution.

There were two significant outcomes of the work by Heaney et al. (2006) at Lake Lacawac. First, they refined the field technique of electrical resistivity surveying for the purpose of characterizing seepage: the equipment they employed for the project was new, and its application to the

characterization of lake seepage untested. Developing field techniques for use of the equipment for the characterization of lake seepage represented an important component of their work. Second, by sampling and analyzing sediment from areas where they had conducted electrical resistivity surveys, they confirmed the efficacy of the technique in identifying geologic heterogeneities. They were able to identify lithologic transitions and likely seepage flow paths on the scale of 1-2 meters. They were unable, however, to definitively link geologic heterogeneity with seepage rates because measured seepage rates at Lake Lacawac were extremely low; maximum measured seepage flux was less than 0.19 cm per day, a quantity within the bounds of measurement error. For a more definitive correlation of the relationship between geophysical signature and seepage, a study site with higher seepage rates was needed.

The work presented in this thesis represents such a continuation of the work begun by Heaney et al. (2006). In this stage of the project, ground-penetrating radar (GPR) is added as an additional survey technique. Under ideal conditions, GPR surveys yield high-resolution images of the geometry of the subsurface environment (summarized by Neal, 2004). Using GPR, the electrical resistivity field techniques developed by Heaney et al. (2006) and the same resistivity survey equipment, our research group conducted geophysical surveys and seepage measurements at Mirror Lake, a small glacial lake in New Hampshire.

## CHAPTER 2 STUDY SITE

### 2.1 Study Site Overview

The site of the study was Mirror Lake, a small (15 hectare), glacially-formed lake in the White Mountains of central New Hampshire (Figure 2-1). The lake has been a National Science Foundation-designated Long Term Ecological Research site (LTER) since the 1980's, and is part of the Hubbard Brook Experimental Forest of the United States Department of Agriculture (Likens, 1984). Of particular importance to this project was that seepage rates up to 250 ml per minute at discrete points were reported (Rosenberry, 2005), implying that the site would offer measurable seepage rates against which to compare the results of geophysical surveys. The availability of other geologic and hydrologic data (e.g., Winter, 1984; Paillet, 1988; Winter, 1989; Harte, 1997; Tiedeman et al., 1997; Johnson, 1999; Ellefsen et al., 2002) also made Mirror Lake appealing as a site for study; it meant we would have multiple measures of ground truth against which to compare the results of geophysical surveys.

### 2.2 Study Site Hydrology and Geology

Mirror Lake has three inlet streams and one outlet (Figure 2-1). It is 11 m deep at its maximum. The sides of the lake are generally steep along the northern, eastern and southeast shores, with water depths often plunging to 6 or 7 meters within 5 or 6 meters from shore. Bedrock beneath Mirror Lake is fractured quartz monzonite, schist, and a variety of igneous intrusives (Winter, 1984; Johnson, 1999). The rock is Early Devonian in age and comprises the igneous and metamorphic Littleton and Kinsman Formations. Schist and slate are the primary constituents of the Littleton; microcline, plagioclase and quartz, in approximately equal parts, are the main constituents of the Kinsman monzonite (Winter, 1984). Bedrock is immediately overlain by a layer of poorly-sorted glacial drift, which ranges in thickness from nearly non-existent at its minimum (the center of the lake) to over 50 meters at its maximum (lake's edge). The drift is clay-poor and ranges in composition from silt to silty sand, with cobbles and boulders distributed throughout (Winter, 1984; Winter, 2000). A thick (3 m+) layer of organic sediment ("gyttja") blankets all depths greater than approximately 7 m.

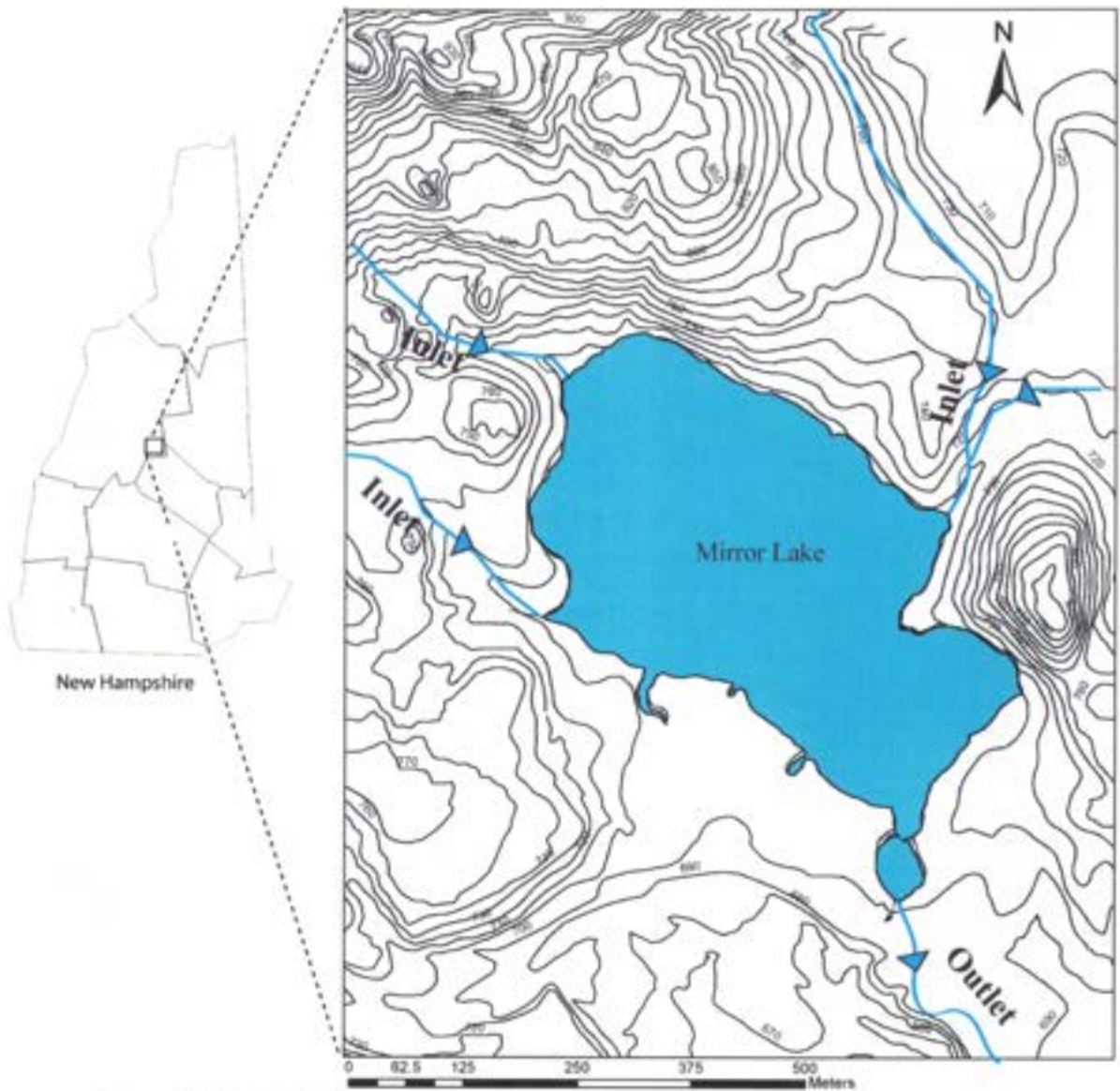


**Figure 2-1: Study Site Overview.** Mirror Lake is a small, glacially-formed lake in the White Mountains of central New Hampshire. It is a flow-through lake with three inlet streams and one outlet. Low mountains surround the lake on its west, north and eastern sides. Black lines show topography (measured in feet above sea level). *Contour Map from Complex Systems Research Center, University of New Hampshire*

Rosenberry et al. (1999) calculate that groundwater seeps into Mirror Lake along approximately 80% of the shoreline, and that that seepage provides 11% of annual influx to the lake (Figure 2-2). Lake water seeps out of Mirror Lake into the groundwater system along the southern shore and accounts for approximately 40 to 47% of lake out-flux (Rosenberry et al., 1999). Rosenberry and Winter (1993) comment that seepage rates at Mirror Lake are in fact lower than might be expected if the lake lay directly atop bedrock rather than atop glacial drift. They attribute the lower-than-expected seepage rates to the low hydraulic conductivity of the drift (range of  $K \approx 10^{-7}$  to  $10^{-5}$  m/sec), and to the presence of the thick layer of gyttja, which has an even lower hydraulic conductivity (Rosenberry and Winter, 1999).

The highest seepage rates at Mirror Lake were generally observed within 1-2 m of shore, with seepage rates decreasing rapidly with distance from shoreline (Asbury, 1990; Rosenberry, 2005). This observation is in keeping with numerical models of seepage, which suggest an exponential decline in seepage with distance from a lake's shore (McBride and Pfannkuch, 1975; Winter, 1976; Genereux and Badopadhyay, 2001; Mikochik, 2008). Seepage rates are highest along the southwest shore of Mirror Lake: rates in excess of 200 cm per day have been reported within a zone approximately 40 meters long (Asbury, 1990; Rosenberry, 2005). On-shore core samples from regions ~10 – 100 m from the locations of high seepage rates record the presence of relatively well-sorted, and therefore relatively porous, sand and gravel within the upper 50 meters of sediment (Wilson, 1991; Tiedeman et al., 1997; Scheutz 2002; Harte, 1997). Because sediment at Mirror Lake is clay poor (Harte, 1997), it is reasonable to consider porosity as a proxy for hydraulic conductivity: porous (i.e. well-sorted) material will conduct water well, and less porous material (poorly-sorted) will conduct it poorly. Where sediment at Mirror Lake is poorly sorted, as it is around much of the lake, seepage rates will be low; where it is better sorted, seepage rates will be higher. The results of slug tests of on-shore wells at Mirror Lake are consistent with this hypothesis; the hydraulic conductivity of well-sorted sand and gravel deposits along the southwest shore of Mirror Lake is approximately 10 to 100 times greater ( $K \sim 10^{-4}$  m/sec) than that measured in more poorly sorted sediment elsewhere around the lake (Wilson, 1991; Harte, 1997; Tiedeman et al., 1997; Scheutz, 2002). Research suggests that this sand and gravel deposit is responsible for the very high out-seepage rates observed along the southwest shore of Mirror Lake, and

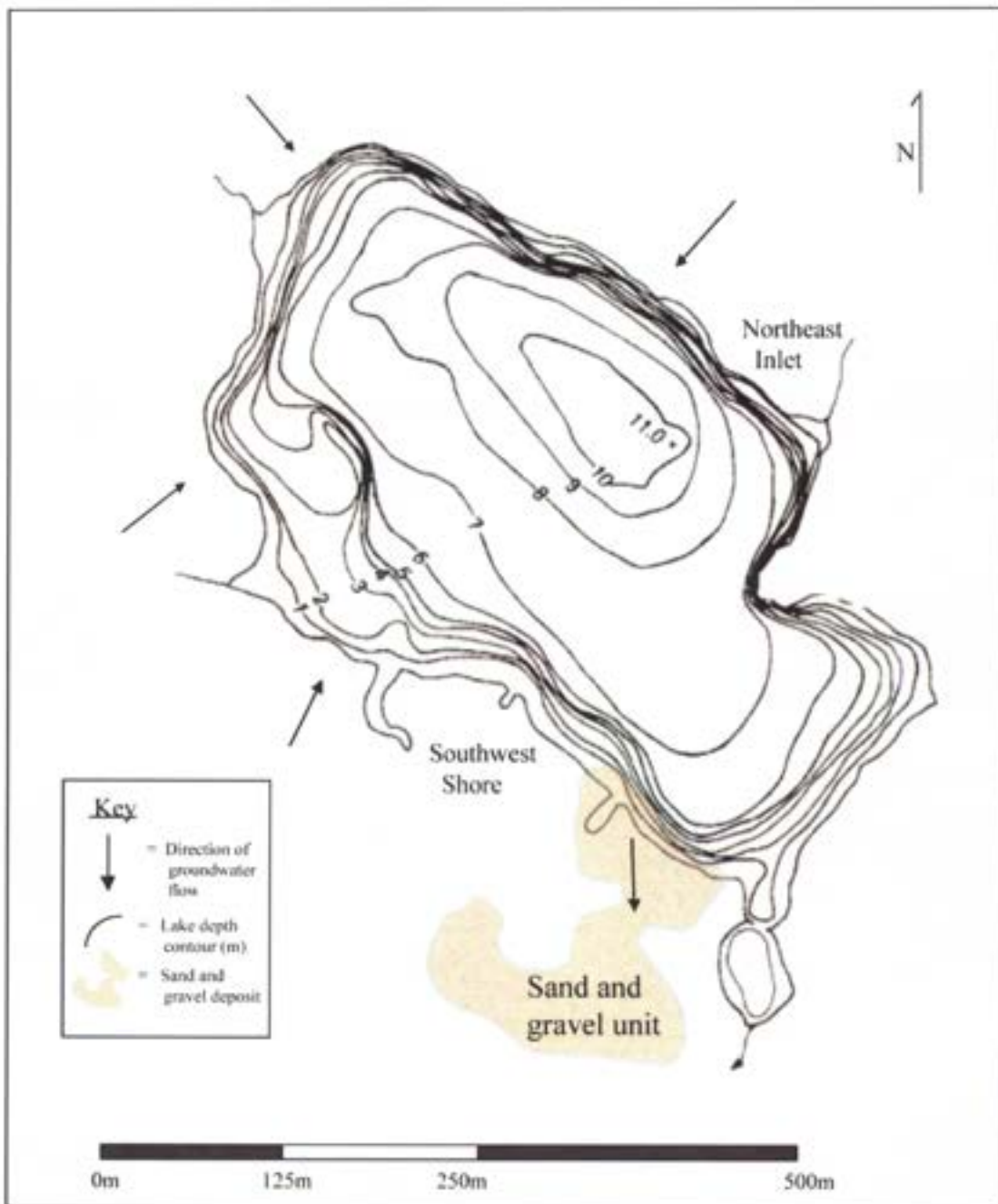


**Figure 2-2: Groundwater Flow at Mirror Lake.** Black arrows indicate approximate direction of groundwater flow (Rosenberry et al., 1999). Seepage rates are highest along the southwest shore, where the results of core analyses, slug and modeling tests suggest the presence of a deposit of well-sorted sand and gravel. *Lake bathymetry sketch from Moeller, 1975. Sand and gravel extent from Scheutz, 2002.*

for the fact that out-seepage represents such a high portion (~47%) of all out-flux for the lake (Tiedeman et al., 1997; Rosenberry et al., 1999; Scheutz, 2002).

The presence of comparatively well-sorted sediment along the southwest shore is geologically plausible. Several lines of evidence suggest that the southwest shore of Mirror Lake represents an outwash lens for the receding glacier that formed Mirror Lake. First, while the topography around much of the lake is steep, the ground adjacent to the southern end of the lake is relatively flat (Figure 2-1). Such comparatively flat terrain is consistent with a zone of high deposition, as would be expected with an outwash lens. Second, as described above, cores along the southwest shore show deposits of sand and gravel up to 50 m thick (Harte, 1997; Tiedeman, 1997). The presence of discrete deposits of sand and gravel is indicative of sorting associated with fluvial processes rather than of simple ablation. A similar model of outwash deposition has been used to explain variations in hydraulic conductivity and seepage rates in Trout Lake, Wisconsin (Krabbenhoft and Anderson, 1986).

### 2.3 Road Salt Contamination at Mirror Lake

The eastern portion of the Mirror Lake drainage basin includes Interstate Highway 93 (Figure 2-3). Since construction of the highway in the 1970's, the concentrations of sodium and chloride in Mirror Lake have risen steadily. Researchers have attributed this rise to the flow of water contaminated with road salt from Highway 93 into Mirror Lake (Rosenberry et al., 1999). The majority of road salt contaminated water entered Mirror Lake through the Northeast Inlet stream, which directly abutted the highway. A diversion berm was constructed to capture contaminated runoff in an artificial wetland and thereby prevent it from entering the Northeast Inlet. Though this berm appears to have slowed overland flow of road salt contaminated water to the Northeast Inlet, the berm leaks in several places and so road salt continues to enter Mirror Lake via the Northeast Inlet stream. Measurement of chloride concentrations in bedrock wells between Highway 93 and Mirror Lake indicate that chloride has entered the groundwater system as well, though not at all measurement points. Piezometer measurements of hydraulic gradient suggest that groundwater seeps into the Northeast Inlet stream and within the cove to which the Northeast Inlet discharges. Seepage therefore also represents a likely mode of delivery for road salt contaminated water to Mirror Lake (Rosenberry et al., 1999). Because dissolved salts like

chloride decrease water resistivity, it was possible that resistivity surveys would respond to road salt contamination of pore-fluid at Mirror Lake.



**Figure 2-3: Road Salt Contamination at Mirror Lake.** Interstate 93 is approximately 100 m from the eastern shore of Mirror Lake at its closest point. Chloride content in Mirror Lake has increased steadily since the 1970's when I-93 was built. A diversion berm (yellow line) pools most highway runoff water and prevents it from entering the Northeast Inlet stream (blue line). Higher-than-baseline chloride concentrations have nonetheless been measured in the Northeast Inlet stream. *Orthophoto from Complex Systems Research Center, University of New Hampshire.*

## CHAPTER 3 METHODS

### 3.1 Electrical Resistivity Survey Overview

Geologic heterogeneity is one factor that controls seepage. Because geologic heterogeneity can cause changes in any of the factors which control electrical resistivity - porosity, pore fluid conductivity, saturation and mineralogy – electrical resistivity profiling offers the potential to image these geologic heterogeneities. To profile the resistivity structure of the subsurface environment, we injected current into the subsurface and measured resultant electric potential across dipoles at known distances from the point of injection. Drop in electric potential at measuring electrodes was a function of the resistivity of the material through which current passed and of the distance between current and measuring electrodes.

Electrical resistivity of geologic materials is a function of porosity, pore fluid conductivity, volume fraction of pores filled with water, and the electrical properties of the minerals that comprise the material and that cement individual grains (Archie, 1942). The relationship between these factors and electrical resistivity is quantified by Archie's law (3.1):

$$\rho = a\phi^{-m}s^{-n}\rho_w \quad 3.1$$

where  $\rho$  is the bulk (overall) resistivity of a substrate,  $\rho_w$  is pore fluid resistivity,  $\phi$  is the porosity,  $s$  is saturation and  $a$ ,  $m$  and  $n$  are constants, characteristic of the electric properties of constituent minerals or of the cement which binds grains. Variation of any of these factors leads to variation in bulk resistivity.

Voltage potential drop is proportional to the length of the current path and inversely proportional to the cross-sectional area through which current flows (Figure 3-1). This constant of proportionality defines a substrate's resistivity and it is typically measured in Ohm-meters ( $\Omega$ -m).

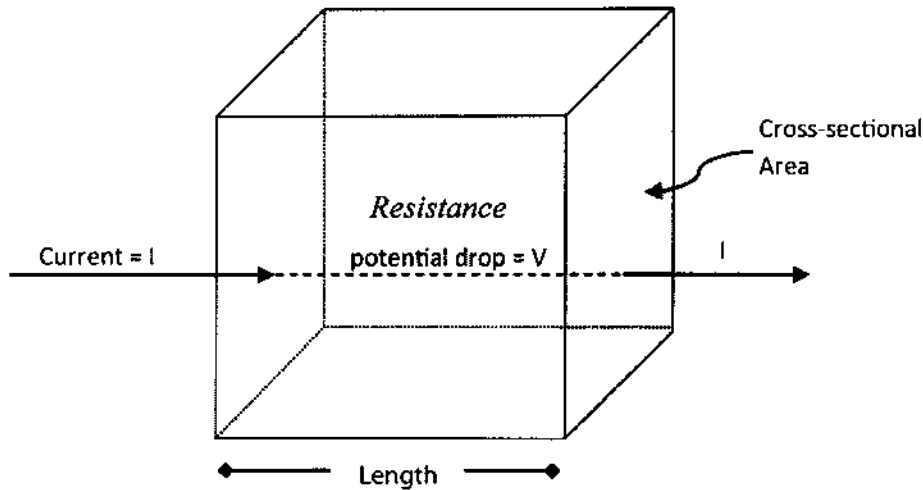


**Figure 3-1. Electrical Resistivity.** The resistivity of a geologic material is defined by the ratio of the drop in Voltage per unit length divided by the cross-sectional area. *Adapted from Reynolds, 1997.*

In a homogeneous half-space of known resistivity  $\rho$ , potential drop from an injection of current at a point source on the surface varies as a function of distance from the source of the current:

3.2

where  $r$  is the distance from current source, and voltage drop is negative overall because potential decreases with distance from the current source (Reynolds, 1997). Greater distance between current and measuring electrodes ( $r$ ) implies that the measuring electrodes will sense current that has penetrated more deeply in the earth. Where the earth is not homogeneous, measured resistivity will reflect the resistivities of all media through which the current has passed in its path through a given section of earth. Such a measurement is known as apparent resistivity ( $\rho_a$ ). If multiple measurements of apparent resistivity are made within a study area, and different electrode spacings used for each measurement, inferences about the distribution of resistive materials can be made. For instance, because wider electrode spacings allow greater depth of penetration, a resistivity survey wherein a wider electrode spacing yielded a lower apparent resistivity value than a closer spacing implies the existence of a low resistivity body at depth. Conversely, a resistivity survey wherein a wider spacing yielded a higher apparent resistivity implies the existence of a high resistivity body at depth.

By comparing and weaving together apparent resistivity measurements from multiple locations and made using multiple electrode spacings, a 2-D image of the subsurface environment can be created. Modern resistivity survey equipment facilitates and automates this process; most, including the SuperSting R8 Marine Resistivity system used in this project (Figure 3-2), have computers which fire electrodes in pre-determined patterns, and multiple channels for measurement of potential drop at multiple locations for each injection of current. Also available is modeling software which solves for the subsurface structure implied by a given set of apparent resistivity measurements.

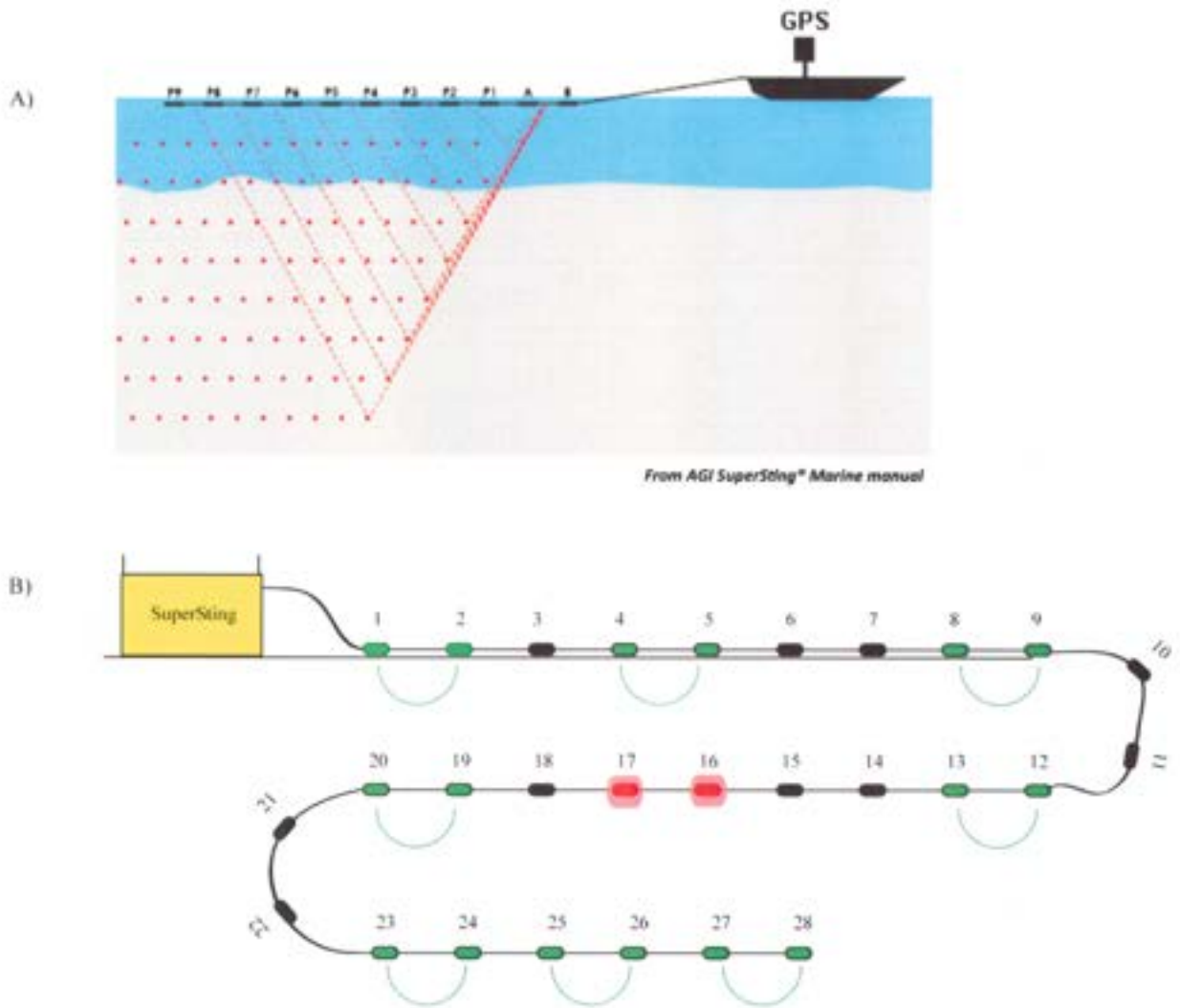
The SuperSting® resistivity survey system, which uses all the features described above, uses watertight electrode cables for current injection and potential measurement. Electrode cables with variable numbers of and spacing between electrodes may be freely interchanged. The Sting is equipped with a variety of pre-set firing patterns, each optimized for a particular survey condition; it also gives the user the option of creating a custom pattern. Electrode number and geometry, along with desired firing/measuring pattern is input to the SuperSting prior to a survey.

We conducted two types of surveys in this project: towed-cable surveys and stationary (lake-bottom) cable surveys. The cable used in the towed survey has a total of 11 electrodes. The first two of these eleven electrodes were dedicated current electrodes and injected current at regular intervals as the cable was towed around the lake. The other 9 electrodes worked in pairs to measure electric potential (Figure 3-3A). The stationary-cable has 28 electrodes and was left in place while its 28 electrodes cycled through a pre-set pattern of firing and measuring (Figure 3-3B). This variable firing pattern allows the stationary-cable survey to gather resistivity measurements from multiple different angles over a given area without physically moving the cable.

Each survey type has advantages. With a towed cable the surveyor can rapidly characterize a large distance; the boat towing the cable generally travels at a rate of 2-3 km/hour, enabling characterization of the subsurface at that same rate. The stationary-cable survey, on the other hand, requires 15-20 minutes to complete a single survey, the coverage of which is never larger than the length of the cable used in the survey (ours was 27 meters). Where it would take a matter of minutes to characterize a 100 meter stretch of shoreline with a towed-cable resistivity survey, it would take several



**Figure 3-2: SuperSting R8 Marine Resistivity System.** SuperSting is shown here on the shore, with electrode cable attached and the battery which powers the SuperSting.



From AGI SuperSting® Marine manual

**Figure 3-3: Survey and Cable Types.** (A) is a cartoon of the cable and firing pattern employed for towed surveys: an 11-electrode cable is used for the towed-cable survey. The first two electrodes (A and B) are dedicated current electrodes, while P1-P9 are dedicated potential electrodes and work in pairs to measure voltage drop for each injection of current. Current is injected every 4 seconds as the boat moves. On-board GPS connected directly to the SuperSting records time and position information for each voltage measurement. (B) is a schematic of the cable used in stationary surveys (shown in curved shape only to conserve space on the page; cable is, in reality, always stretched straight). The cable has a total of 28 electrodes; each electrode may operate as either a current or a measuring electrode. A sample firing moment is shown: electrodes 16 and 17 (shown in red) are current electrodes, while 8 other pairs of electrodes measure potential (shown in green). Electrodes shown in black are not firing.

hours to cover the same ground with a series of stationary-cable surveys. What the stationary-cable survey lacks in rapidity, however, it makes up for in resolution: with a stationary-cable survey the current does not have to penetrate a thick water column before reaching the target of the survey, so there is less attenuation of the resistivity signal. The density of resistivity measurements per unit length surveyed is also far greater with a stationary-cable survey than it is for towed surveys, and the spacing between electrodes in our stationary-cable was 1 meter rather than the 2- or 4 meter spacing of our towed-cable survey. The collective impact of these differences between the towed- and stationary-cable surveys is that resolution in our stationary-cable surveys was 4 to 5 times that of our towed cable surveys. The strengths and limitation of the two techniques make them complimentary; with a rapidly acquired towed resistivity profile, regions of interest can be identified for detailed survey via a stationary-cable survey.

### 3.2 Towed-Cable Surveys at Mirror Lake

We conducted 4 towed-cable resistivity surveys at Mirror Lake: two surveys using a 2-m electrode spacing and two using a 4-m spacing. Because previous studies of seepage showed that the highest seepage rates were within 2 m of shoreline (McBride and Pfannkuch, 1975; Winter, 1976; Asbury, 1990; Rosenberry, 2005), that region was of great interest to us. It was, however, generally not possible to approach the shoreline with the towed survey closer than 3 meters; shallow water and an abundance of boulders and fallen trees precluded closer passes. Surveys at two distances from shore, one nearest possible (2-5 m) and one slightly further out (5-8 m) were conducted (Figure 3-4). In some cases, shallow water or irregular shoreline, as exists in the southern and eastern portions of the lake, precluded any approach to the shore closer than 5, 10 or even 20 m. Where the water was shallow or there were peninsulas, it was necessary to detour from the desired path to avoid grounding the boat or snagging the cable on land. Where there were coves, the electrodes at the tail-end of the cable traveled a different path than those closest to the boat, which reduced the accuracy of the data.

The procedure for conducting a towed resistivity survey was as follows: the SuperSting control unit was placed in the boat. The cable was attached to the SuperSting, and then hooked to the boat by means of a large metal loop embedded in the cable. The cable, which was fed out from the back of the

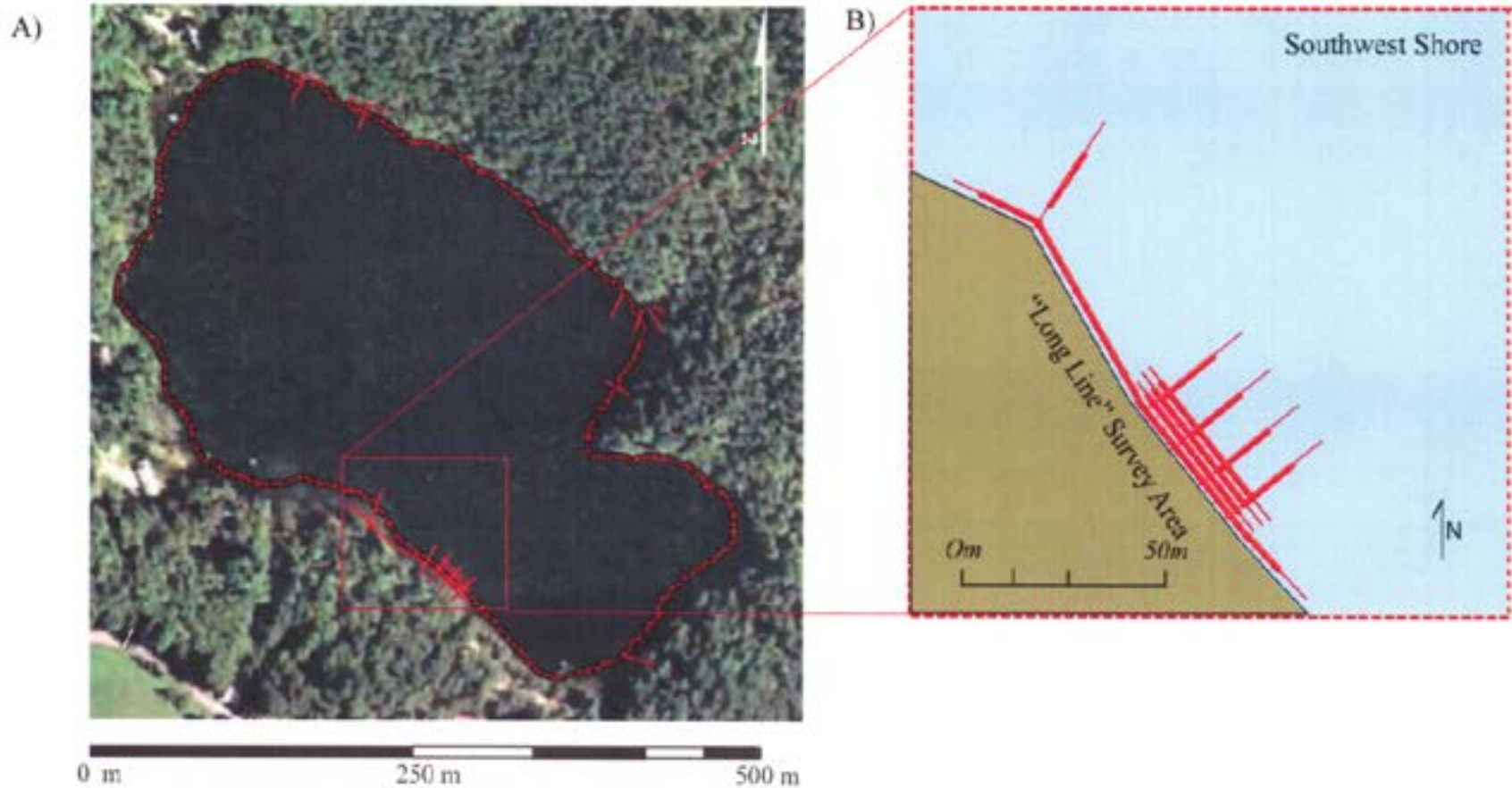


**Figure 3-4: Locations of Towed- and Stationary-Cable surveys at Mirror Lake.** All survey locations are approximate, accurate  $\pm 10$  m. Tree cover makes it appear some surveys were made on land. The red dots (A) indicate the approximate path taken for the near-shore (2-3 m) towed-cable surveys. Solid red lines indicate the location of stationary cable surveys (A and B). Thicker red lines in the cartoon of the southwest shore (B) indicate where stationary cable surveys were overlapped to cover distance greater than permitted by single stretch of the cable. *Orthophoto from National Agricultural Imagery Program (NAIP), 2003.*

boat as the boat moved forward so that it was ultimately in a straight line, was kept afloat by small (~15cm) sections of pool floats attached, via plastic wire ties, to the section of cable between each of the electrodes (Figure 3-5a). Another port in the SuperSting was attached to a Lowrance GPS and sonar unit which recorded position and water depth information used later in the data inversion process. The GPS receiver was mounted to the top of the trolling motor, where reception of the GPS signal was best. The sonar transducer was attached, by means of a metal collar, to the bulb which housed the propeller motor (Figure 3-5b).

Survey parameters, including electrode geometry, GPS and sonar connection information, transmitter voltage, firing and measuring patterns, were entered into the SuperSting by means of a keypad prior to the start of a survey. Once the cable had been fed out behind the boat and the boat was in position to begin the survey, the "Start" key was pressed and the Sting launched its survey, requiring, if all went well, no further input from the user. Current was injected and potential measured every four seconds as the cable was towed along the perimeter of Mirror Lake. At typical speeds (2-3 km/hour), this produced a set of resistivity measurements on average every 3.5 m. A constant towing velocity of 2-3 km per hour was maintained until the survey was finished. Survey data were stored by the SuperSting's internal computer and downloaded once the survey was complete. Apparent resistivity measurements were integrated during the processing stage of the survey using the GPS information recorded with each resistivity measurement: because electrode array geometry was constant (except when making sharp turns), it was possible to interpolate all electrode positions from a single GPS reading. Resistivity values could in this way be assigned to particular places along a survey track and easily plotted on a map

### 3.3 Stationary-Cable (Lake-Bottom) Survey

For the lake-bottom survey we used a 28-electrode cable, where each electrode was capable of functioning as either a current or measuring electrode (Figure 3-3b). This ability to toggle between modes allowed the stationary-cable to accomplish from a single position what the towed-cable did as it was physically moved about the lake; that is, by injecting current and measuring potential drop from multiple different positions, we gathered resistivity data about a region from multiple angles.



 = pool float wire-tied to cable

 = electrode

Figure 3-5a. Cartoon of Towed-Cable With Pool Floats.



Sonar transducer with collar

Figure 3-5b. Cartoon of Trolling Motor with Sonar Transducer and GPS Antenna Mounted.

Completing all possible permutations of electrode pairs is not only impractical but also unnecessary because certain combinations of electrodes duplicate others. Studies have been conducted (e.g., Peake, 2005) to determine optimum survey patterns in terms of both time and data quality, survey patterns. The dipole-dipole array, in which a pattern of 56 different pairs of current electrodes is used and potential measured at between 3 and 8 different “dipoles” (pairs of measuring electrodes) for each injection of current, is particularly effective for mapping shallow lateral variation (Peake, 2005). It was employed for all stationary-cable surveys in this project.

Stationary-cable surveys were conducted with the survey cable approximately perpendicular to or parallel with the shoreline: such a regular measurement pattern made comparing profiles easier in the analysis phases of the investigation. We conducted a total of 18 perpendicular-to-shore resistivity surveys and 25 parallel-to-shore surveys (Figure 3-4). The majority of these (33 of 43) were conducted along a 130-meter stretch of the SW shore of Mirror Lake. We placed flags every meter along this stretch of shoreline to facilitate measurement reference. Locations of resistivity and radar surveys, seepage measurements, and sediment samples were all referenced against this “Long-Line.” The other stationary-cable surveys were conducted along the eastern shore of Mirror Lake and within the Northeast Inlet area.

The procedure for conducting a stationary-cable survey was as follows: one person stood on shore with the SuperSting control unit and one end of the electrode cable while the other backed away from the shoreline in the boat and fed the remaining cable from the boat into the lake. The cable was pulled taut once the end was reached, and then released to sink to the bottom of the lake, with a float attached to the lake ward end of the cable to facilitate retrieval. Electrodes were metallic and usually visible through the water column. Depth to each electrode was measured using a measuring tape with a weight attached to it. The shoreward, connection end of the cable was then attached to the SuperSting and the survey begun. As with the towed-cable survey, once a survey had been launched no further input was required from the user until the preset measuring pattern was completed.

### 3.4 Data Inversion

Once an electrical resistivity survey was completed, the resistivity data was processed (“inverted”) into a form interpretable by the surveyor. We used EarthImager 2D for this purpose. Preparatory steps were required before data were passed to EarthImager for inversion. These steps varied depending on the type of survey conducted. In the case of towed-cable resistivity surveys, GPS and depth data gathered from the Lowrance unit needed to be synchronized with the resistivity data. A second program, Marine Log Manager®, facilitated this process by tying resistivity data to the appropriate coordinate location by time stamp, extracting sections of long surveys, and creating depth profiles from the sonar data which would be used to constrain the inversion process. Marine Log Manager also allowed us to correct minor user errors made during the survey. It was possible, for instance, to correct for the input of a 4-m electrode spacing when a 2-m spacing was actually employed. In the case of the stationary-cable survey, it was necessary to create a file with water depths to constrain the inversion process.

The inversion process, by which images of the subsurface are generated from a set of resistivity data, is straightforward in theory. The inversion software creates a model of the subsurface environment and then conducts an “imagined” resistivity survey over that model (Figure 3-6). It then compares resistivity data from that imagined survey with the resistivity data actually gathered from the field. Regions of the resistivity profile where the match between actual resistivity data and modeled resistivity values is good are kept; in regions where the fit between observed and modeled values is poor, model resistivity values are modified. The entire process is then repeated, with iterations continuing until the rate of decrease in variance between modeled and actual resistivity values (where variance is quantified by Root Mean Square error, described in Section 3.5) approaches zero or falls below some other specified tolerance. The final image of the subsurface environment is a graphic representation of the program’s model of a subsurface environment that generates the best fit to the observed field resistivity values.

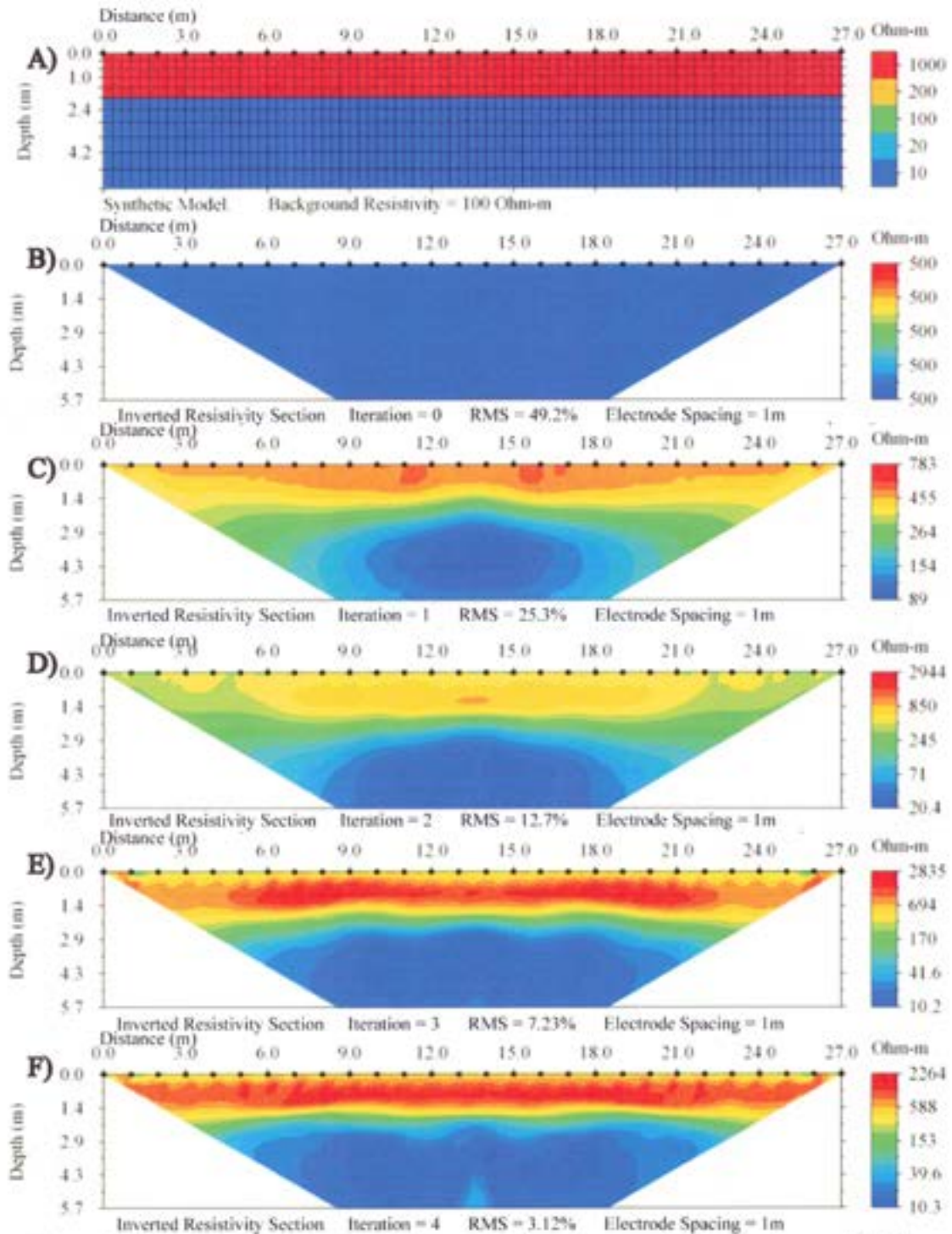


**Figure 3-6. The Inversion Process.** (A) is a synthetic two-layer earth, the upper layer of which is highly resistive, the lower of which is highly conductive. (B)-(F) show the successive inversion iterations: (B) represents the starting "guess", a half-space with uniform resistivity (in this case 500  $\Omega$ -m). (C) represents the first improvement on the starting model, (D) the improvement on (C) and so on as EarthImager attempts to determine what kind of earth would yield the observed apparent resistivity values. Root Mean Square error (RMS) decreases with each iteration as calculated resistivity values converge towards measured resistivity values.

### 3.5 Inversion Error Analysis

Although the theory behind inversion of resistivity data is relatively straightforward, the process is mathematically complex. A fundamental difficulty is that there may exist multiple solutions for a single inversion problem; that is, there are potentially multiple different subsurface environments that could generate a particular set of observed field resistivity values. There are many different ways of modeling and sorting through data to help mitigate this issue of non-unique solutions. Inversion software such as EarthImager offers multiple different processing settings which affect starting models and algorithms for inversion, thresholds for the discarding of bad data, iteration cutoff limits, and so on. Broadly speaking, the analyst can be most confident in her data set and inversion settings when inversion of the same data using multiple different settings yields similar final images, and least confident when it yields very different ones. There exist a number of mathematical measures of model accuracy, including assessments of average variation between modeled and measured resistivity values, data misfit plots, and analysis of the sensitivity of models to depth.

EarthImager offers several built-in tools for such error analysis. With its “Data Misfit” tool, for example, relative model accuracy is assessed by subtracting measured apparent resistivity from calculated apparent resistivity, and dividing that quotient by measured apparent resistivity:

$$\mathbf{Data\ Misfit} = \frac{\rho_{meas} - \rho_{calc}}{\rho_{meas}} \quad \mathbf{3.3}$$

Results of this data misfit analysis may be displayed graphically as a “pseudosection”, in which data misfit values are assigned a color and displayed as a function of their location along the survey line, or as a cross-plot (Figure 3-7) (Advanced Geosciences Incorporated, 2007).

Variance between observed and modeled resistivity values can also be quantified by averaging the square roots of the squares of the difference between the apparent resistivity values at each equivalent point within the two models (“Root Mean Square error”) (Advanced Geosciences Incorporated, 2007).

$$RMS = \sqrt{\frac{\sum_{i=1}^N \left( \frac{\rho_i^{pred} - \rho_i^{meas}}{\rho_i^{pred}} \right)^2}{N}} \times 100\% \quad 3.4$$

$\rho_i^{pred}$  = predicted apparent resistivity value at each point;  
 $\rho_i^{meas}$  = measured apparent resistivity value at each point;  
 $N$  = total number of measurements

The final assessment of the root mean square error (RMS) of an inverted resistivity dataset gives the surveyor a quick sense of the accuracy of that inverted section. This measure is useful not only for assessing the accuracy of given models but also for determining at what point the iteration process ought to be halted. Where a successive iteration of the model generation/pseudo-survey process resulted in, for instance, a 20% improvement in fit between modeled and actual resistivity values, the new model could reasonably be kept. Where successive iteration resulted in a 0.5% improvement in model fit, on the other hand, the iteration process is halted; such small improvements in model fit are not supported by actual data but instead represent a fitting of the model to noise.

A sensitivity analysis may be used to quantify how strongly supported a model is at different depths and at different regions. We used the method proposed by Oldenburg and Li (1999) and further modified by Marescot and Loke (2003). This method quantifies the degree to which the use of different starting models or inversion parameters yields a common final model of the earth. In this technique, the resistivity data is inverted twice; once using a very high starting resistivity value and once using a much lower one. The resistivity values of each block of the model generated from the lower starting value of

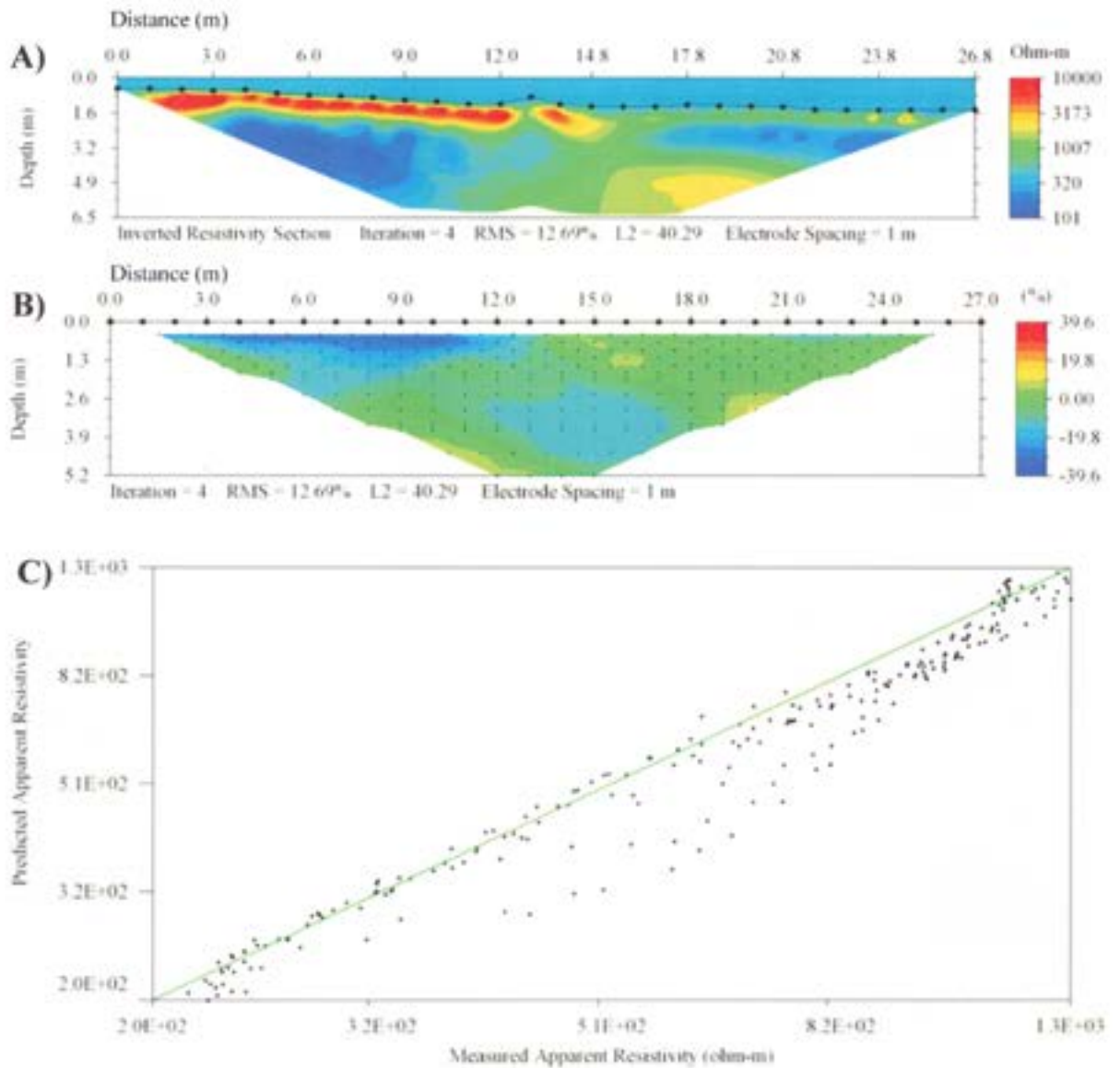


**Figure 3-7. Sample Inverted Resistivity Section with Error Assessment.** (A) shows an inverted resistivity section. (B) Shows error assessment, as measured by the percent difference between measured and calculated resistivity values, by approximate location within the inverted section. Percent error is color coded. (C) is a cross-plot of error assessment, with measured apparent resistivity on the x axis and predicted (calculated) apparent resistivity on the y axis.

these two inversions are subtracted from the values of each block of the model generated by inversion of the larger one, and that value is divided by the difference between the two starting average resistivity values.

$$R_{AB}(x, z) = \frac{q_A(x, z) - q_B(x, z)}{q_A - q_B} \quad 3.5$$

Where inversions are well constrained by data points,  $R_{AB}$  will approach 0 because there exists enough apparent resistivity data that the inversion routine can calculate true resistivity. Where the model is not well constrained by data,  $R_{AB}$  will be large because there is not enough data to calculate true resistivity, so the starting “guess” about the resistivity of the subsurface strongly influences the final solution. In this way the accuracy of a given model can be assessed on a cell-by-cell basis.

### 3.6 Resistivity Test Box

We used the resistivity test box to assess directly the resistivity of small (~330 cm<sup>3</sup>) sediment samples. The resistivity test box is a 3 x 5 x 33 cm plastic box with 2 current and 2 potential electrodes (Figure 3-8). It connects with an earlier version of the SuperSting resistivity system, the Sting R1 IP resistivity system. This single-channel resistivity system measure potential drop across measuring electrodes M and N for each injection of current through electrodes A and B. An on-board computer calculates and reports resistivity from that potential drop.

### 3.7 Sediment Sampling

We collected sediment samples using clear plastic collection tubes, approximately 5 cm in diameter (Figure 3-9), to assess the resistivity of saturated sediment samples using the resistivity testbox. We collected cores from locations where it was possible to insert the collection tube (approx. 5 cm in diameter) at least approximately 10 cm directly into sediment. This was generally only possible where sediment was very soft, as it tended to be in regions where there were thick deposits of organic-rich material. We also collected sediment samples from regions where it was not possible to insert the tube directly into sediment (i.e., in regions where sediment was hard-packed) by scraping samples from the upper few cm of sediment into collection tubes. We assessed the resistivity of saturated sediment samples using the resistivity test box.

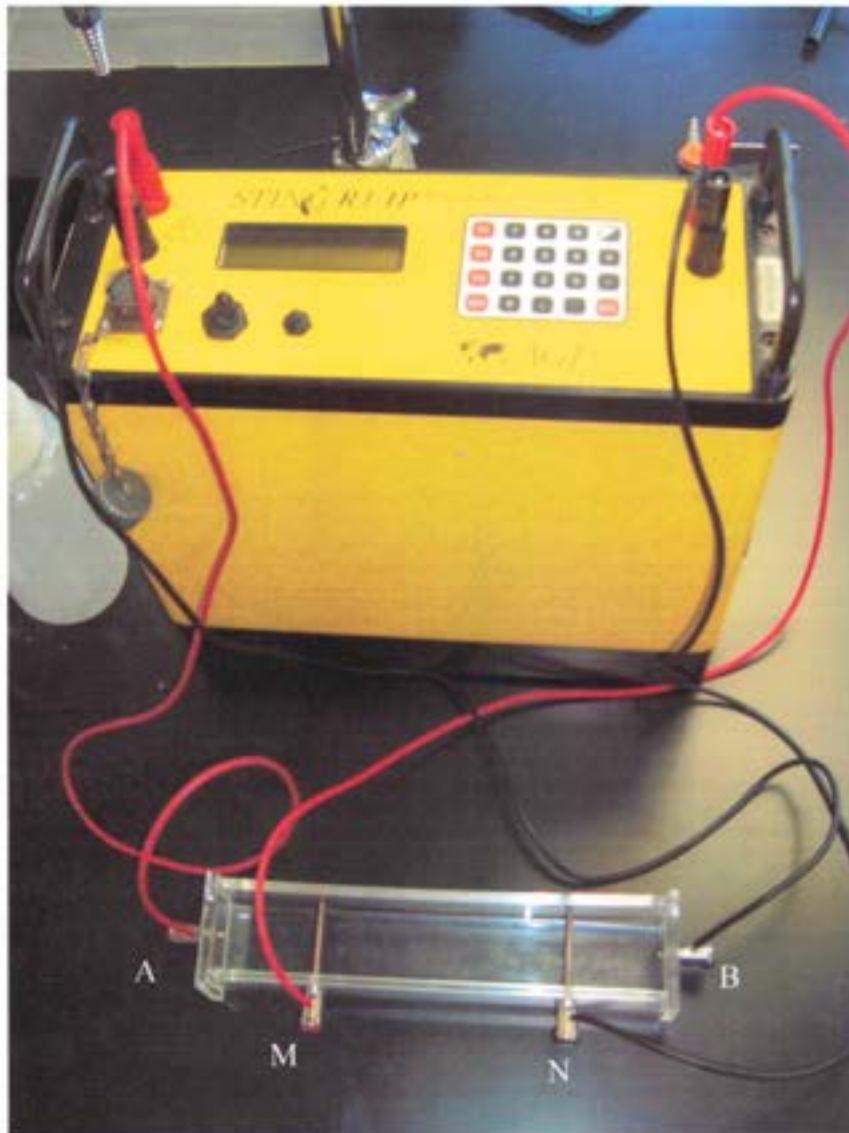


**Figure 3-8. Resistivity Test Box.** A small (~3 x 5 x 22 cm) plastic box with measuring electrodes (A and B) and potential (M and N) electrodes is connected to the Sting R1 IP resistivity system. Resistivity of a small sediment sample can be measured directly with the test box.

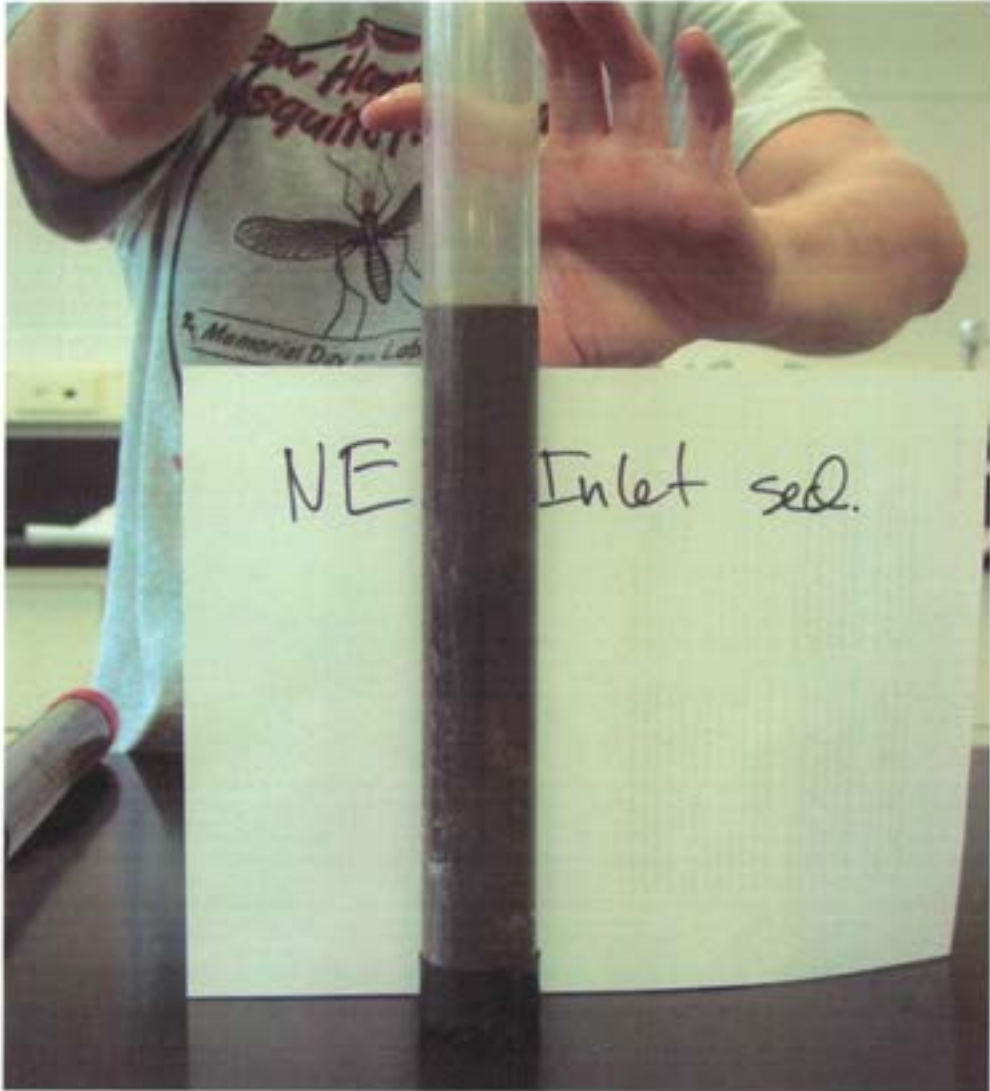


**Figure 3-9. Sediment Core in Collection Tube.** Sample sediment core from the northeast inlet area. It was only possible to collect such cores in regions where sediment was very soft, as it tended to be in regions with thick deposits of organic matter. The dark brown color of this sample reflects high organic matter content.

### 3.8 Ground Penetrating Radar

Ground penetrating radar was employed in this project as an adjunct to electrical resistivity profiling. Whereas electrical resistivity profiling introduces an electric current into the earth and measures how well the earth conducts that current, ground penetrating radar (GPR) introduces electromagnetic waves to the subsurface and measures how those waves reflect. The technique is useful to geologists because radar waves are reflected by bedding planes and other major changes in sedimentation, and can reveal a detailed image of subsurface structure.

The behavior of radar waves in a given medium is controlled by the dielectric permittivity ( $\epsilon$ ) of that medium, its electrical conductivity ( $\sigma$ ) and its magnetic permeability ( $\mu$ ), properties that are primarily functions of freshwater content of the substrate and of more difficult to quantify structural properties (Neal, 2004; Reynolds, 1997). The relationship of these properties to wave velocity in a substrate ( $v$ ) is described by:

$$v = \frac{c_0}{\sqrt{\epsilon_r \mu_r \frac{1 + \sqrt{1 + \left(\frac{\sigma}{\omega \epsilon}\right)^2}}{2}}} \quad 3.6$$

where  $c_0$  is the velocity of electromagnetic waves in a vacuum,  $\omega = 2\pi f$  and is the angular frequency of the signal in radians/sec,  $\epsilon$  is the dielectric permittivity of free space,  $\epsilon_r$  is the host medium's dielectric permittivity relative to free space,  $\sigma$  is its bulk conductivity at the given frequency, and  $\mu_r$  is its relative magnetic permeability, and  $\frac{\sigma}{\omega \epsilon}$  describes attenuation of the signal as it passes through host media (Neal, 2004). A wave's amplitude ( $A$ ) also changes as it passes through a medium, that amplitude declining exponentially from its initial value and described by the equation

$$A = A_0 e^{-\alpha z} \quad 3.7$$

where  $\alpha$  is an attenuation constant caused by loss of energy via conversion of the radar signal to heat and is dependent upon the dielectric and conductive properties of the host medium,  $A_0$  is a wave's initial amplitude, and  $z$  is distance traveled by the wave.

Where  $\epsilon$ ,  $\sigma$ ,  $\omega$  and  $\mu$  remain constant, radar waves will be transmitted through the medium without reflection. Where  $\epsilon$ ,  $\sigma$ , and  $\omega$  vary through the course of a geologic section ( $\mu$  generally remains constant) as the result of changes in porosity, grain composition, orientation and packing, or amount and type of pore fluid, reflections will be generated at the points where those properties change over a zone greater than or equal in length to approximately three times the dominant radar wavelength (Neal, 2004). Objects such as cobbles and boulders represent sudden, marked variations in  $\epsilon$ ,  $\sigma$ , and  $\omega$ ; such objects reflect electromagnetic energy strongly, and produce characteristic diffraction hyperbolae in radargrams (Figure 3-10). The amplitude of reflected waves is quantified by  $R$ , the coefficient of reflection,

$$R = \frac{\sqrt{V_2} - \sqrt{V_1}}{\sqrt{V_2} + \sqrt{V_1}} \quad 3.8$$

where  $V_1$  and  $V_2$  are the velocities of radar waves in adjacent layers 1 and 2. It is these reflections which are collected and plotted in a GPR survey and which collectively comprise the images of the subsurface. If average radar velocities for a given medium are known, reflections can be plotted as a function of depth by measuring time between the introduction of an electromagnetic wave to a substrate and the return of reflections to a receiving antenna. Shading the positive (or negative) portions of the plots of reflected waves, as is done to create radargrams (Figure 3-10) can yield an image of the sub-surface environment. Since radar surveys are sensitive to changes in grain size, porosity, packing, orientation and other sedimentological factors that tend to be associated with bedding planes, such plots can image bedding planes, lithologic, and other structural features.

Selection of antenna frequency for a GPR survey depends upon the aims of the survey. It is generally possible to resolve features as small as approximately one quarter the wavelength of the dominant radar frequency, so with higher frequency comes improved resolution (Reynolds, 1997). Higher frequency signals, however, do not penetrate as deeply into the subsurface. A good first approximation of the depth of penetration for any GPR survey is given by the so-called skin depth,

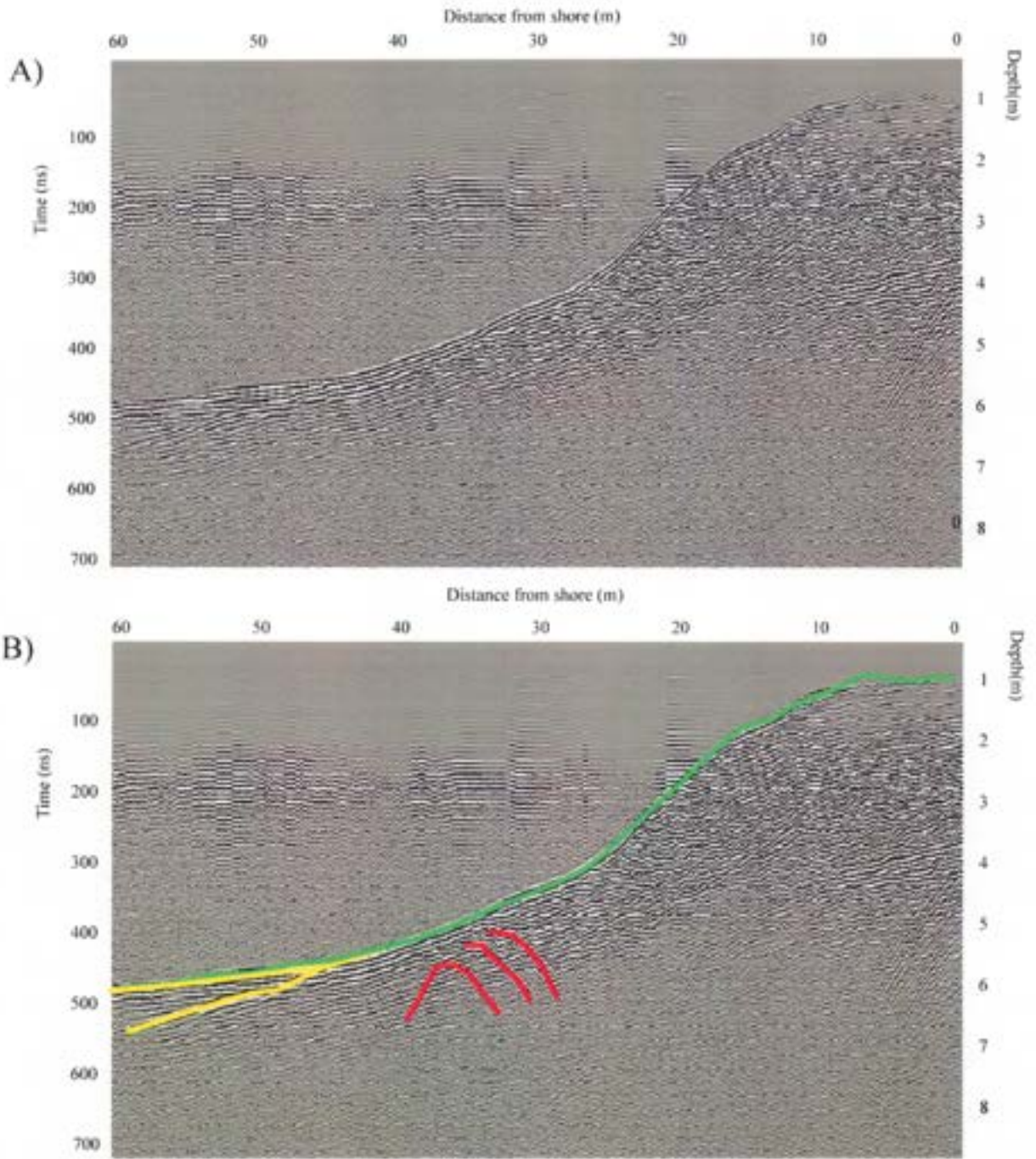


**Figure 3-10. Sample Radargram.** (A) and (B) are the same radargram. The bottom of the lake (green), layer of organic matter, and bedding within that organic matter (yellow) and diffraction hyperbolae (red) are highlighted in (B). Sometimes only one half of a diffraction hyperbola is visible. Radar reflections are generated any time there is a change in the conductivity or dielectric permittivity of sediment.

defined as the depth at which wave amplitude has decreased to  $\frac{1}{e}$  (approximately 37%) of its original amplitude (Reynolds, 1997). Skin depth is defined mathematically as

$$\delta = \left( \frac{2}{\omega \sigma \mu} \right)^{\frac{1}{2}} \quad 3.9$$

where  $\delta$  is skin depth (in meters),  $\omega$  is angular frequency,  $\mu$  is magnetic permeability and  $\sigma$  is conductivity (Reynolds, 1997). Depth of penetration, therefore, is not only dependent upon frequency but also upon the nature of the material being studied. Highly conductive materials such as clay and sea water are virtually opaque to radar waves. Highly resistive materials, on the other hand, such as unfractured granite, can transmit radar waves for many tens of meters. We used a MALA geosciences 250 MHz antenna in this project, which represents a frequency middle ground in terms of vertical resolution vs. depth of penetration.

Our 250 MHz GPR system included a transmitting and a receiving antenna housed in a plastic case 0.73 meters apart and connected to a computer recording system. To this computer recording system we attached a Trimble GPS unit, which recorded position information for the radar data. We loaded the entire suite of into the bow of our polyurethane boat, with the bottom of the antennae nearly flush with the floor of the boat (Figure 3-11).

We conducted a total of 40 GPR surveys: 20 perpendicular to shore at regular intervals (every 50 meters) around the perimeter of the lake to develop a sense of the basic lithology, and 20 perpendicular to shore at closer intervals (approximately every 10 meters) within our southwest shore study area (Figure 3-12). We also conducted a parallel-to-shore survey of the lake's perimeter, keeping a distance of 3-5 meters from the shore so as to traverse the same area covered by the outer of our towed-cable resistivity surveys.

Several data processing steps facilitated interpretation of GPR data. We processed GPR data using both Reflex 2-D Quick® and MatGPR software. First, reflector depths were calculated and assigned to radargrams, using a wave velocity of 0.033 m/ns, the speed with which radar travels through fresh water. Next, linear coordinates were extrapolated from GPS data and assigned to the radargrams.

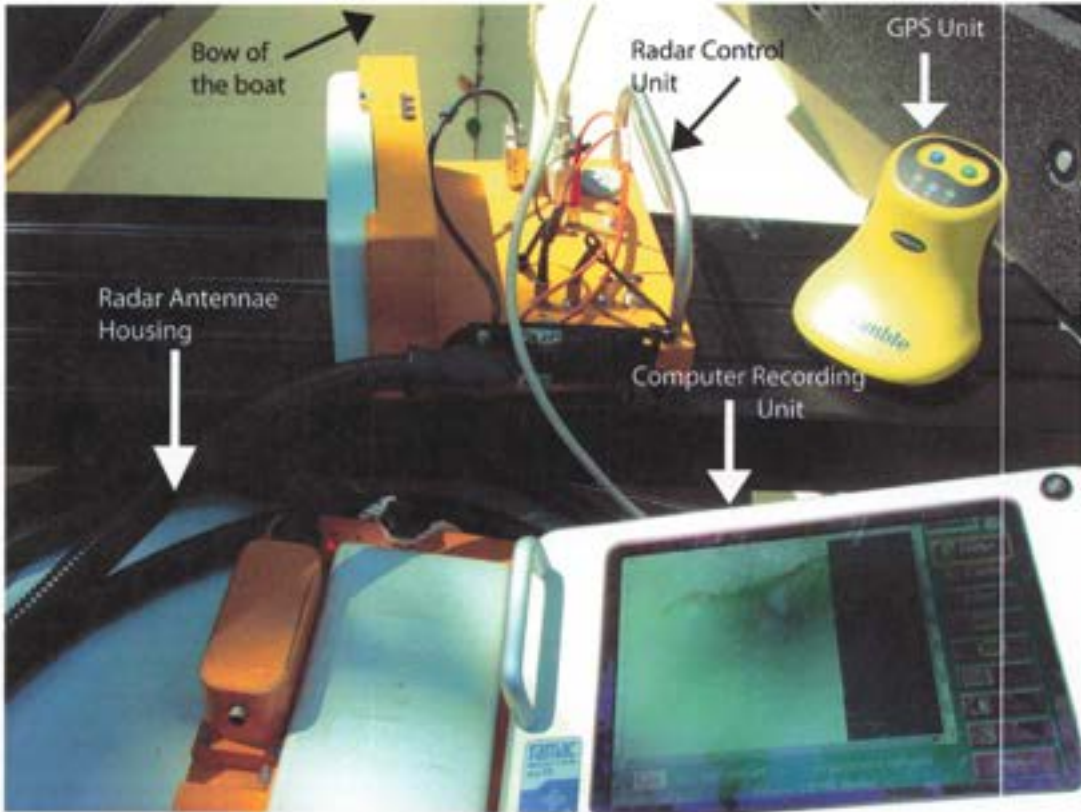


**Figure 3-11. Radar Equipment in Boat.**



**Figure 3-12. Location of Radar Surveys at Mirror Lake.** ~50 m GPR transects were conducted at 50 m intervals around Mirror Lake. Transects were conducted at approximately 10 m intervals along the southwest shore. Two parallel-to-shore surveys were conducted: one about the perimeter of the lake and one along the southwest shore. Lines (A), (B), (C), and (D) are discussed in the Results Chapter.

Third, an automatic gain control (AGC) function was applied to amplify radar reflections as a function of depth. Without such amplification, all but the nearest-surface reflections would be invisible because signal strength decreases exponentially with distance from the source. Finally, the appearance of noise in radar data, primarily caused by reverberation and by scattering, was reduced using a variety of filtering functions. The same processing steps and setting were applied to all radargrams.

### 3.9 Seepage Meters

In-situ measurements of the exchange between groundwater and the lake was measured with seepage meters of the design suggested by Lee (1977) as modified by Rosenberry et al. (2005) (Figure 3-13). A seepage meter works by sealing a selected region of sediment from the water column around it. A measuring bag attached to an outlet in this sealed zone, filled with a small quantity of water, will respond to local flow patterns.

We used one half of a 55-gallon (0.208 m<sup>3</sup>) plastic drum for these purposes. A hole (approximately 1.8 cm<sup>3</sup>, the size of a common garden hose) was drilled in the top of each half-drum. A threaded brass fitting was placed in the hole and sealed against the sides of the hole by means of caulk and plumber's tape. A length of garden hose and a measuring bag was attached to the metal fitting. The drum was pressed into the sediment above the region of interest. The entire unit was then allowed to sit undisturbed for at least one hour to allow re-equilibration of seepage in the region. At the end of this re-equilibration a period an approximately 1.5 liter plastic bag, filled approximately half-way with water and weighed, was attached to the free end of the hose by means of a brass fitting. The bag was placed in a protective plastic case to prevent waves, wind and other disturbances from affecting seepage from or to the collection bag. The shut-off valve of the brass-fitting was opened to allow exchange between the local hydrologic system and the water in the measuring bag. All seepage from the area beneath the drum changed the quantity of water in the bag. Where seepage was from the lake to the groundwater system ("out-seepage"), the contents of the plastic bag was drawn down. Where seepage is from the groundwater system to the lake ("in-seepage"), the measuring bag filled. After an appropriate length of time (hours to days if the seepage rates are low, minutes if rates are high) the shutoff valve of the measuring bag was closed and the bag removed from the seepage meter and weighed. From the known



**Figure 3-13. Seepage Meter.** Seepage Meter (blue cylinder) attached to measuring bag, which is protected from waves and wind by the clear plastic case and held in place by a large rock (foreground).

cross-sectional area of the seepage meter, the weight of the collection bag before and after the measurement, and the length of the measurement period, seepage rates are calculated, generally expressed in centimeters per day.

We made seepage measurements at a total of 74 points in Mirror Lake, the vast majority of which (72 out of 74) were within our intense study area of the southwest shore of that lake. Seepage measurements were made every 10 meters along the 130 meter stretch of our southwest shore “Long Line” (all of which were at a distance of approximately 2 meters from the shoreline) and at several intermediate points as well. We made additional measurements further from shore, including five seepage “transects” in which seepage meters were placed at 2-3 m intervals along a straight line out into the lake to a maximum of 16 meters from shore. At least three repeat measurements were made at each seepage meter site to ensure reproducibility of results.

### 3.10 Bathymetry

We gathered detailed bathymetric information for the southwest shore of Mirror Lake by traversing the area with our boat while we logged Sonar depth and GPS data (both given by the Lowrance navigation unit we used for SuperSting towed-cable resistivity surveys) with a laptop computer. By “zigzagging” over the southwest shore area and collecting depth and position information every second, we collected a dataset from which we could create a contour map of the area. We did so using the Kriging interpolation method via the Surfer® (Golden Software) gridding and plotting program. The resulting bathymetry map is included in Appendix A.

### 3.11 Data Coordinates

We collected GPS data for nearly all measurements conducted at Mirror Lake using a Trimble Geo XT GPS unit and a Lowrance GPS & sonar unit. Much of the data collected with the Trimble unit were logged directly by that unit. Data logged directly into the Trimble could be differentially corrected during post-processing, a step which improved precision to approximately  $\pm 0.5$  m. Where signal quality was poor, the Trimble would not allow logging directly into the unit; in those cases, we recorded approximate coordinate locations by hand as they could be read from the Trimble display screen.

Precision in those cases was approximately  $\pm 5$  m. The Lowrance unit was employed only during towed-cable resistivity surveys; that unit connected and communicated directly with the SuperSting resistivity survey system. No differential correction of the Lowrance GPS data was possible, and position data collected with the Lowrance unit were accurate  $\pm 5$  m. ArcGIS mapping software was used to plot the position data.

## CHAPTER 4 RESULTS AND DISCUSSION

### 4.1 Introduction

Our work at Mirror Lake aimed to test the hypothesis that geophysical techniques can image geologic heterogeneities which control seepage, or image seepage itself. To test this hypothesis we made seepage measurements at regular intervals over areas where we conducted electrical resistivity and ground-penetrating radar (GPR) surveys. We conducted a total of 4 around-the-lake towed-cable resistivity surveys, 43 stationary-cable resistivity surveys, 2 parallel-to-shore GPR surveys (including one round-the-lake survey), and 57 perpendicular-to-shore GPR surveys. We measured seepage at a total of 74 locations around Mirror Lake, 72 of which were along its southwest shore. Finally, we collected sediment samples at 22 locations, 20 of which were along the southwest shore.

### 4.2 Resistivity Survey Results Overview

We employed both 22-m and 44-m cables in the towed surveys, with electrode spacings of 2-m and 4-m respectively. We conducted two surveys with each of these cables, one attempting to stay within 2-3 m of shore and one slightly further away (4-5 m). Total depth of penetration, including the water column, was approximately 5 m with the 22-m cable and approximately 10 m with 44-m cable. Where the slope of the lake was gentle and where there were near-shore debris and man-made obstacles such as rafts, it was not possible to approach the shoreline by closer than 5-20 m. It was also not possible to maintain the desired distances where the shoreline was irregular, as where there were coves and peninsulas. Such difficulties were more frequently encountered and were more pronounced with the longer cable. The 22-m cable survey therefore generally returned the longest uninterrupted data streams. In particular, the 22-m cable survey conducted 2-3 m from shore returned the most useful data; water depths at the furthest distance were 3-4 m, so depth of penetration into sediment was only 1-2 m. All towed-cable resistivity profiles presented in the body of this thesis are therefore from the 22-m cable survey at a target distance of 2-3 m from shore. Portions of the survey omitted are places where irregular shoreline or near-shore debris precluded towing the cable in a straight line and in sufficiently shallow water.

Results from the 22-m cable survey are presented in Figure 4-1A-G. Resistivity values are contoured by color; a constant color scale is used throughout this thesis. The highest resistivity values (~3000  $\Omega$ -m) are in red. Intermediate resistivity (~1500  $\Omega$ -m) values are in yellow. The lowest resistivity values (<200  $\Omega$ -m) are in blue. The white line indicates lake-bottom, inferred from sonar data collected with the towed-cable surveys. Depth scale is provided on the left hand side of the inverted images. Inversions were constrained using lake depth. Lake water conductivity, a second inversion constraint, was established via a conductivity-meter as 330  $\Omega$ -m. That value was consistent with the results of inversion of a section of resistivity survey conducted over open water. Root mean square error (RMS) for the towed-cable surveys ranged from approximately 3 -10%. Sensitivity analyses (described in Section 3.5) suggested that  $R_{AB}$  (Equation 3.5) was  $\leq 10\%$  in the upper 1-3 m, with a gradual transition to greater than 30% below 4m. The surveys have therefore been truncated at a depth of approximately 4 meters.

Towed-cable resistivity surveys indicated that the resistivity of most sediment at Mirror Lake was 1000 – 3000  $\Omega$ -m, with discrete zones of low ( $\leq 200$   $\Omega$ -m) resistivity (Figure 4-1A-G). In some regions, sediment resistivity was relatively homogeneous (e.g., Figure 4-1A). In others, it was heterogeneous (e.g., 4-1B). Some features observed in resistivity profiles were easily related to geologic features. Along the eastern peninsula bedrock was exposed; along the northern shore, boulders were exposed. In both cases, sediment resistivity was high ( $> 3000$   $\Omega$ -m) (Figure 4-1C and G). In the region of inlet and outlet streams, and in a few other locations, thick ( $> 0.5$  m) deposits of organic matter were apparent (discussed in more detail in Section 4.4). Where such deposits were observed, resistivity was low ( $\leq 200$   $\Omega$ - m) (Figure 4-1B, C, D, F, and G). Where a curved path was taken to navigate a cove, electrodes at the tail end of the cable were pulled across open water; such paths produced resistivity profiles wherein the upper few meters of “sediment” were apparently equal in resistivity to lake water. Such resistivity values do not accurately reflect the resistivity of sediment traversed by the boat and the electrodes nearest to it but rather the resistivity of the open water traversed by the tail-end electrodes.

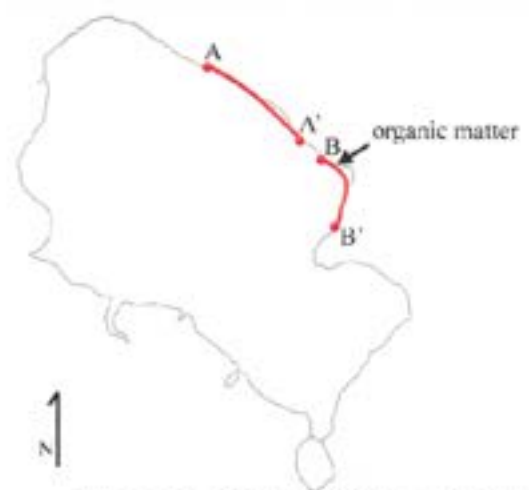
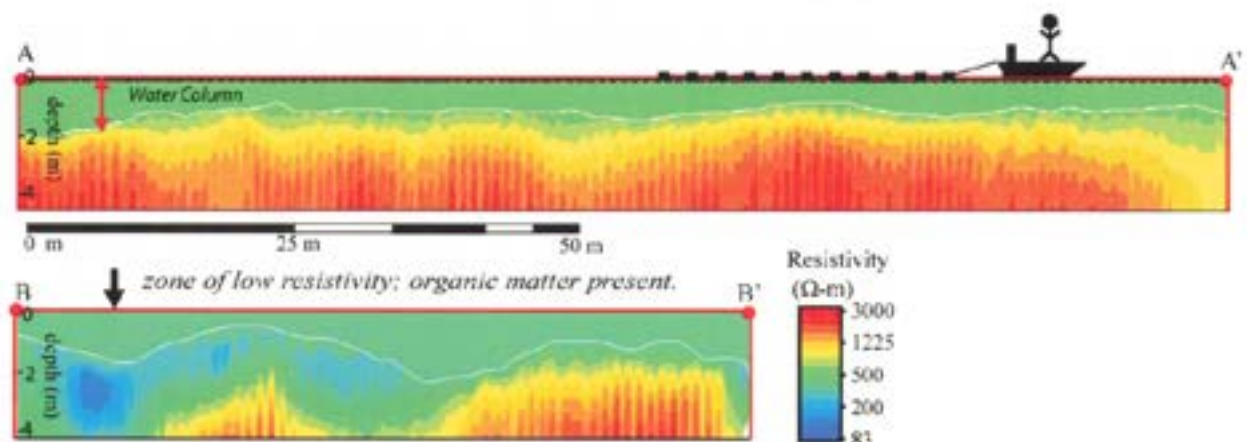
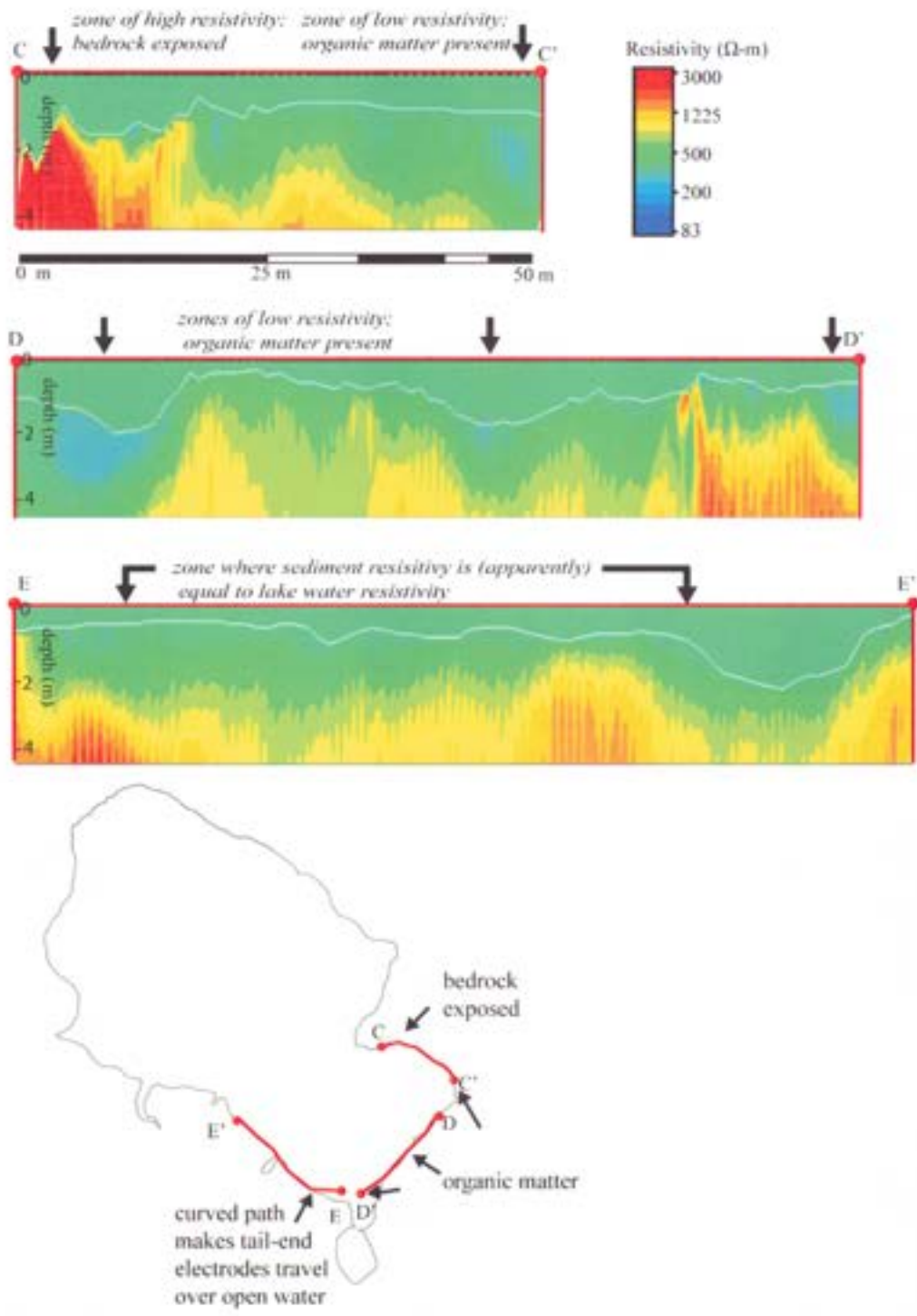
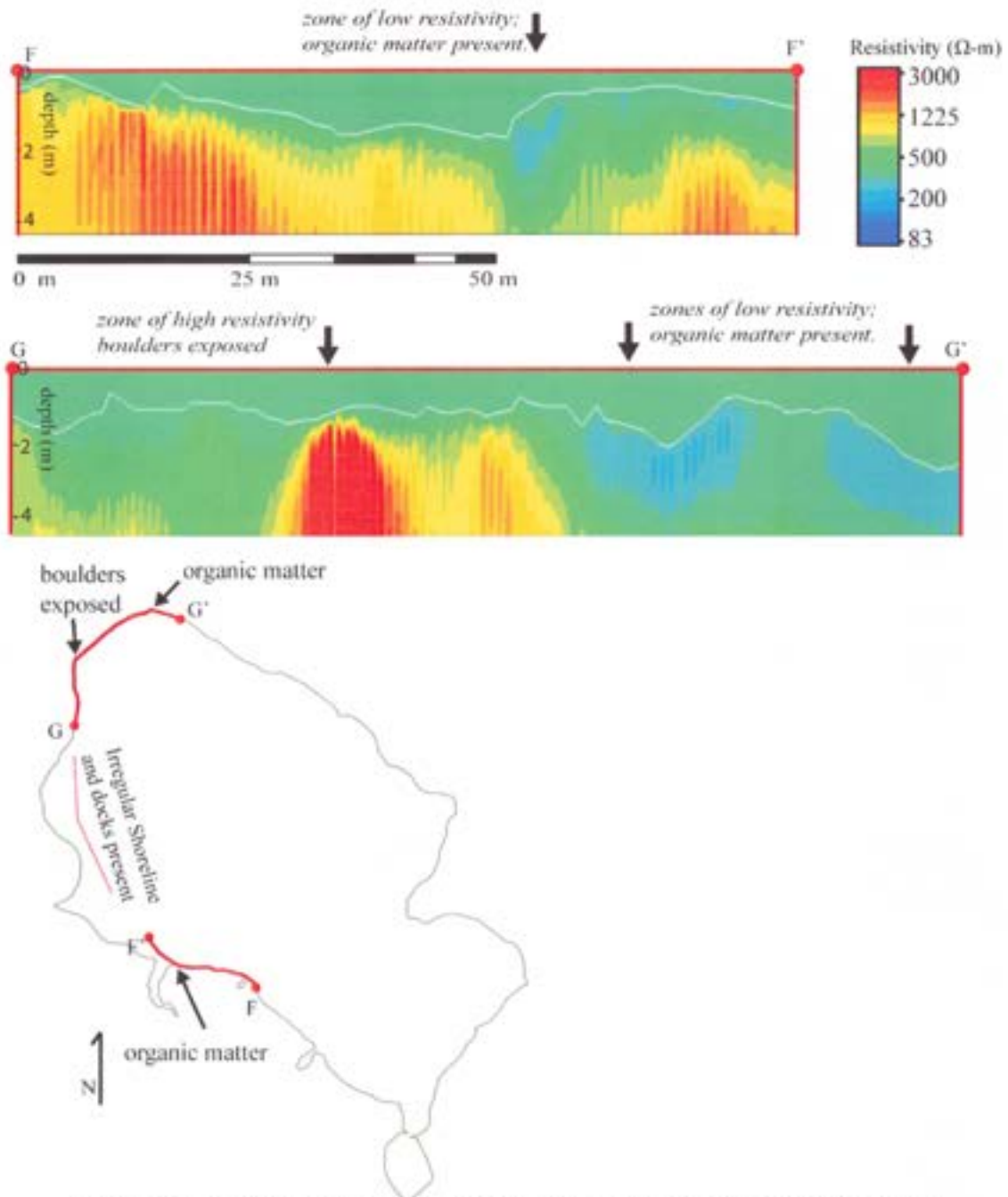


Figure 4-1A/B: (22m) Towed-Cable Resistivity Survey Results for Eastern Shore and Northeast Inlet Area. Towed-cable resistivity survey results showed that sediment resistivity at Mirror Lake ranged from less than 200  $\Omega$ -m to approximately 3000  $\Omega$ -m. (A) shows homogeneity within the sediment of the eastern shore of Mirror Lake. (B) shows heterogeneity within sediment of the northeast inlet area: a zone of low resistivity (< 200  $\Omega$ -m) exists at the northern end of the profile, while high resistivity (~3000  $\Omega$ -m) sediment exists at the south end. This low resistivity zone is discussed further in Section 4.7.



**Figure 4-1C-E: (22-m) Towed-Cable Resistivity Survey Results for Southeastern Corner of Mirror Lake.** The zone of high resistivity ( $> 3000 \Omega\text{-m}$ ) in (C) reflects a zone where bedrock was exposed. The zones of low resistivity ( $< 200 \Omega\text{-m}$ ) in (C) and (D) reflect deposits of organic matter. Regions in (E) which have the same resistivity as the lake water reflect regions where electrodes at the end of the streamer cable did not travel the same path as those near the boat.



**Figure 4-1F-G: (22-m) Towed-Cable Resistivity Survey Results for Western and Northwestern Shores of Mirror Lake.** Zones of low resistivity reflected deposits of organic matter. The zone of high resistivity in (G) corresponded to a region dense with boulders. The shoreline between the end of segment F and the beginning of segment G was highly irregular and also had several docks; these features precluded approach of the shoreline there by closer than approximately 20 m. Water depth at that distance from shore was too great to allow penetration into sediment greater than approximately 1 m, so no image is presented.

The results of stationary-cable resistivity surveys are presented in Figure 4-2A-K. One line (Perpendicular Line 3) is omitted because that survey was influenced by proximity to an electromagnetic flow meter. Two others, perpendicular resistivity surveys of the eastern shore, have been omitted because the very steep terrain along the shoreline there prevented inversion of those data. The black dots in stationary-cable profiles represent the location and depth of electrodes. The same color and depth scale used for presentation of the towed-cable results is used for the results of the stationary-cable surveys. Because the cable used in stationary-surveys is only 27 m long, any inversion images which show an inverted section longer than that represent the merged results of two or more overlapping stationary-cable surveys. RMS was less than 5% for inversion of single stationary-cable surveys, and 7-15% for merged datasets.  $R_{AB}$  values for inversions of single stationary-cable surveys were similar to those associated with towed-cable surveys;  $R_{AB}$  was  $\leq 10\%$  in the upper 1-3 m, with a gradual transition to greater than 30% below 4 m. Like the towed-cable profiles, stationary-cable surveys have therefore been truncated at a depth of approximately 4 meters. Even with this truncation, however, zones of lower resistivity (highlighted in Figure 4-2A) appeared at the bottom of all stationary-cable profiles. Zones of low resistivity at depth also appeared in the inversion of synthetic, uniform earth resistivity data. Low resistivity at depth is therefore an artifact of inversion and does not necessarily reflect actual low resistivity at depth. For inversion of merged datasets,  $R_{AB}$  was up to 50%, with an average of approximately 30%.

Stationary-cable surveys allowed the approach of terrain inaccessible to towed-cable resistivity surveys, such as coves, peninsulas, and shallow water. The stationary-cable surveys also offered resolution which was 4-5 times that of the towed-cable surveys. The higher resolution of stationary-cable surveys was a product of several factors: first the electrodes in a stationary-cable survey lay directly upon lake-bottom, so electrical current did not have to penetrate a thick water column before reaching the target of the survey. Second, many more measurements per unit length were made in the stationary-cable surveys than in towed surveys. Finally, the electrode spacing of our lake-bottom cable

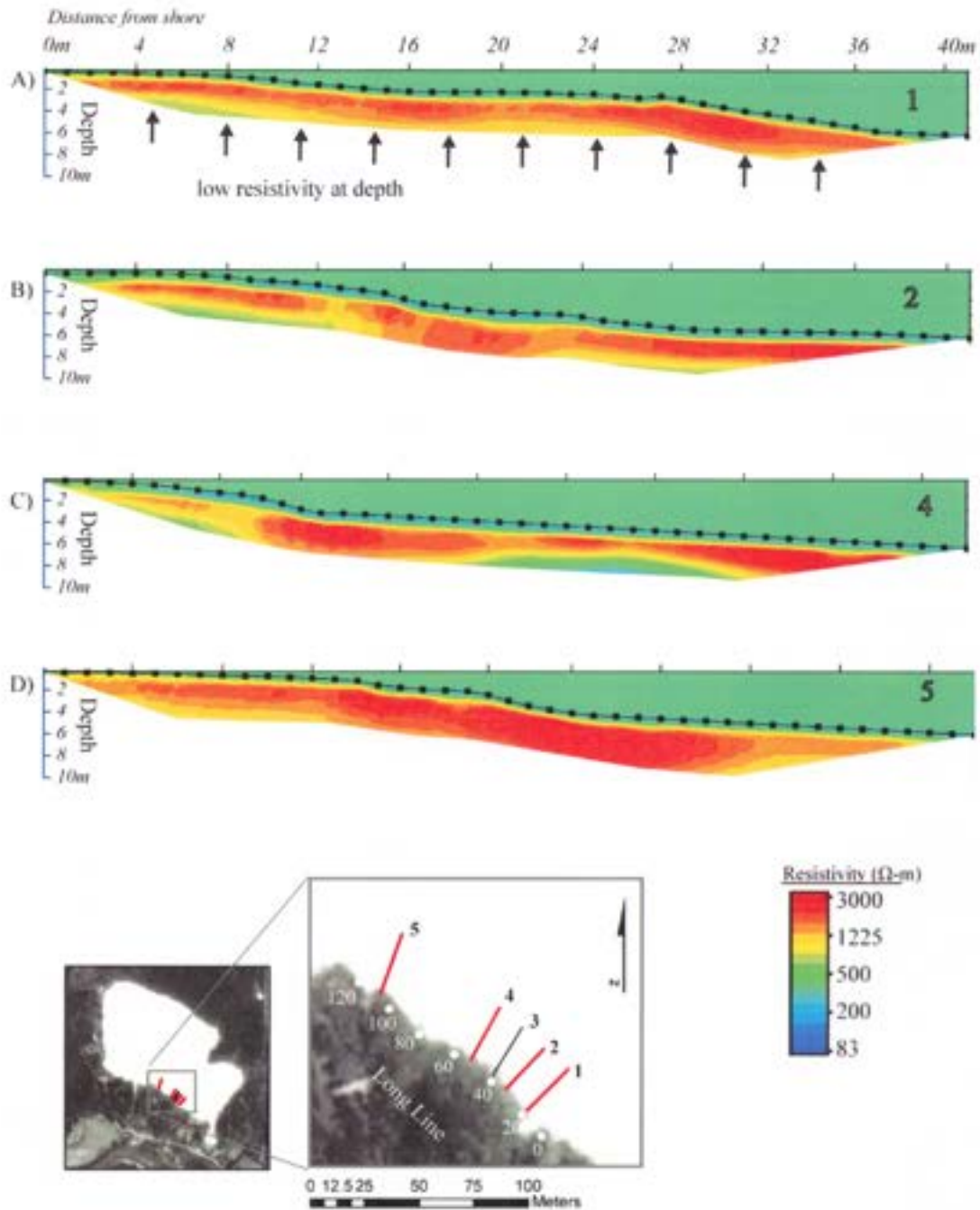


**Figure 4-2A-D: Southwest Shore Perpendicular Resistivity Profiles.** The results of 8 resistivity surveys, 2 merged for each 40 m transect, are presented here. The results are discussed in detail in Section 4.3. Average sediment resistivity increased with distance from shore, from approximately 1500  $\Omega\text{-m}$  to 3000  $\Omega\text{-m}$ . Proximity of an electromagnetic flow meter to the cable in survey 3 (omitted) made the results of that survey inconclusive. The low resistivity indicated at depth, highlighted only in (A) but present in all stationary-cable profiles, is an artifact of inversion and does not necessarily reflect low resistivity at depth.

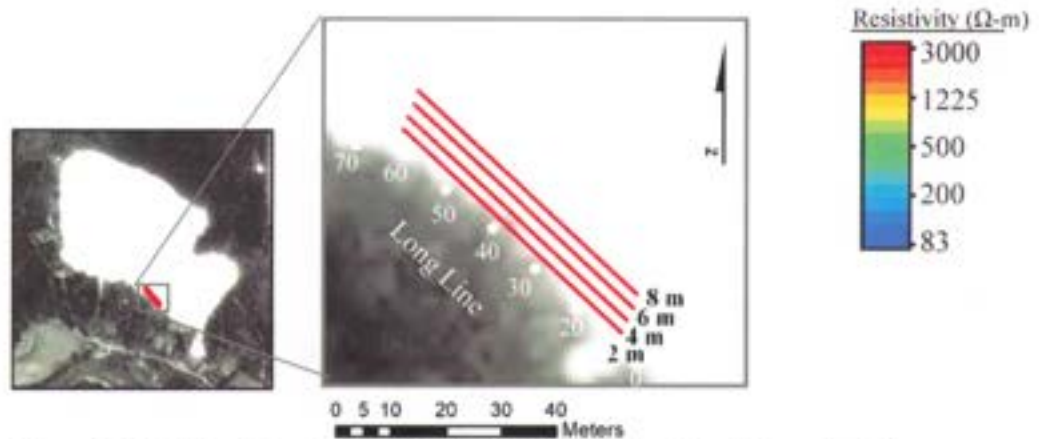
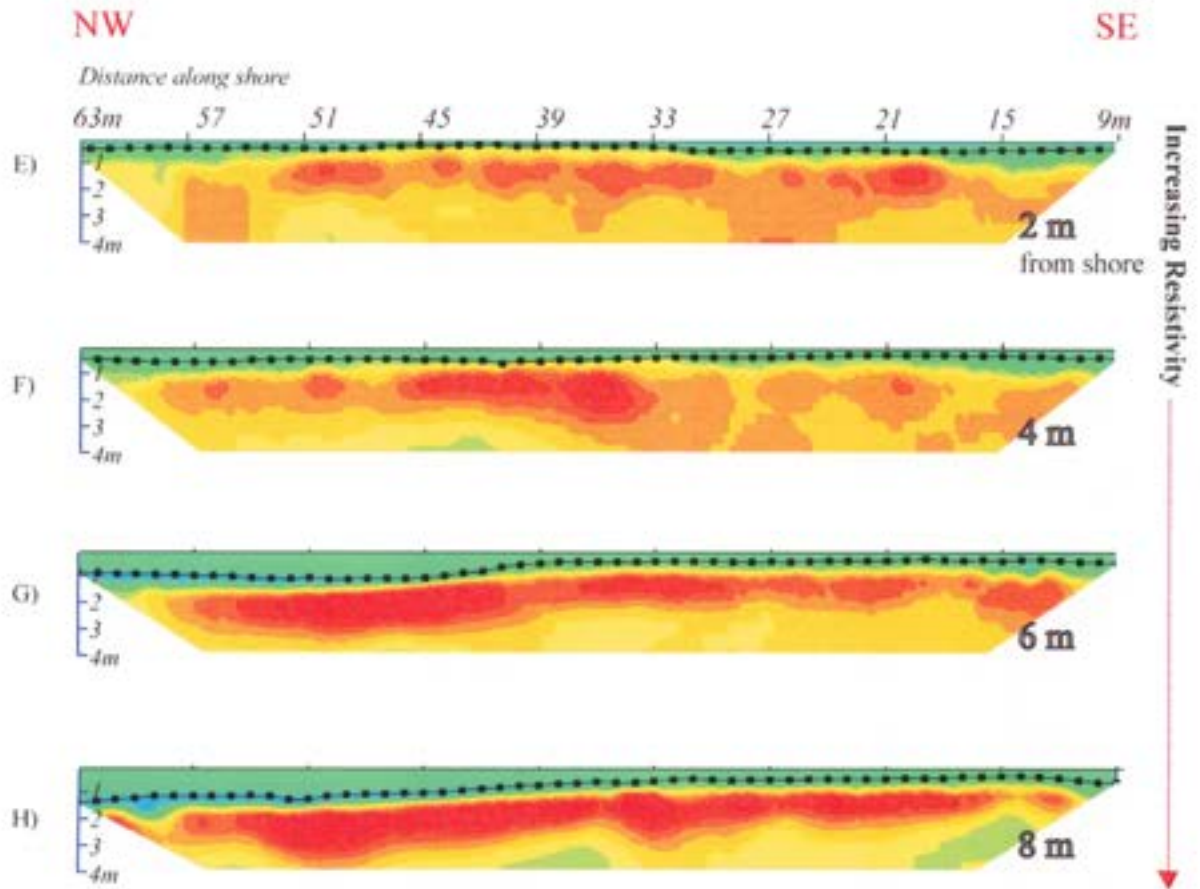


**Figure 4-2E-H: Southwest Shore Parallel Resistivity Profiles.** The results of 9 stationary-cable surveys, 3 merged for each 54 m transect, are presented here. They are discussed in detail in Section 4.3. Average sediment resistivity increased with distance from shore, from approximately 1500  $\Omega\text{-m}$  to 3000  $\Omega\text{-m}$ . As was the case in all stationary-cable surveys, the low resistivity indicated at depth is an artifact of inversion and does not necessarily reflect low resistivity at depth.

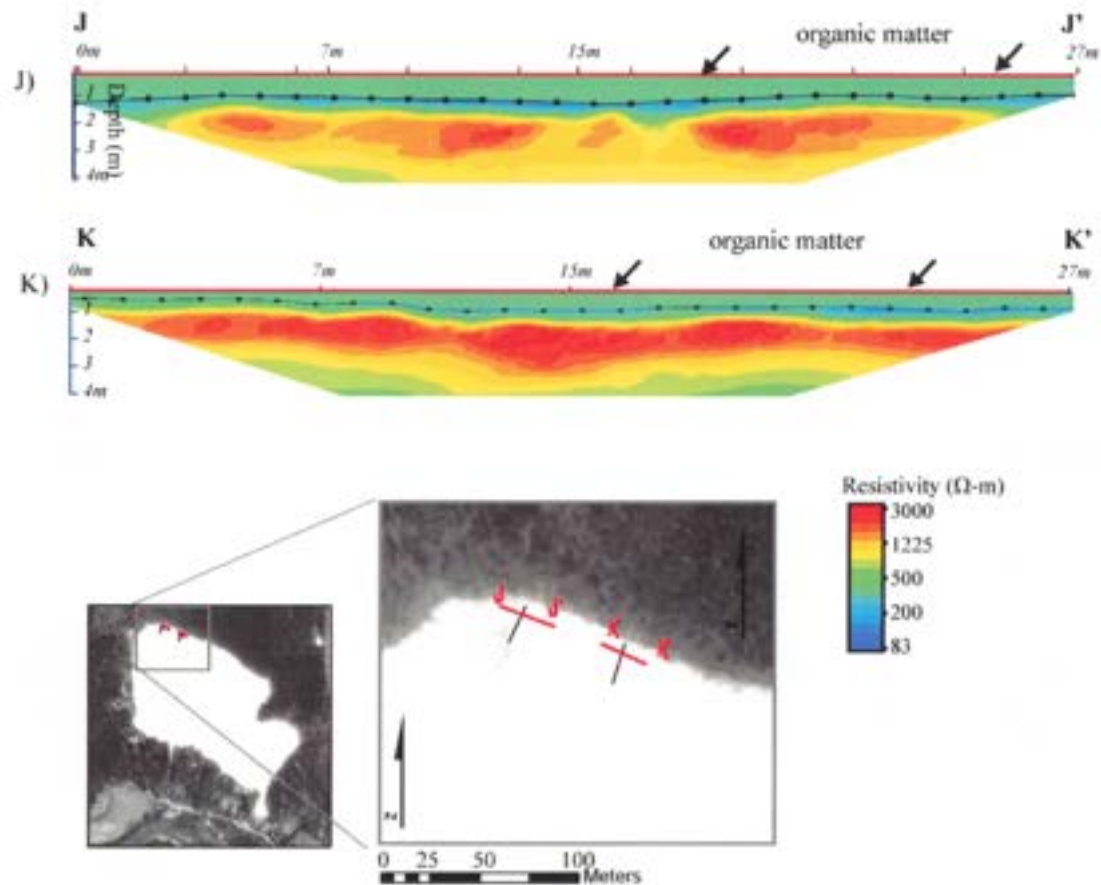


**Figure 4-2J-K: Eastern Shore Resistivity Profiles.** We conducted 2 perpendicular- and 2 parallel-to-shore stationary-cable resistivity surveys along the eastern shore of Mirror Lake. Results of the parallel-to-shore resistivity surveys are presented here and are discussed in detail in Section 4.4. Both (J) and (K) show homogeneity in sediment resistivity. Average sediment resistivity was approximately 1500  $\Omega\text{-m}$  in (J) and 3000  $\Omega\text{-m}$  in (K). A thin layer of low resistivity ( $\sim 200 \Omega\text{-m}$ ) material is present at the surface of both and reflected a layer of organic matter. The results of the perpendicular-to-shore surveys conducted coincident with (J) and (K) have been omitted because the very steep terrain along the shoreline there prevented inversion of those surveys.

was 1-m rather than the 2-m and 4-m spacing we used in the towed-cable surveys. This higher resolution and greater versatility, in terms of where the cable could be deployed, however, came at the expense of slower data acquisition.

Like the towed-cable resistivity surveys, stationary-cable surveys showed that sediment resistivity ranged from less than 200  $\Omega$ -m to approximately 3000  $\Omega$ -m. Where towed- and stationary-cable surveys were conducted on overlapping terrain, however, the towed-cable survey consistently returned lower measurements of resistivity highs than did the stationary-cable surveys. A comparison of the results of towed- and stationary-cable surveys is presented in Figure 4-3. Along the eastern edge of Mirror Lake, towed-cable surveys returned maximum average resistivity values of approximately 1500  $\Omega$ -m, while the stationary-cable surveys returned values of approximately 3000  $\Omega$ -m (Figure 4-3A). Towed-cable surveys of the northeast inlet area of Mirror Lake returned maximum average resistivity values of approximately 1500  $\Omega$ -m, whereas highest average resistivity values from the stationary-cable survey were in the 3000  $\Omega$ -m range (Figure 4-3B). Along the southwest shore, towed-cable surveys conducted at a distance of approximately 10 m from shore showed resistivity values which average around 1500  $\Omega$ -m (Figure 4-3C). Parallel-to-shore stationary-cable surveys conducted at a distance of 8 m from shore, showed average resistivity values to be about 3000  $\Omega$ -m. In all three cases, un-inverted apparent resistivity values as well as the inverted data were lower in the towed-cable surveys, suggesting that the discrepancy observed in inverted sections was the product of differences in raw data rather than a product of inversion.

I believe that the discrepancy is likely the product of differences in current travel path between towed- and stationary-cable surveys. Towed-cable surveys were conducted where water depths were approximately 2 m, which corresponded to being generally over or just beyond the edge of a narrow (~ 2 m) underwater plateau which rings the lake; beyond that plateau the sides of the lake are much steeper, plunging steeply towards the maximum lake depth of 7m+. Stationary-cable surveys, however, were generally conducted atop these plateaus: that is, regions where we conducted stationary-cable surveys had to be flat enough that the towed-cable would not roll down the banks of the lake. They were therefore necessarily along the plateaus. A greater portion of each resistivity "signal" was therefore

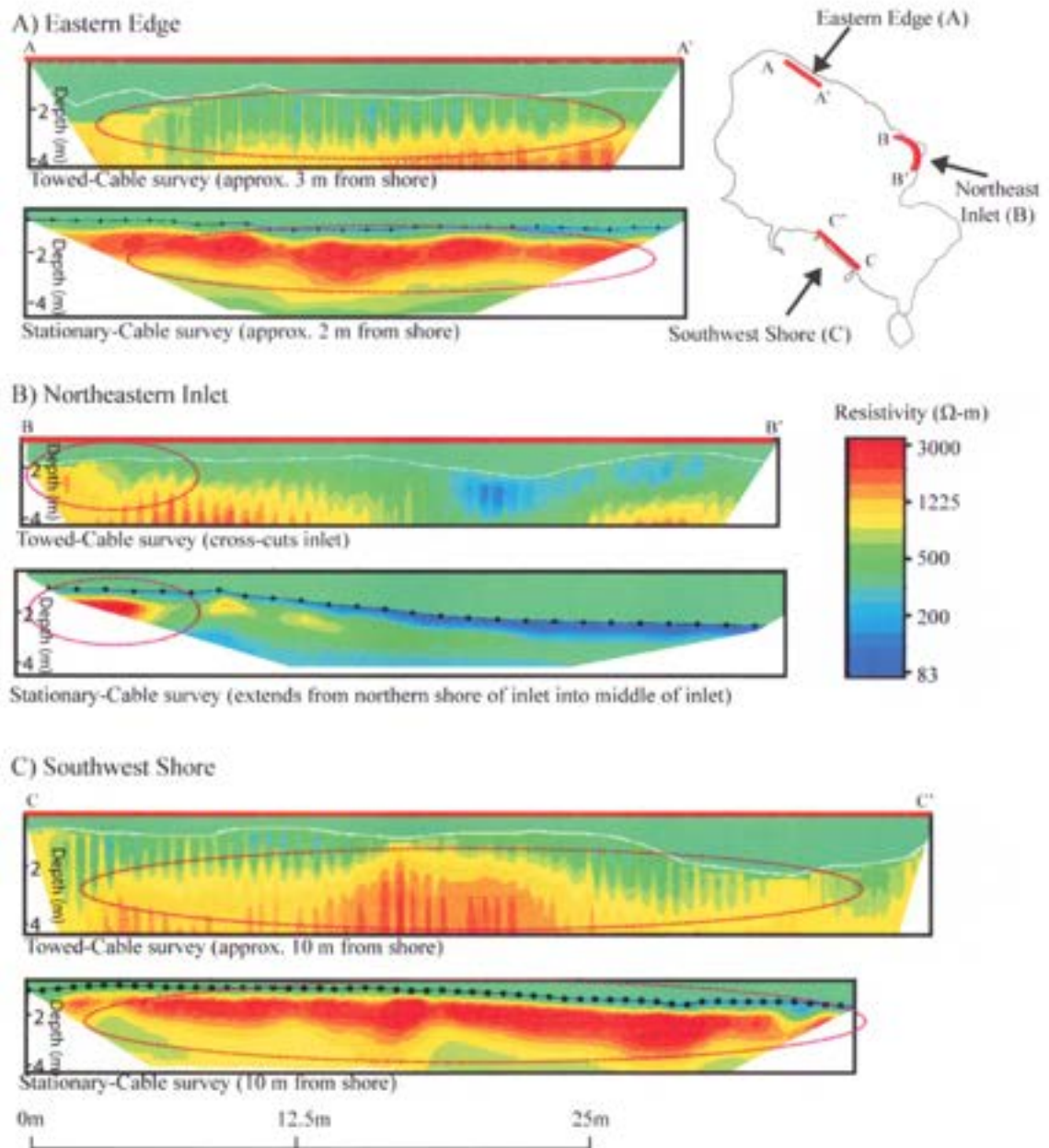


**Figure 4-3: Towed- vs. Stationary-Cable Resistivity Values.** Towed-cable resistivity surveys consistently returned sediment resistivity values which were lower than those returned by stationary cable surveys. (A), (B), and (C) show the results of stationary and towed- cable resistivity surveys conducted over duplicate or nearly duplicate terrain. Dashed red ovals highlight regions where resistivity values differ significantly.

likely influenced by lake water in the towed-cable surveys. Towed-cable resistivity surveys were subject to more sideswipe – survey of terrain adjacent to the survey cable (in this case lake water) rather than immediately below it – than were stationary-cable surveys. The lower resistivity values returned by towed-cable surveys therefore probably reflect the fact that proportionally more current flowed through the water. Because more of the current in a stationary-cable survey will interact with the geology, and because the density of resistivity measurements per unit area with the stationary-cable survey is approximately 6 times that of the towed-cable survey (thereby providing significantly greater constraint on the models generated by the inversion), I believe the resistivity values returned by the stationary-cable surveys more accurately reflect the resistivity of sediment. Towed-cable resistivity values therefore ought to be considered underestimates of true sediment resistivity. The majority of interpretation about resistivity survey results in relation to seepage is limited, in this thesis, to the results of the stationary-cable surveys.

#### 4.3 Southwest Shore Resistivity and Seepage Results

We focused study along the southwest shore of Mirror Lake where high seepage rates were previously observed (Asbury, 1990). We placed flags every meter along a 130 m stretch of that shore at a distance of 2 m from land. We conducted seepage measurements every 10 m along that “Long Line”, and at several intermediate points as well. We also conducted 5 seepage “transects”, measuring seepage every 2-3 m extending out perpendicular to shore, to a maximum distance of 16 m from shore. We conducted parallel-to-shore stationary-cable resistivity surveys over the entire length of the Long Line at a distance of 2 m from shore, overlapping adjacent surveys by approximately 50% so that we could generate a single resistivity profile for the Long Line. We also conducted parallel-to-shore surveys at 4, 6 and 8 m from shore within a zone where seepage rates were highest. Finally, we conducted perpendicular-to-shore surveys along each of the seepage transects. The results of Perpendicular Survey 3, the location of which was shown in Figure 4-2, are ignored in the interpretation because proximity to an electromagnetic flow meter influenced those data.

#### 4.3.1 Resistivity Values 1500 to 3000 $\Omega$ -m and Seepage Rates

The results of southwest shore seepage measurements are shown in Figure 4-4. The highest seepage rates were observed within 2 m of shore. These highest seepage rates (average = -80 cm/day, with a high of -277 cm/day) were clustered within a zone approximately 40 m long. Two of the five seepage transects were within the zone of very high seepage. Seepage rates declined to close to 0 cm/day by 12 m from shore in seepage transects 1 through 4. Transect 5 represented an exception to the pattern of decreasing seepage rates with distance from shore: slightly positive values were observed at 12 and 16 m from shore.

Parallel-to-shore resistivity surveys indicated that average sediment resistivity increased with distance from shore (Figure 4-2E-H). At 2 m from shore, average sediment resistivity was approximately 1500  $\Omega$ -m (Figure 4-2E). At 8 m from shore, it was approximately 3000  $\Omega$ -m (Figure 4-2H). There is some evidence in the perpendicular-to-shore surveys for increasing resistivity with distance from shore, but the variation is not clear-cut. No decrease in resistivity with proximity to shore appears in the Survey 1 (Figure 4-2A), the near-shore end of which overlapped with the southern end of the parallel-to-shore surveys (Figure 4-2E-G). Sediment resistivity in Survey 2 (Figure 4-2B), which also overlapped with the parallel surveys, appears to decrease within 4 m of shore; this apparent decrease, however, does not necessarily reflect a decrease in sediment resistivity. Data are sparse at the ends of stationary-cable surveys and so inversions are not well constrained there. Perpendicular surveys 4 and 5 (Figure 4-2C & D), indicate that average sediment resistivity is about 1500  $\Omega$ -m until approximately 10 and 12 m from shore respectively, several meters further than is indicated by the parallel-to-shore surveys. Because the increase in resistivity from 1500 to 3000  $\Omega$ -m indicated by the parallel-to-shore profiles occurs in the middle of the profiles where inversion models are well-constrained, I believe it is fair to assert that sediment resistivity does indeed increase in such a manner. The fact that perpendicular-to-shore surveys are inconclusive in this regard and in some cases differ from the parallel lines is likely a product of the fact that data are sparse at the ends of the surveys. In short, the results of parallel-to-shore resistivity provide more information about the near-shore environment than do the perpendicular-to-shore surveys.

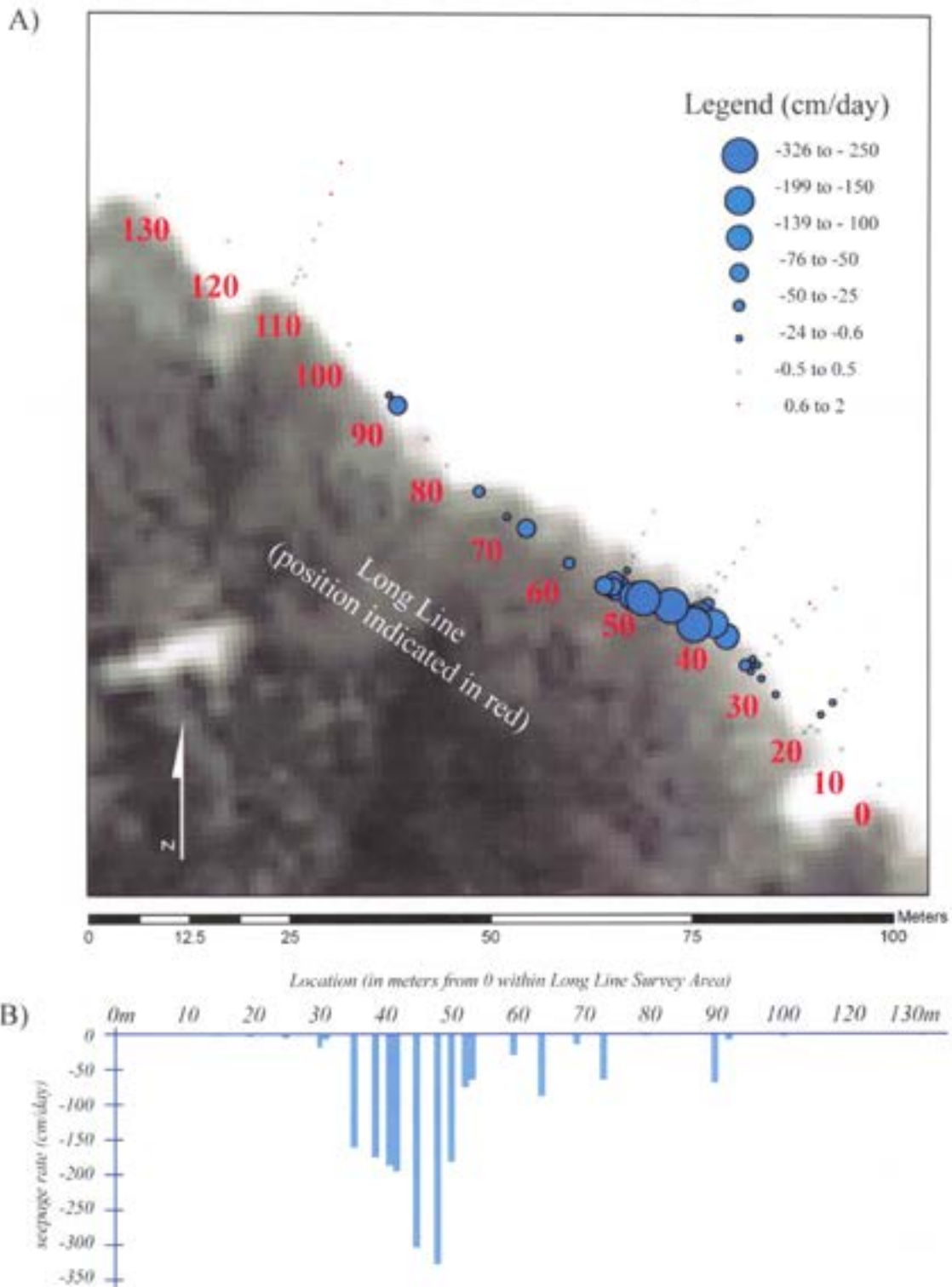


**Figure 4-4: Seepage Rate By Location Within Long Line Survey Area.** (A) reports the results of all seepage measurements along the southwest shore, with dot size proportional to seepage rates at a given position. (B) plots the results of seepage measurements at 2 m from shore only. Tree cover makes the locations of some seepage measurements appear as if they were made on-shore.

As stated previously, parallel-to-shore resistivity surveys at 2, 4, 6, and 8 m from shore (Figure 4-2E-H) within the zone of highest seepage rates showed that average sediment resistivity was approximately 1500  $\Omega$ -m at a distance of 2 m from shore and 3000  $\Omega$ -m at a distance of 8 m from shore. Seepage measurements showed that seepage rates decreased with distance from shore. That is, lower seepage rates were coincident with higher resistivity. A similar coincidence between lower resistivity ( $\sim$ 1500  $\Omega$ -m) values and higher seepage rates was observed at a distance of 2 m from shore, where a transition in sediment resistivity was observed approximately midway along the Long Line survey (Figure 4-5A and B): average sediment resistivity is approximately 1500  $\Omega$ -m until meter 70 of the Long Line, and approximately 3000  $\Omega$ -m after meter 70. Seepage rates were highest along the Long Line (average = -80 cm/day, with a high of -277 cm/day) where resistivity values were intermediate ( $\approx$  1500  $\Omega$ -m). Seepage rates were lowest (average = -20 cm/day, with a high of -90 cm/day) where resistivity values were  $\geq$ 3000  $\Omega$ -m or  $\leq$ 100  $\Omega$ -m.

I have interpreted the relationship between intermediate ( $\sim$ 1500  $\Omega$ -m) resistivity and high seepage rates based upon Archie's law. Bulk resistivity is, according to Archie's law, dependent upon porosity, pore fluid conductivity, saturation, and mineralogic and cementing characteristics inherent to a given lithology (Equation 3.1). Saturation was constant in the case of our study because sub-bottom sediment represents a fully-saturated environment. We also expected pore fluid conductivity to remain constant because in all but a few cases all seepage was out-seepage, so pore fluid would have had the same conductivity as lake water. The source of variation in resistivity was therefore either a change in porosity, mineralogy, or cementing factors. Major shifts in mineralogy or a change in clay content, reflected in variables a, m, and n, are necessary to cause significant changes in resistivity. Clay content at Mirror Lake is uniformly low, and mineralogy relatively consistent (Harte, 1997). Variation in porosity is, by process of elimination, a likely source of the variations in resistivity observed along the southwest shore of Mirror Lake.

The results of textbox analysis of sediment resistivity are consistent with this interpretation; textbox values of the resistivity of siliceous sediment were 300-1000  $\Omega$ -m. These values were lower than the field values of 1500-3000  $\Omega$ -m. Testbox values for the resistivity of organic-rich sediment

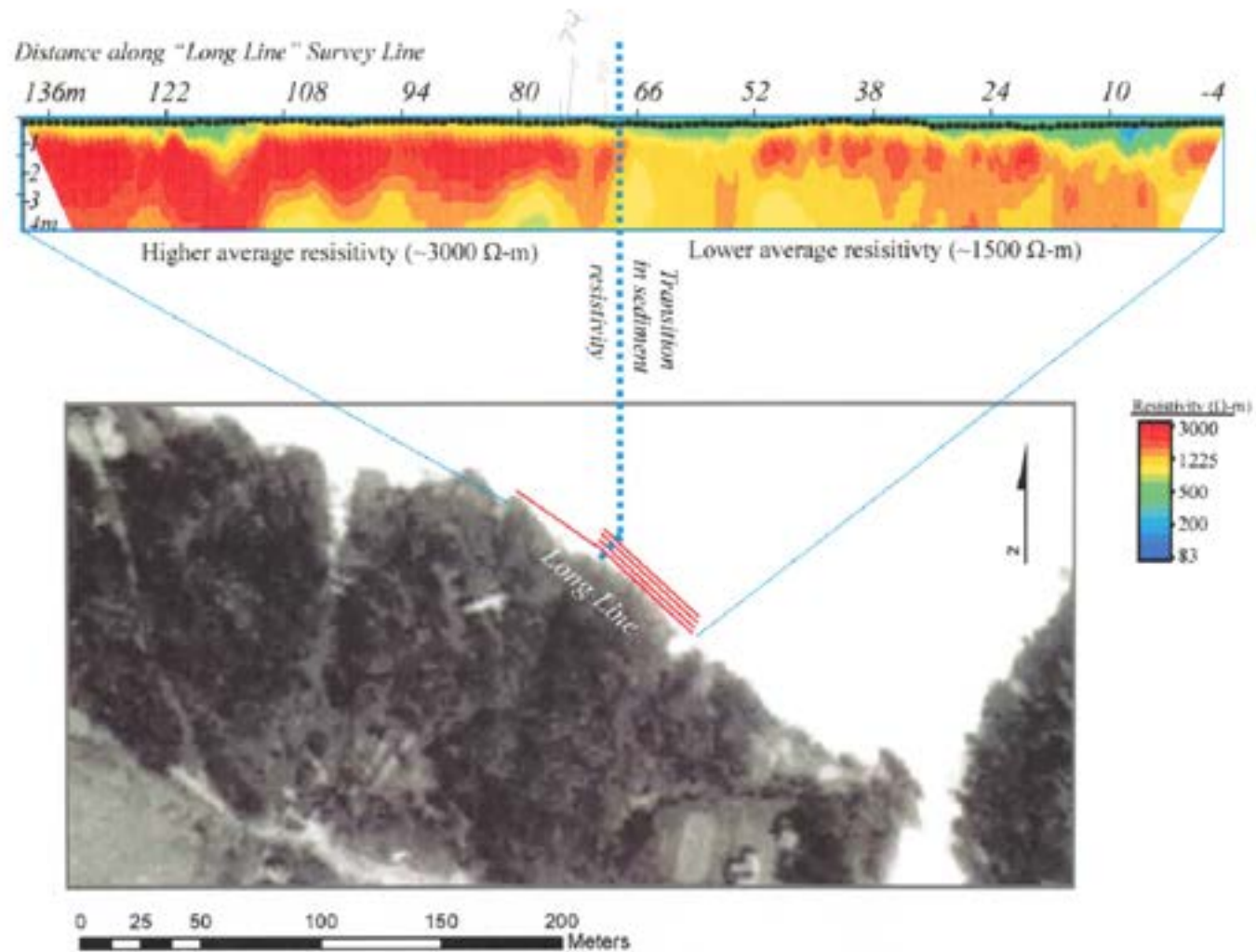


**Figure 4-5A: Long Line Resistivity Survey.** Average sediment resistivity was 3000 Ω-m within the northern end of the southwest shore "Long Line" survey line, while it was 1500 Ω-m in the southern end. The transition from intermediate to higher average resistivity occurred at approximately meter 70 of the Long Line survey line.

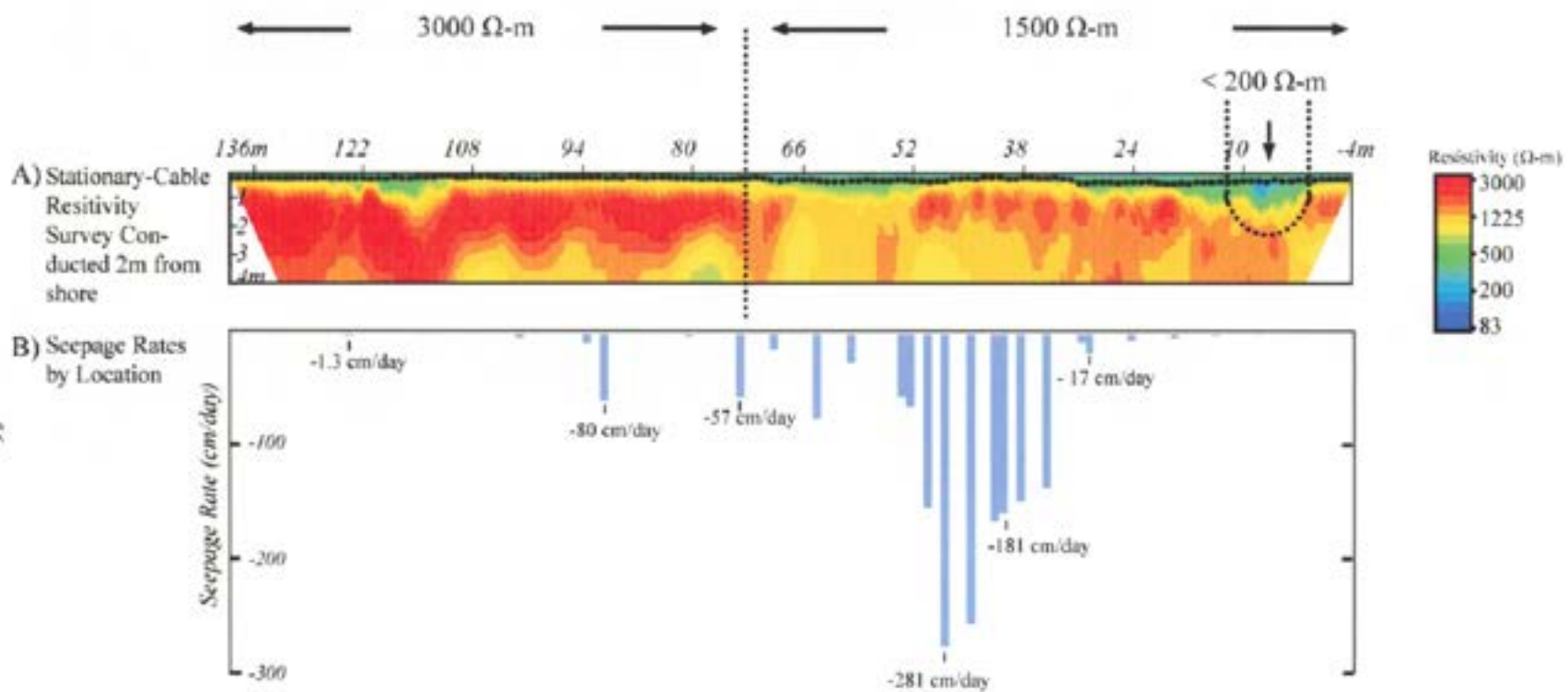


**Figure 4-5B: Relationship Between Average Resistivity and Seepage Rates Along Southwest Shore of Mirro Lake.** Where average resistivity values were ~ 1500 Ω-m, seepage rates were highest. Where average resistivity values were ~3000 Ω-m and < 100 Ω-m, seepage rates were lowest.

resistivity were 150 - 300  $\Omega$ -m, where field values were < 200  $\Omega$ -m. I believe this discrepancy arises because the sediment samples were disturbed during the process of transferring samples from collection tubes to the testbox: this disturbance almost certainly increased porosity and affected the resistivity values. In the case of siliceous sediment, increased porosity led to lower resistivity. In the case of organic-rich sediment, an increase in porosity increased bulk resistivity because there was a lower concentration of high-conductivity material.

To test the hypothesis that changes in porosity were responsible variations in resistivity along the southwest shore of Mirror Lake, I used Archie's Law to model the effects of a change in porosity on resistivity values. Because sediment is unconsolidated at Mirror Lake and because the lake water was resistive (330  $\Omega$ -m), only the lowest published (Reynolds, 1997) values of variables  $a$  and  $m$  (0.5 and 1.3 respectively) yielded resistivity values consistent with those observed at Mirror Lake and within a reasonable range of sediment porosity values (12-40%) (Harte, 1997); higher values of  $a$  and  $m$  yielded resistivity values higher than any observed at Mirror Lake. Holding those variables constant at the lowest published values, models showed that an approximately 12% change in porosity can cause a 1500  $\Omega$ -m change in resistivity (Figure 4-6).

It is reasonable to assume that porosity varies along the southwest shore because that shore likely contains an outwash lens from the receding glacier which formed Mirror Lake (Section 2.2). While sediment underlying most of a glacially derived lake tends to be poorly sorted, sediment within its outwash lens is sorted by stream action. Degree of sorting within these systems will vary depending upon the position of channels, with discrete zones of more poorly-sorted material and also discrete zones of more well-sorted material (Ritter et al., 1995). Because porosity is affected by degree of sorting, porosity will vary with sorting within outwash fields. In a clay-poor environment such as Mirror Lake, variations in porosity are related to variations in hydraulic conductivity. The results of previous core, hydrologic and modeling studies at Mirror Lake provide evidence of variable sorting along the southwest shore of Mirror Lake, and associated variations in hydraulic conductivity. In particular, there is evidence for a deposit of well-sorted sand and gravel along the southwest shore (Figure 2-2). Archie's law suggests that such a deposit would have a lower bulk resistivity than more poorly sorted sediment

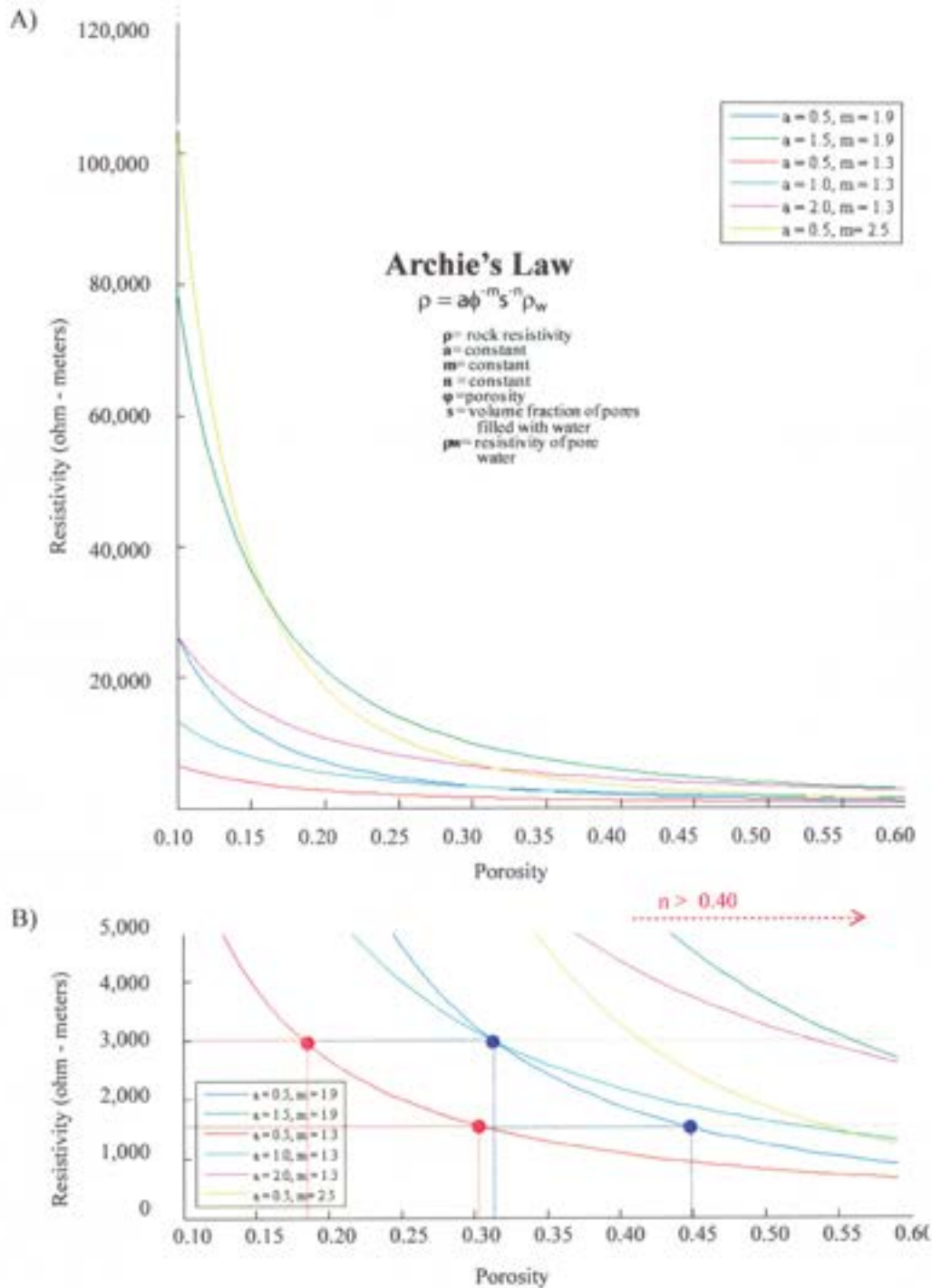


**Figure 4-6: Model of Effect of Variations in Porosity on Resistivity, with Different Values of a and m.** (A) shows the impact on bulk resistivity of variations in porosity under a variety of conditions for a and m. (B) shows the impact of those variations within the range of resistivities observed at Mirror Lake. The red and blue lines represent the most reasonable approximations to porosity and resistivity values observed at Mirror Lake (Harte, 1997); both show that a 12% change in porosity leads to a 1500  $\Omega$ -m change in resistivity.

because it has a higher porosity. The bounds of the southwest shore sand and gravel deposit coincide approximately with the transition from intermediate (1500  $\Omega$ -m) to higher (3000  $\Omega$ -m) average resistivity within our Long Line survey area (Figure 4-7). There are, therefore, multiple lines of evidence to suggest that the transition from intermediate (1500  $\Omega$ -m) to higher (3000  $\Omega$ -m) average resistivity within the Long Line survey area reflects variations in sorting, porosity and hydraulic conductivity.

Where there is an exception to the pattern of low seepage rates coincident with high (3000  $\Omega$ -m) resistivity, (i.e., at meter 90 of our Long Line, where a -62 cm/day seepage rate was measured within a region where average sediment resistivity is 3000  $\Omega$ -m) I believe it is likely that a zone of lower resistivity is present but that it was small or slightly offset from the resistivity line and could not be resolved with the equipment used in this study. The fact that a considerably lower seepage rate (-8 cm/day) was observed at meter 92 of the Long Line, just 2 m from the higher rate, is consistent with the interpretation of small-scale geologic heterogeneity. Further study with a resistivity survey with a smaller electrode spacing, sensitive to features on the sub-meter scale, would provide more information.

#### 4.3.2 Low (200 $\Omega$ -m) Resistivity and Low Seepage Rates

Zones where resistivity was less than or equal to 200  $\Omega$ -m coincided with deposits of organic-rich matter at least 0.5 m thick. Organic matter was readily distinguishable from siliceous deposits in the field by color (organics were dark brown-black, siliceous sediment was grey and tan), texture (organics were fine and smooth where siliceous sediment was gritty) and smell (organic deposits had a distinct sulfurous odor where siliceous sediment was odorless). The low resistivity (<200  $\Omega$ -m) of organic material was confirmed in the lab with the resistivity test box; where organic matter content was high, as judged from color, texture, and odor, resistivity was approximately 150-300  $\Omega$ -m; where organic matter content was lower, resistivity was approximately 300-1000  $\Omega$ -m. Organic content was confirmed in the lab via drying and sieving the sediment; pieces of sticks, bark, and leaves were observed in the sieved, dried samples along with siliceous sediment. Permeameter tests of the hydraulic conductivity of

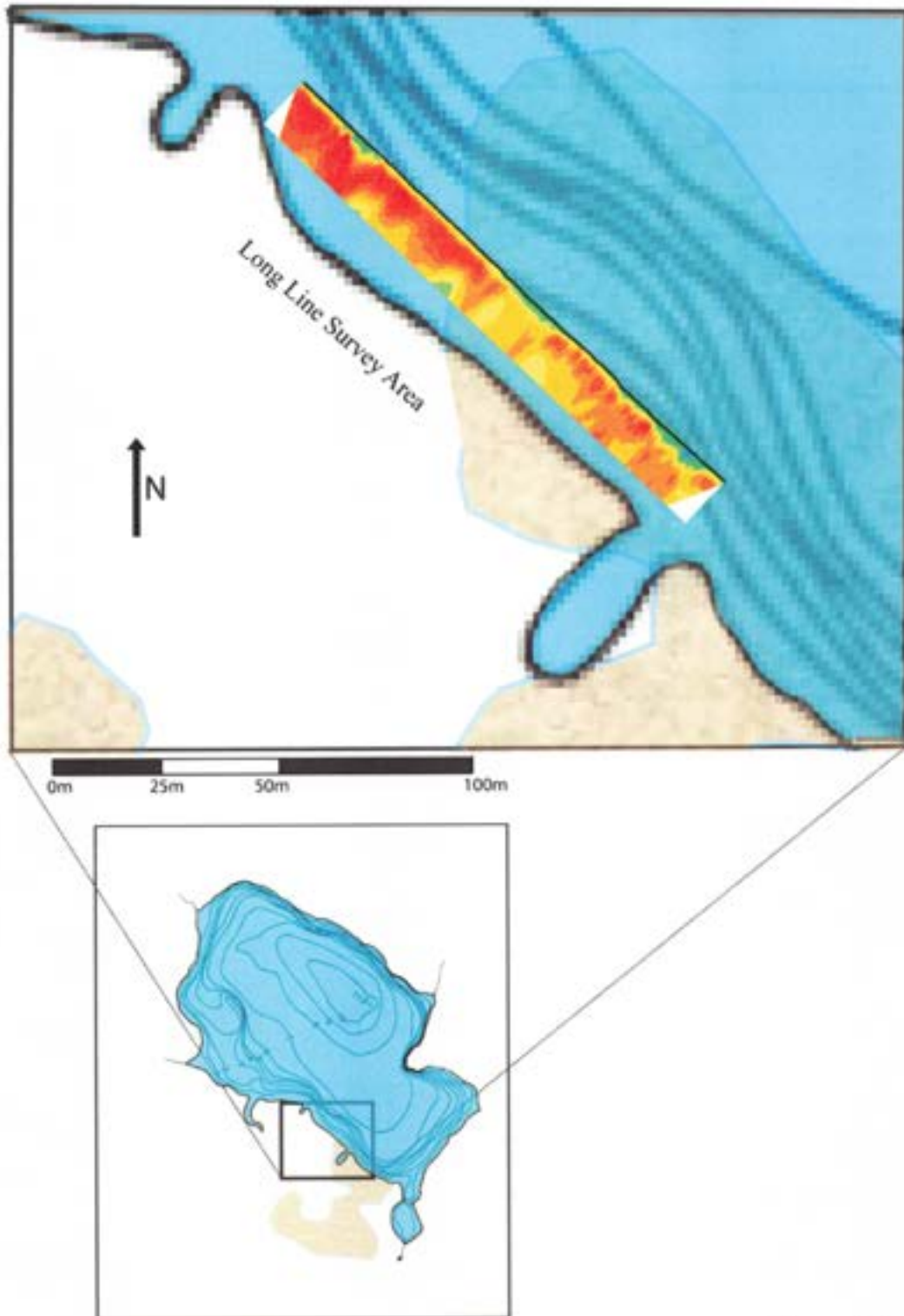


**Figure 4-7: Coincidence of Resistivity Results with Sand and Gravel Deposit.** The transition in average sediment resistivity observed along the southwest shore of Mirror Lake coincides approximately with the bounds of a sand and gravel deposit there. *Extent of sand and gravel deposit from Scheutz, 2002.*

this sediment suggested K was lower than that of organic poor sediment: K values of  $3 \times 10^{-3}$  and  $5 \times 10^{-4}$  cm/sec were measured in organic-rich sediment, whereas K in more organic-poor samples was greater than  $5 \times 10^{-3}$  cm/sec, with an average of  $1 \times 10^{-2}$  cm/sec (Dr. Laura Toran, personal communication, 6/15/08). The low seepage rates observed where resistivity surveys indicate sediment resistivity values of  $\leq 200 \Omega\text{-m}$  are attributed to the low hydraulic conductivity of organic-rich sediment.

#### 4.4 Eastern Shore Seepage and Resistivity

The results of parallel-to-shore resistivity surveys, conducted approximately 2 m from shore along the steep eastern shore of Mirror Lake, were presented in Figure 4-2J and K. Those sites were chosen to test the hypothesis that geologic heterogeneities observed with the towed-cable survey would relate to seepage rates. The results of the 22-m towed-cable resistivity survey indicated average sediment resistivity transitioned from approximately 1000  $\Omega\text{-m}$  to approximately 2500  $\Omega\text{-m}$  within the span of approximately 30 m along the northeastern shore. Stationary-cable surveys conducted over that terrain confirmed a transition in sediment resistivity, though with slightly higher values than indicated by the towed-cable surveys; average sediment resistivity, as assessed with the stationary-cable surveys, was 1500 -2000  $\Omega\text{-m}$  in the more northern of those surveys and approximately 3000  $\Omega\text{-m}$  in the more southern. A layer of organic-rich material, which varied in thickness from approximately 0.10-0.5 m thick, was also indicated in the stationary-cable surveys, and was confirmed through examination of hand-samples of sediment there. Seepage rates were measured coincident with those resistivity surveys, at distances of approximately 2 and 6 m from shore and approximately in line with the perpendicular-to-shore resistivity surveys there (shown in Figure 4-1A)\*. Seepage rates at both locations were slightly positive (<0.06 cm/day) but below detection limits. These low seepage rates were likely influenced by the presence of the organic matter deposits. That is, though a geologic heterogeneity was identified with the towed-cable survey which might have related to seepage (i.e., a transition from intermediate to

---

\* Tree cover along the Eastern Shore prevented the collection of firm coordinate data for both seepage and resistivity measurements made there. Map locations of all data are therefore approximate.

higher average resistivity), finer-scale features observed with the follow-up, stationary-cable surveys (i.e., organic matter) were likely a more powerful control on seepage.

#### 4.5 Northeast Inlet: Resistivity and Road Salt Contamination

Towed-cable resistivity surveys indicated a zone of low ( $\leq 200 \Omega\text{-m}$ ) resistivity in the Northeast Inlet area (Figure 4-8A). This zone extended to a depth of approximately 4 m in sediment. We followed up with stationary-cable resistivity surveys there, which also imaged a zone of  $\leq 200 \Omega\text{-m}$  resistivity extending from the surface of the lake-bottom to a maximum depth of 4 m (Figure 4-8B and C). In other regions of the lake, zones of low resistivity were related to deposits of organic matter. Sediment samples from the northeast inlet region indicated that there were significant organic matter deposits there. The deposits of organic matter, however, ranged in thickness from approximately 0.1 to 0.5 m. The zone of low ( $\leq 200 \Omega\text{-m}$ ) resistivity in the northeast inlet area extends to a depth of approximately 3-4 meters, more than 2 meters past the organic matter deposits into the siliceous drift.

I hypothesize that the source of this zone of very low resistivity within the siliceous sediment of the northeast inlet area is a decrease in pore-fluid resistivity caused by the presence of road salt. Since the construction of a Highway 93 along the eastern edge of Mirror Lake in the 1970s, sodium and chloride concentrations in the lake have risen steadily (Rosenberry et al., 1999). Research on the delivery mechanism of this road salt contamination suggests that both groundwater and surface water transport sodium chloride to the lake. Rosenberry et al. (1999) estimate that, on average, 2.2% of total chloride contamination is delivered to Mirror Lake by groundwater, and 49% via the Northeast Inlet stream. A pore water sample from the shallow ( $\approx 40$  cm) subsurface revealed chloride content three times the level observed in the lake (9 mg/L  $\text{Cl}^-$  in northeast-inlet area pore water versus 2.5 mg/L  $\text{Cl}^-$  in the lake). We also found that the resistivity of this pore water was 3.3 times lower than the background level (approximately 200  $\Omega\text{-m}$  rather than 330  $\Omega\text{-m}$ ).

To test whether the presence of chloride could cause the very low resistivity observed beneath the organic matter deposits of the northeast inlet area, I used Archie's law to model the impact of an increase in pore fluid conductivity on bulk resistivity. The results of these calculations show that a 3.3x

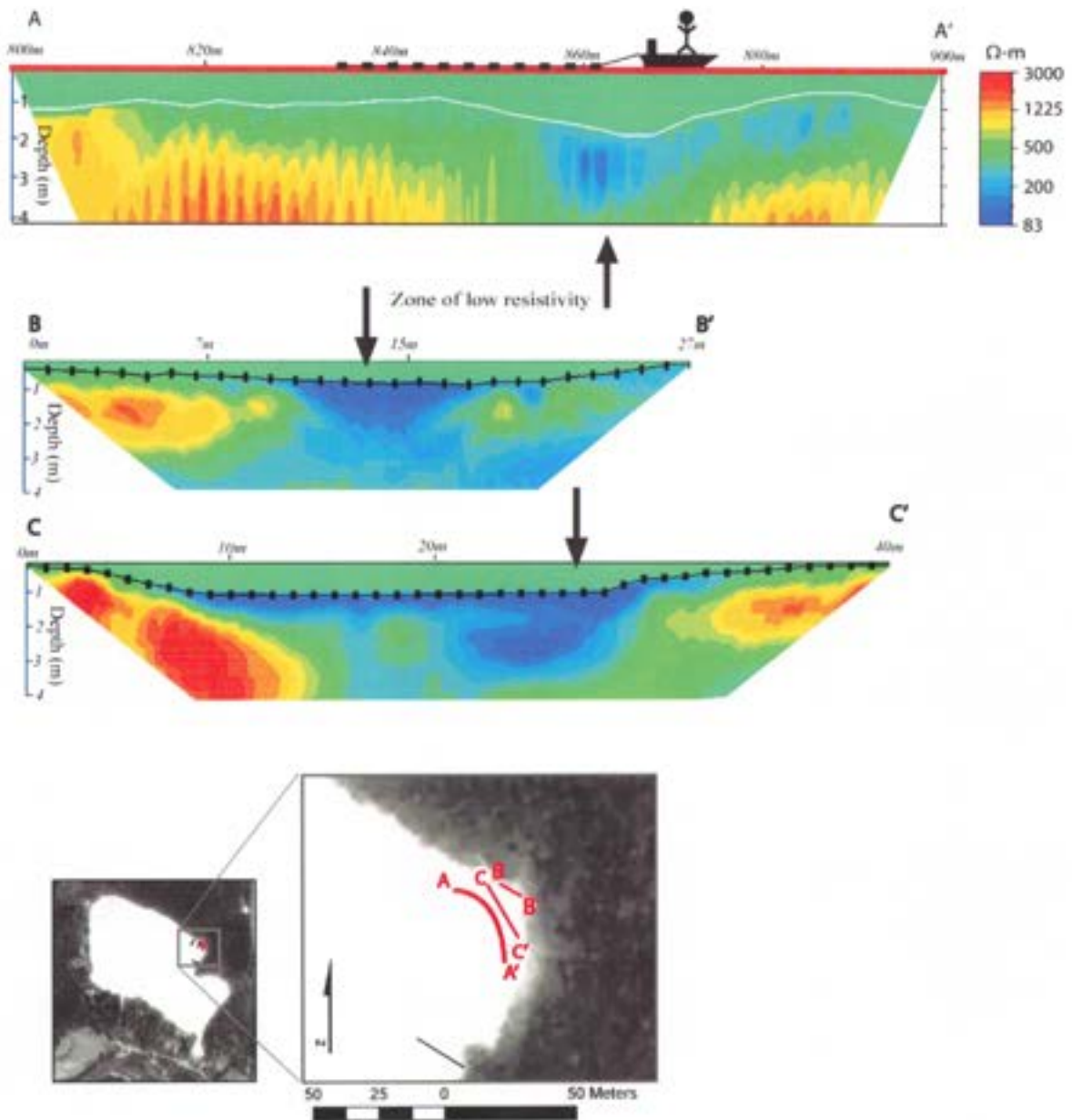


**Figure 4-8: Zones of Low Resistivity Below 2 m depth in Northeast Inlet Area.** Towed (A) - and stationary (B and C) - cable surveys both revealed zones of low resistivity at greater than 2 m depth in the northeast inlet area of Mirror Lake. We have attributed these zones of low resistivity to chloride contamination of pore water. Tree cover along the Eastern Shore prevented the collection of firm coordinate data for both seepage and resistivity measurements made there. Map locations of all data are therefore approximate.

increase in pore fluid conductivity ( $\rho_w$ ) will lead to a 3.3x decrease in resistivity. The range of resistivity we measured for the drift which underlies Mirror Lake was approximately 1500 to 3000  $\Omega$ -m. A 3.3x decrease in pore-fluid conductivity would lower that range to 450 - 900  $\Omega$ -m. Our resistivity surveys of the northeast inlet indicated minimum resistivities of less than 100  $\Omega$ -m at 3-4 m depth. This suggests that chloride concentrations were likely even greater at depths of 3-4 meters within sediment than that measured at 0.4 m. Such a conclusion is also suggested by the nature of resistivity data inversion, which tends to smooth transitions between adjacent survey areas, and to thereby underestimate resistivity contrasts. It is therefore likely that the hypothesized zone of chloride contamination is even more conductive than is indicated by the inversion image.

These results collectively suggest that resistivity surveys were able to confirm the presence of road salt contamination and to partially map its extent. The results suggested highly localized, concentrated deposits of chloride within the northeast inlet area, consistent with a contaminant plume. It is likely, in fact, given that resistivity surveys underestimate and smooth resistivity contrasts in adjacent regions, that the zone of chloride contamination is both smaller and more concentrated than is indicated by the zone of low resistivity observed in the profiles from the contaminated region. It is not possible to tell from the resistivity surveys alone whether road salt is delivered to northeast inlet via groundwater or surface water. Given, however, that previous research has measured chloride contamination in groundwater wells between the northeast inlet area of Mirror Lake and the highway which is the source of the chloride, and hydraulic gradient measurements suggest groundwater discharges to Mirror Lake within the Northeast inlet area (Rosenberry, 1999), it is likely that seepage of contaminated groundwater to the northeast inlet area contributes to the chloride concentrations in the lake.

#### 4.6 Ground Penetrating Radar Surveys

We conducted a total of 54 radar surveys at Mirror Lake: 34 perpendicular-to-shore at 50-m intervals along the lake's perimeter, 19 perpendicular-to-shore surveys at approximately 10 m intervals along the southwest shore, 1 parallel-to-shore survey about the entire perimeter of the lake and 1 parallel-to-shore survey within the Long Line survey area of the Southwest Shore (shown in Figure 3-12). Representative samples of the perpendicular-to-shore surveys are presented in Figures 4-9A-D.

Resolution in the parallel-to-shore surveys was poor because the shallow water in which we conducted them caused significant reverberation of the radar signal (highlighted in Figure 4-9A); the results of those surveys are omitted from the body of this thesis.

Several features appeared consistently in the radargrams we collected at Mirror Lake: diffraction hyperbolae (produced by objects such as cobbles and boulders which scatter electromagnetic energy), bedding planes, and the organic sediment (“gyttja”) which covers the bottom of Mirror Lake. The distance scale along the top of each radargram represents distance from shoreline. The depth (in meters) on the right y axis represents the inferred depth of features that reflected a radar pulse. The wavy lines within the water column are noise amplified by the application of automatic gain control to raw data. Upside-down U-shaped features with very straight edges are interpreted as diffraction hyperbolae and are highlighted in red (Figure 4-9A’). Roughly linear features which extend for at least several meters and that are not parts of diffraction hyperbolae are interpreted as bedding planes. Bedding planes are highlighted in yellow and in green (Figure 4-9A’). Where bedding planes existed within the smooth, flat sediment of the lake bottom they were interpreted as bedding within gyttja (yellow). Where bedding was observed within sediment at the side of the lake it was interpreted as stratification of sediment (green).

Stratification within the sediment at the sides of the lake was observed in only 3 radargrams at Mirror Lake: radargrams B and C (the map locations of which are shown in Figure 3-12), radargrams for which are shown in Figure 4-9B and C) and the line in between them. That stratification was observed at distances of approximately 15 to 45 m from shore at depths of 2-3 m in sediment. It corresponded with water depths of approximately 2-7 m. All other radargrams from Mirror Lake showed bedding only within the organic sediment (gyttja) which covers the bottom of the lake (e.g., as shown in Figure 4-9D).

Depth of penetration into the stratified bedding shown in radargrams B and C was greater than into glacial till elsewhere around the lake (e.g., that shown in D): it was approximately 2-4 m into sediment rather than 1-2 m. The glacial sediment elsewhere around the lake strongly scattered the electromagnetic signal, and showed few coherent reflectors; diffraction hyperbolae were ubiquitous.

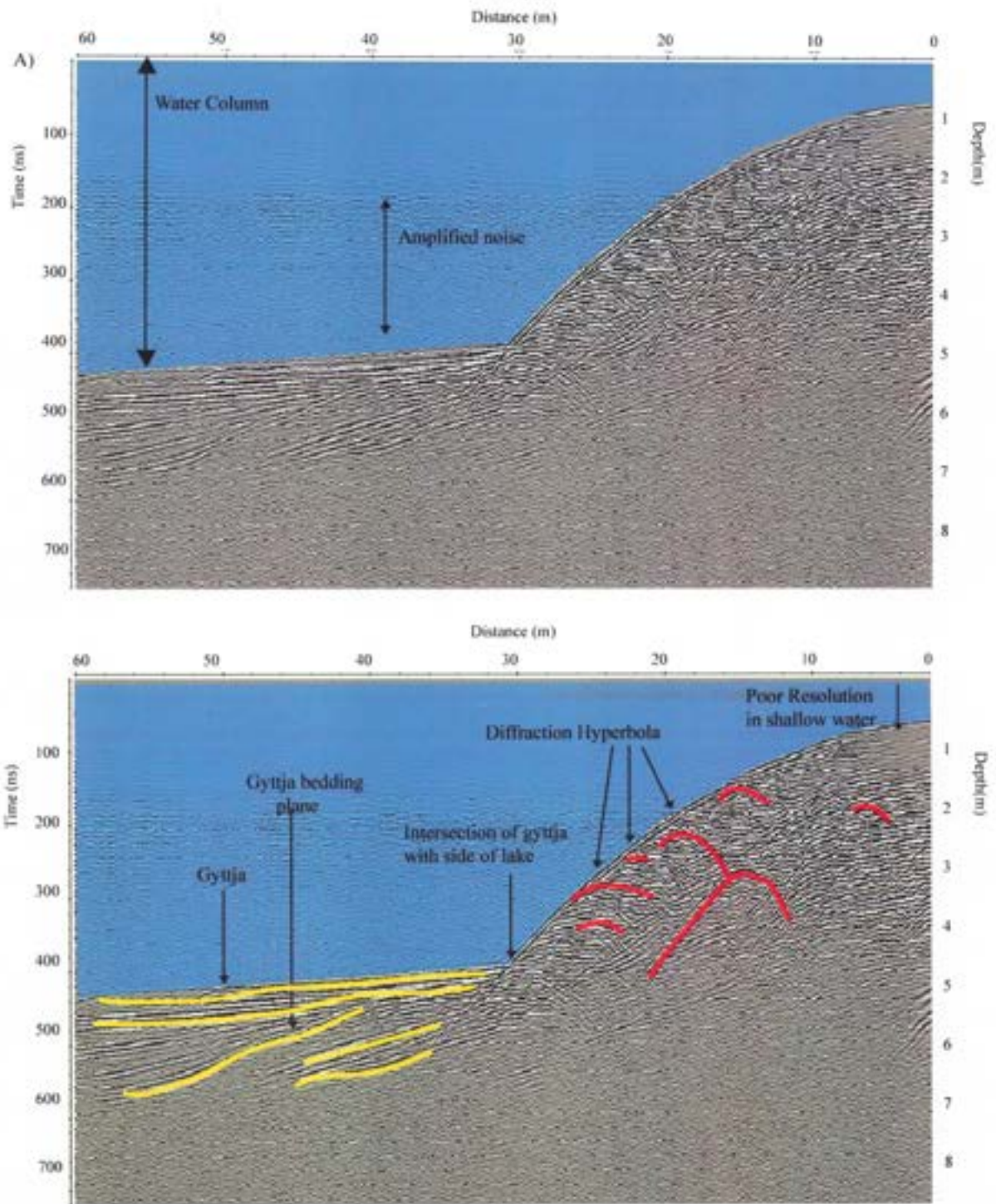


**Figure 4-9A. Overview of Features Observed in Radargrams.** The upper and lower images are the same radargram. The upper image highlights the water column and explains the presence of wavy lines within the water column. The Lower image highlights the gyttja, gyttja bedding planes, intersection of the gyttja and till, diffraction hyperbolae, and the poor resolution in shallow water. The map location of this surveys is shown as A in Figure 3-12.

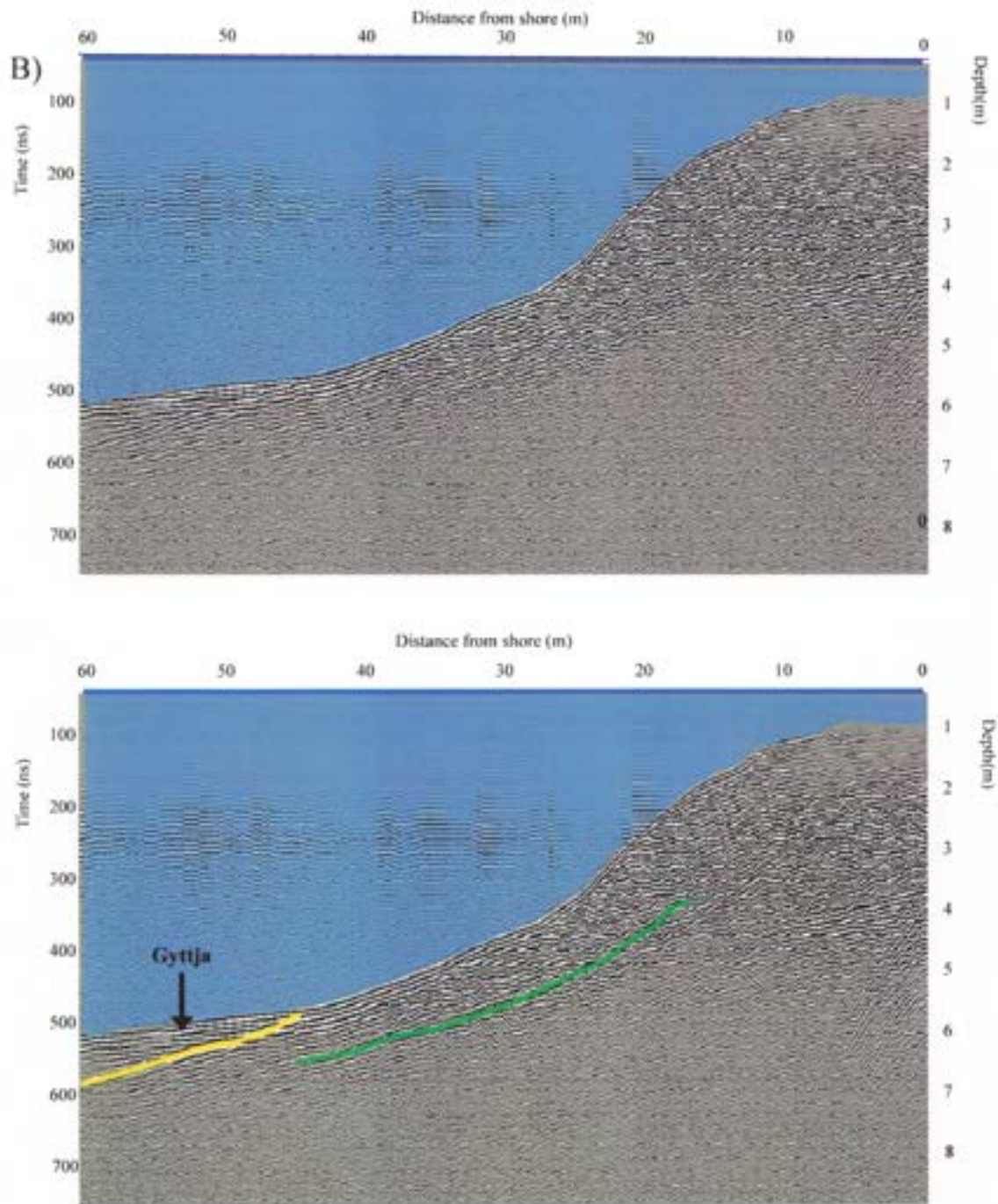


**Figure 4-9B. Radargram from Southwest Shore.** A continuous reflector exists within sediment at the sides of the lake and is highlighted in green. This reflector is interpreted as bedding within siliceous sediment. Bedding within gyttja is shown in yellow. The map location of this radargram is shown as B in Figure 3-12.

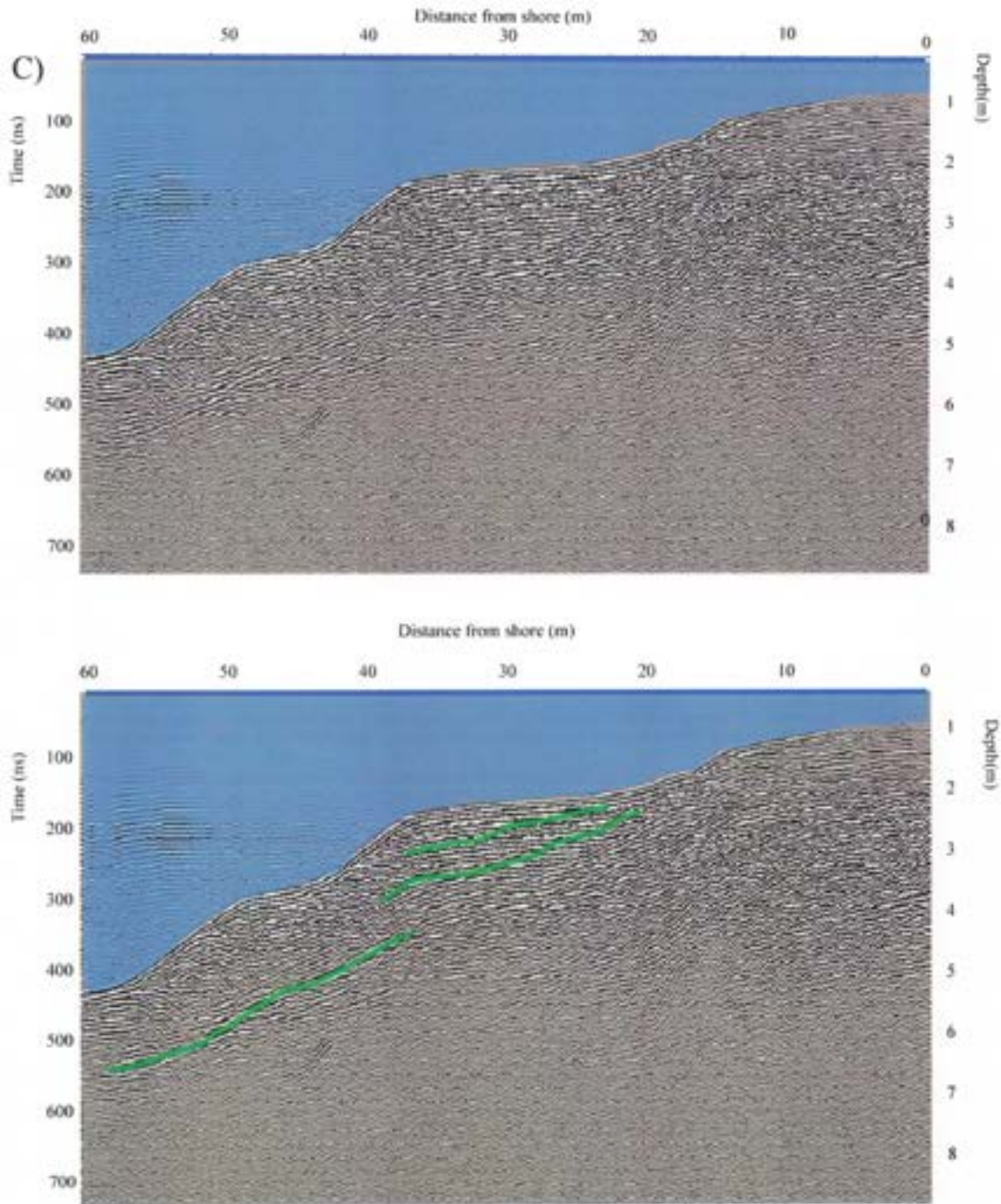


**Figure 4-9C. Radargram from Southwest Shore.** Several reflectors exist within sediment at the sides of the lake (highlighted in green). These reflectors are interpreted as bedding within siliceous sediment. The map location of this radargram is shown as C in Figure 3-12.

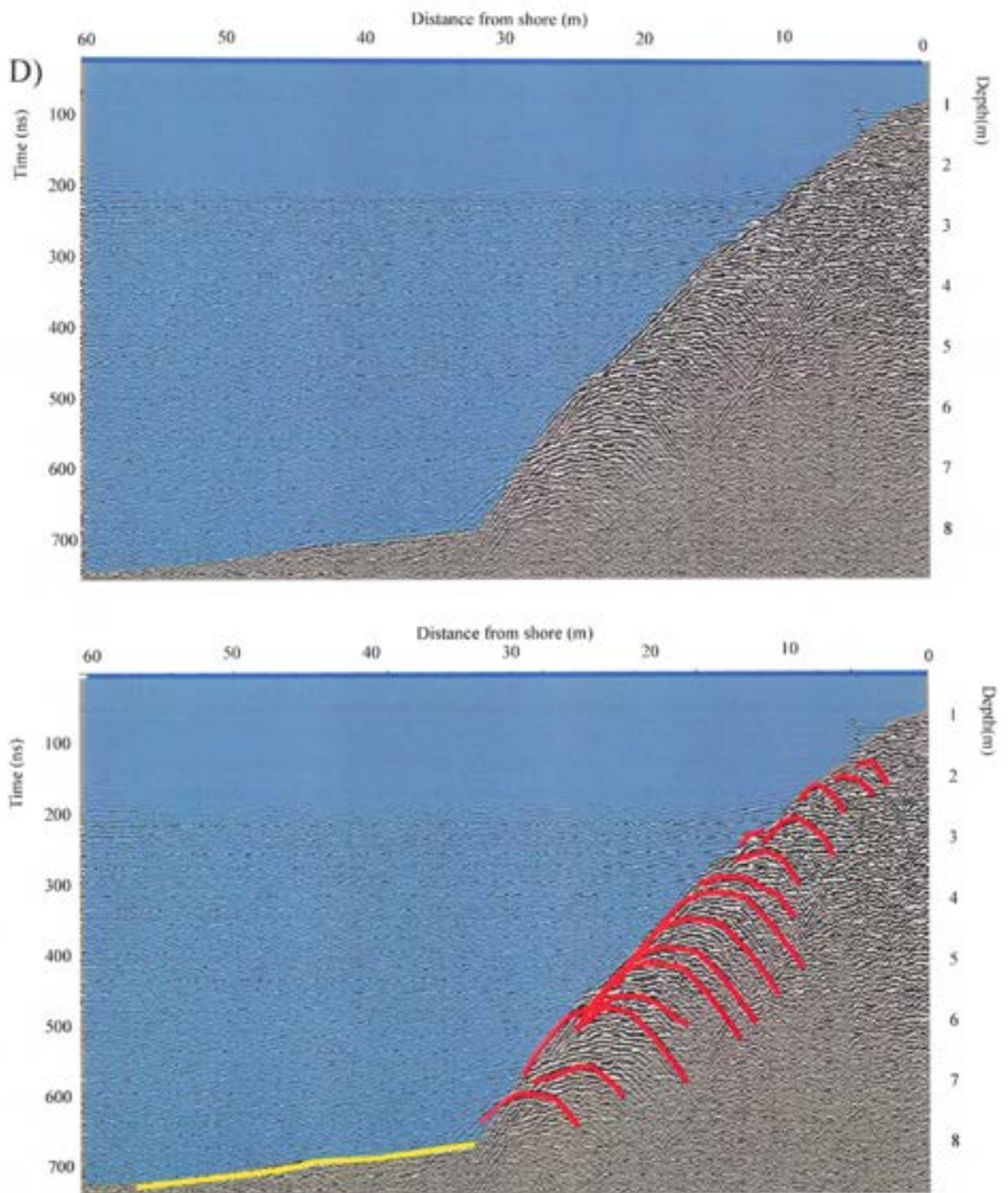


**Figure 4-9D. Radargram from Eastern Shore.** No bedding, except within gyttja (highlighted in yellow) is observed within this radargram.; diffraction hyperbolae (highlighted in red) are ubiquitous, and penetration is minimal. The map location of this radargram is shown in Figure 3-12D.

The fact that few coherent reflectors were observed within most sediment at Mirror Lake, along with the ubiquity of diffraction hyperbolae in all radargrams confirmed the results of earlier research that the glacial sediment under Mirror Lake is boulder and cobble rich (Likens, 1984). The stratification observed in radargrams B and C, was, however, unexpected. Those radargrams were conducted over terrain near the mouth of a canal dug to Mirror Lake during the 19<sup>th</sup> century (Likens, 1984). It is possible that the stratification observed in them reflects deposition of sediment from recent, anthropogenic activity.

The contact between the smooth, flat gyttja blanket and the diffractor-rich till was readily identifiable in all radargrams (highlighted in Figure 4-9A). I created a map of the boundaries of the gyttja by locating the interface between the gyttja and the sides of the lake on each of the perpendicular-to-shore radargrams, measuring the distance of that interface from shore, and then plotting a point to represent the location of that interface on a pre-existing map of Mirror Lake (Figure 4-10). I then drew a line to connect all the points, thereby estimating the bounds of the gyttja layer. The map I constructed coincided approximately with the map created by an earlier research group (Moeller, 1975), though there were some discrepancies (Figure 4-11). Discrepancies are likely the result of both geologic ambiguity and because the earlier gyttja map was created without GPS data. In cases where the earlier map shows gyttja blanket approaching the shoreline more closely than the map created in this project, it is likely that thin deposits of organic material on the sides of the lake led the divers who created the first map to conclude those deposits were gyttja when in fact they were simply thin organic “skins” or isolated deposits. Similarly, gyttja mapped by radar closer to the shore may be covered by thin sediment deposits. The sharpness of the contact of the edge of the gyttja blanket with the sides of the lake as illustrated in the radar surveys eliminated such ambiguity. Registration of our GPS data against the results of previous location data was another source of error. The bounds of the lake shown in the 1975 map of sedimentation there did not line up perfectly with the shape of the lake as it was indicated in 1992 and 2003 orthophotographs of it. I estimate that the error associated with matching our data to previous, non-GPS derived location data was up to 10 m. It is likely, therefore, that in registering the



**Figure 4-10: Extent of Gyttja Blanket as Inferred from Radargrams.** Brown dots represent the edge of the gyttja blanket, as inferred from radargrams. The brown polygon connects those dots and represents the extent of the gyttja. The inset cartoon on the lower left side of that diagram shows the seepage pattern at the interface of the gyttja with the sides of the lake, as inferred by Rosenberry et al. (1999).

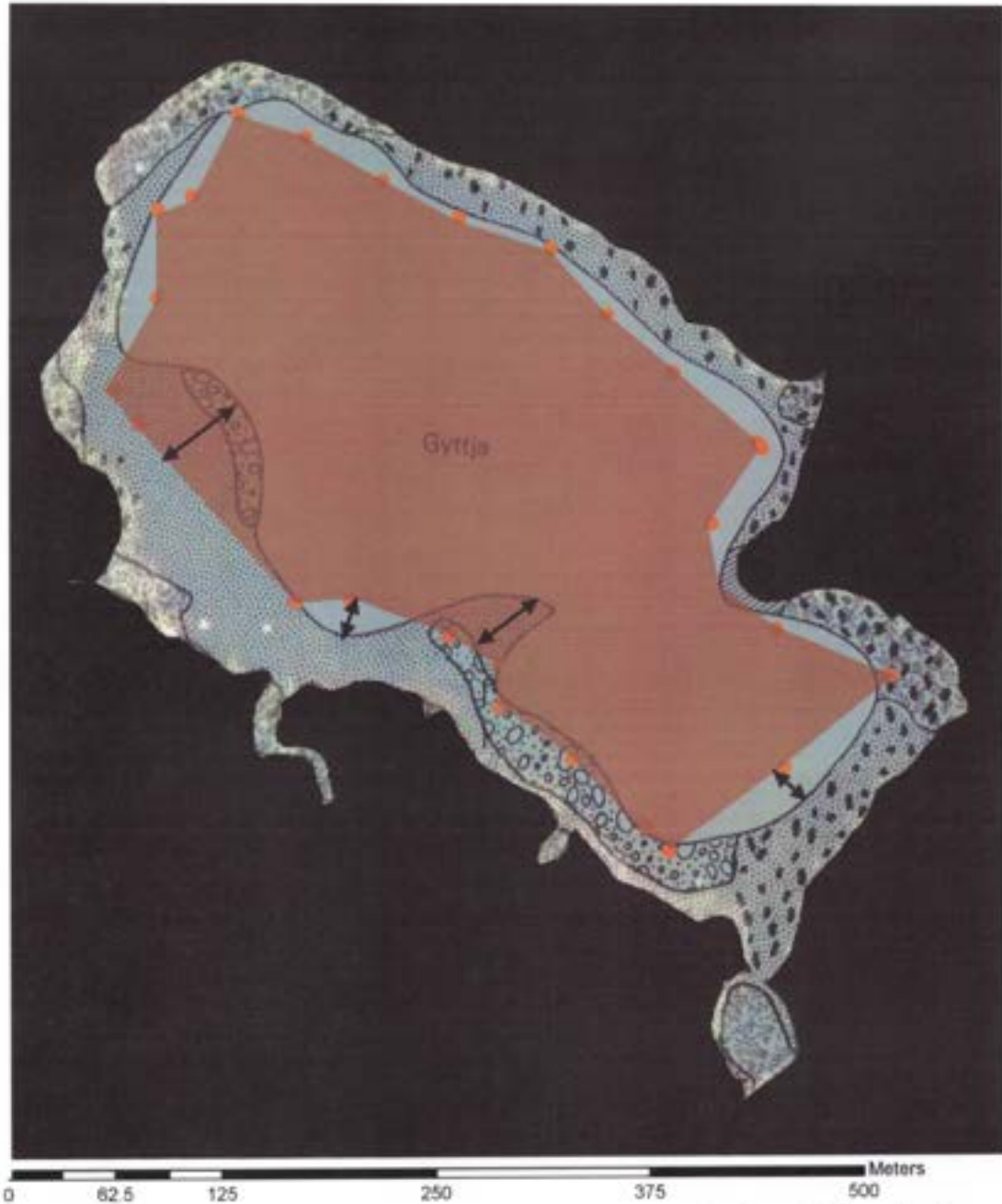


**Figure 4-11: Comparison of Old and New Map of Gyttja Blanket.** The bounds of the gyttja is indicated in the sketch-map of Mirror Lake by the gray space at the center of that sketch map. The brown polygon indicates the extent of the gyttja as we inferred it from radargrams we gathered at Mirror Lake. Black arrows indicate regions where the two maps disagree. *Sediment sketch map from Moeller, 1975.*

1975 map of the gyttja blanket against GPS data we collected there was misalignment which contributed to the apparent disagreement between the two maps.

The ability to map the location of gyttja has implications for seepage: while head measurements reveal an upward hydraulic gradient beneath much of the gyttja at Mirror Lake, seepage likely is at a minimum within zones of gyttja. Rosenberry and Winter (1993) believe that a pattern of out-seepage followed immediately by in-seepage may be characteristic of the edge of the gyttja (Figure 4-10inset). This conceptual model has not been tested thoroughly with seepage meter measurements, but the map provided through radar surveys would facilitate such testing.

## CHAPTER 5 CONCLUSIONS

### 5.1 Electrical Resistivity

Electrical resistivity surveys at Mirror Lake imaged subsurface heterogeneities. In some cases, as with deposits of organic matter, it was a relatively straightforward matter to link resistivity variations to geologic variations. In other cases, as where a zone of lower ( $1500 \Omega \cdot m$ ) average resistivity along the southwest shore of Mirror Lake did not correspond to any obvious surficial geologic heterogeneities, interpreting resistivity results was more difficult. There it was possible to use knowledge of Archie's law to facilitate interpretation: we were able to eliminate pore fluid conductivity and saturation as variables, thereby pointing toward variations in porosity as a factor which influenced resistivity along that shore. Knowledge of the process by which resistivity data are inverted was also useful for interpreting results. In the case of the northeast inlet area, for instance, knowing that inversion smoothed transitions between adjacent features and also tended to underestimate resistivity contrasts allowed us to conclude that a zone of chloride contamination was probably both smaller and more intense than indicated by the resistivity surveys.

Features the size of or smaller than electrode spacing were unlikely to be imaged in resistivity surveys. Resolution was poorer for merged datasets, where overlap data did not always agree and a large number data points were therefore discarded. In the case of the southwest shore, for instance, where high seepage rates were observed in a region where resistivity surveys suggested little seepage would occur, we speculated that a heterogeneity existed which was too small to be resolved by the merged dataset from which that profile was created.

### 5.2 Electrical Resistivity Field Techniques

Towed- and stationary-cable electrical resistivity surveys had different strengths. The rapidity of the towed-cable technique made it ideal for generating a preliminary sketch of the subsurface environment. This first sketch could be used to guide placement of the more time-consuming stationary-cable surveys, as it was in the case of the northeast inlet area of Mirror Lake. The 22-m towed-cable was generally more useful than the 44-m cable; the small size of the lake (0.5 km maximum diameter) made

the 44-m cable particularly prone to snagging on peninsulas and to cross-cutting inlets. At a larger lake or one with longer stretches of straight shoreline, use of the longer towed-cable would be more feasible.

The stationary-cable surveys were useful because of their higher resolution (4-5 times that of the towed-cable surveys) and because they could be deployed over terrain not approachable with the towed-cable survey. In particular, stationary-cables could be used in the near-shore (< 3m depth) environment, where a majority of seepage occurs, and in coves and peninsulas, where use of the towed-cable was limited.

Parallel-to-shore stationary-cable resistivity surveys were useful for providing cross-sectional images of the near-shore environment. Variation with distance from shoreline could be observed in the series of 4 parallel-to-shore surveys at 2, 4, 6, and 8 m from shore we conducted along the southwest shore. Perpendicular-to-shore resistivity surveys were useful for imaging variations with distance from shoreline in more detail. The near-shore environment, however, was more difficult to image with perpendicular-to-shore surveys because measurement density is low at the ends of stationary-cable surveys. Steep terrain was difficult to image with both the parallel- and perpendicular-to-shore cables; because of side-swipe in the case of the parallel-to-shore surveys and because inversion software could not accommodate very steep terrain changes sometimes encountered with the perpendicular-to-shore cables. Further software development could eliminate the latter problem.

In many cases we wished to survey a distance greater than that permitted by a single stretch of the stationary-cable. In such cases we found a 50% overlap between survey lines was desirable. Precise duplication of electrode placement in these cases minimized error associated with merging datasets. Flagging of the survey area facilitated such placement.

### 5.3 Ground Penetrating Radar

GPR surveys at Mirror Lake provided information about the texture and layering of sediment beneath the lake. The smooth, layered appearance in radargrams of the organic sediment (“gyttja”) which blankets the bottom of the lake was unique; it allowed us to easily identify the boundaries of that blanket. Boulders and cobbles had characteristic diffraction hyperbolae and were also readily mapped

with GPR, though depth of penetration into heavily cobbled areas was only 1-2 meters maximum. The fact that GPR surveys imaged boulders mapped by previous research (Moeller, 1975) boosted our confidence in the accuracy of both.

Stratification within non-organic sediment was also identifiable in a few radargrams. It is not clear whether this stratification, observed clearly only along portions of the eastern shore, is related to outwash processes or to the construction of the canal. The fact that stratification was observed, however, made us confident that GPR could image it, even in the scatterer-rich environment of Mirror Lake. No such stratification was observed in radargrams from within the zone where previous research had indicated a transition from glacial till to comparatively well-sorted outwash. A small change in degree of sorting, however, would not create horizontal reflectors and would therefore not be visible with GPR.

#### 5.4 Ground Penetrating Radar Field Techniques

The folding, polyurethane boat we used in this survey was ideal for conducting GPR surveys of the lake: its nearly flat bottom allowed the GPR antennae unit to be placed directly on the floor of the boat, and allowed us to approach the shoreline very closely. It also allowed us to conduct surveys rapidly. Resolution was best in water depths greater than  $\frac{1}{4}$  the wavelength of the dominant frequency of our antenna (i.e., > 1.5 m). It was worst in water depths closest to that wavelength, and improved slightly in shallower water.

#### 5.5 Using Electrical Resistivity and Radar In Tandem

Electrical resistivity and Ground Penetrating Radar were complementary techniques. Heterogeneities were imaged in one technique that were not in the other; a property contrast within the Long Line survey area of the southwest shore was apparent in resistivity surveys but not in GPR surveys. Stratification within sediment, on the other hand, was apparent in GPR surveys along the eastern shore where no property contrast was evidenced by resistivity surveys.

#### 5.6 Position Data

The GPS spatial data we collected at Mirror Lake to tie resistivity, radar and seepage data to measurement locations were self-consistent. It was difficult, however, to align this data with that

collected by previous research groups: many of those measurements (e.g. seepage and core analysis) were made prior to the development of or without the use of GPS location.

The resolution of our own spatial data was also sometimes limited. Occasionally satellite distribution was such that our GPS unit could not gather enough signals to fix the coordinates of our location; this condition was perhaps worsened by the low mountains around the lake. Signal reception was poorest within approximately 10 m of shoreline: the presence of trees there often inhibited the collection of GPS data. In such cases we interpolated the missing data during processing, generally by extending a line from data points collected where signal strength was good towards where it was lost. It is likely that the ability to gather position data will improve in coming years as GPS technology continues to advance.

#### 5.7 Suggestions for Further Study

There are several features which we would be interested to investigate in future work at Mirror Lake. First, we would be interested to conduct resistivity surveys using smaller electrode spacings. Seepage rates varied on a finer scale than was imaged by the 1-m electrode spacing we used in this project. Modeling experiments suggest that variations in the upper 0.5 m of sediment exert the greatest control on seepage rates (Mikochik, 2008). An electrode-cable with 0.5 m spacing or smaller could potentially image the small-scale features which control seepage rates. Work with such a cable is planned for the summer of 2008, as part of the next phase of the project of which this thesis was a part.

A radar antenna which could effectively be used in the very near-shore (< 3m water depth) could potentially yield useful results since the near-shore environment tends to have the highest seepage rates. A waterproof, shielded GPR unit, with which the radar antennae could be coupled directly with the lake bottom, would serve this purpose well. A small raft, with which the antenna could be pulled in the shallowest water, might also serve the purpose; reverberation was worst in water depth approximately equal to dominant wavelength, and was slightly better in water shallower than that. It would be particularly interesting to gather a parallel-to-shore GPR survey; bedding features not apparent in perpendicular-to-shore surveys might be obvious in parallel-to-shore surveys.

Finally, it would be useful if GIS data for Mirror Lake were compiled and posted to a central location. There exists vast quantity of data about the region, collected by diverse research groups and across many disciplines. A central database would facilitate comparison of data from these different studies.

#### 5.8 Implications for understanding groundwater-lake interaction

Our work at Mirror Lake highlighted the versatility of correlating electrical resistivity surveying to seepage. Variations in resistivity along the southwest shore of Mirror Lake probably resulted from changes in porosity, which at that site appear to relate to the hydraulic conductivity of sediment. Variations in resistivity within the northeast inlet were the product of changes in pore-fluid conductivity and were probably indicative of road salt contamination. Both have implications for characterizing underwater seepage: the former in terms of its ability to suggest the geologic variations which control seepage, the latter in terms of evidence of flow paths within a lake. Radar was able to image location of the gyttja boundary, which previous work has shown to be related to seepage rates. Radar also showed stratification within sediment, which might in some cases have implications for seepage, though not in this case. Radar surveys can highlight features which resistivity cannot, and vice versa. Together or separately these techniques can highlight geologic heterogeneities and guide point measurement of seepage.

Our work at Mirror Lake confirms the efficacy of electrical resistivity as a tool which can image geologic heterogeneity which controls seepage and can guide point measurement of seepage. The controls on electrical resistivity and seepage rates were different at Mirror Lake than they were at Lake Michigan where the first work relating resistivity profiles to seepage rates was conducted (Taylor and Cherkauer, 1984): clay content in sediment at Lake Michigan was high and represented a dominant control on resistivity and also on seepage rates. Clay content at Mirror Lake was low; organic matter content, road salt contamination and porosity represented primary controls on resistivity. The first and third of these (organic matter and porosity) likely represented major controls on seepage at Mirror Lake. The substantial technological advances which have evolved in the time which has passed since Taylor and Cherkauer (1984) conducted their pioneering study have made the electrical resistivity survey

technique more powerful and more versatile. We hope that further study at Mirror Lake, scheduled for the summer of 2008, will deepen our understanding of the geophysical signatures of seepage.

## REFERENCES

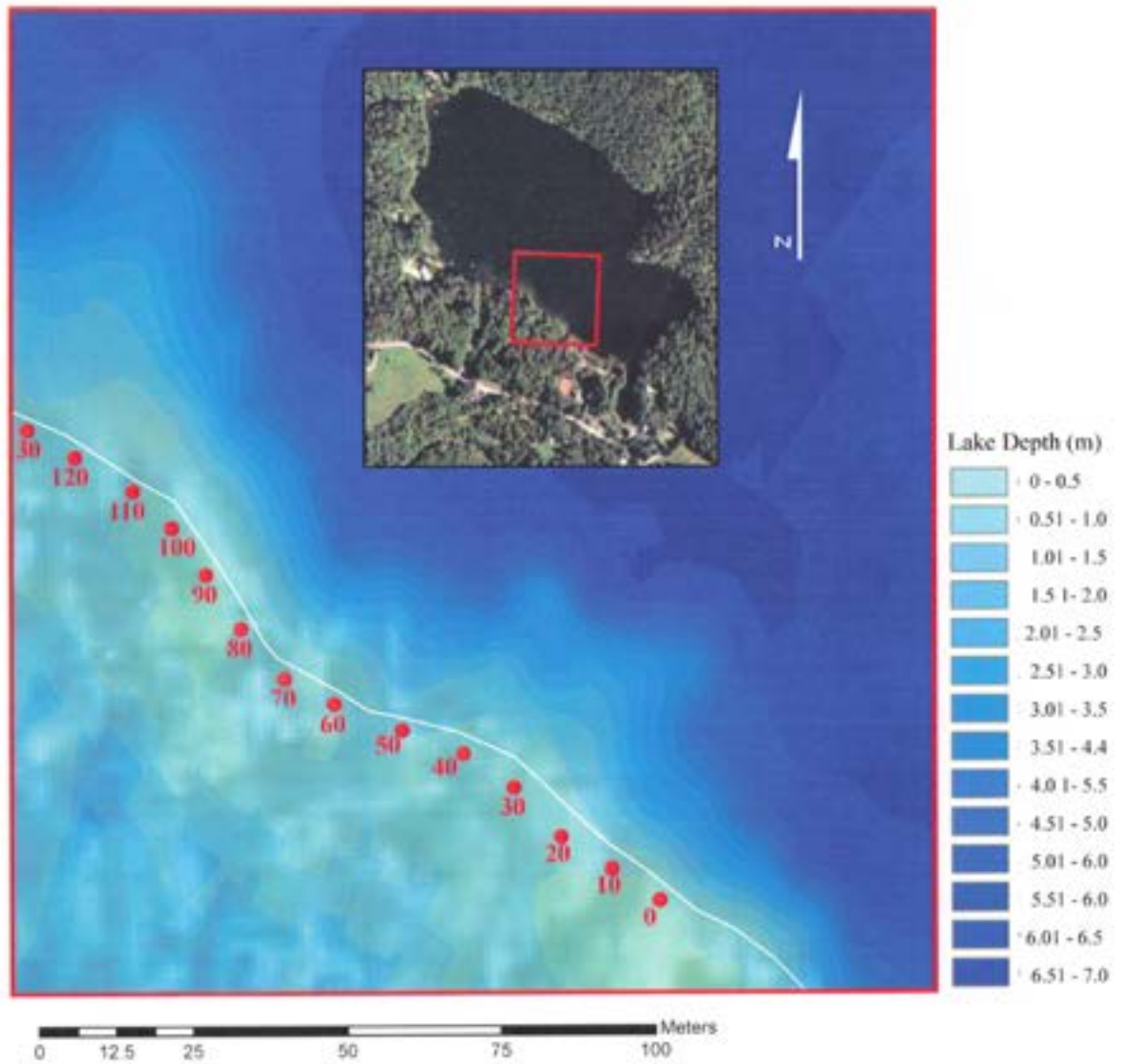
- Advanced Geosciences Incorporated company website. SuperSting R8 Marine Logging System Instrument Manual.  
[www.agiusa.com/files/eicust/earthimageruser.shtml#EI2D](http://www.agiusa.com/files/eicust/earthimageruser.shtml#EI2D). PDF accessed 10/07.
- Asbury, C. E., 1990. The role of groundwater seepage in sediment chemistry and nutrient budgets in Mirror Lake, New Hampshire. PhD dissertation, Cornell University, Ithaca, NY, 1 - 275.
- Archie, G., 1942. The electrical resistivity log as an aid in determining some reservoir characteristics. *Journal of Petroleum Technology*, Vol. 5, 1-8.
- Ball, L. B., Wade, H. K, Cannia, J. C., 2006. Determination of canal leakage potential using continuous resistivity profiling techniques in western Nebraska and eastern Wyoming. Proceedings of the 2008 Symposium on the Application of Geophysics to Engineering and Environmental Problems (SAGEEP), Environmental and Engineering Geophysical Society, April 2-6, Seattle, Washington, 851-862.
- Brunke, M. and Gonser, T. 1997. The ecological significance of exchange processes between rivers and groundwater. *Freshwater Biol.*, Vol. 37, 1-33.
- Cherkauer, D.S., 1991. Geophysical mapping of pathways for entry of contaminated groundwater to lakes and rivers: application in the North American great lakes. *Hydrological Science and Technology*, American Institute of Hydrology, Vol.7, no. 1-4, 35-44.
- Cherkauer, D. S. and Carlson, D. A., 1997. Interaction of Lake Michigan with a layered aquifer stressed by drainage. *Ground Water*, Vol. 35, Issue 6, pp. 981-989.
- Complex Systems Research Center, University of New Hampshire, Durham, 1992. Digital Orthophoto quadrangle, 1:12,000 series, Quad 73, Woodstock, New Hampshire. From University of New Hampshire GIS Clearinghouse, [www.granit.unh.edu](http://www.granit.unh.edu), accessed 11/06.
- Day-Lewis, F.D., Singha, K., Binley, A., 2005. Applying petrophysical models to radar travel time and electrical resistivity tomograms: resolution-dependent limitations. *Journal of Geophysical Research*, Vol. 110, B08206, 1-17.
- Day-Lewis, F.D., White, E.A., Johnson, C.D., and Lane, J.W. Jr., 2006. Continuous resistivity profiling to delineate submarine groundwater discharge – examples and limitations. *The Leading Edge*, June, 2006, 724-728.
- Ellefsen, K. J., Hsieh, P. A., Shapiro, A.M., 2002. Crosswell seismic investigation of hydraulically conductive, fractured bedrock near Mirror Lake, New Hampshire. *Journal of Applied Geophysics*, Vol. 50, 299-317.
- Fogg, G. E., Noyes, C.D., and Carle, S. F., 1998. Geologically based model of heterogeneous hydraulic conductivity in an alluvial setting. *Hydrogeology Journal*, Vol. 5, 131-143.

- Genereux, D., and I. Badopadhyay, 2001. Numerical investigation of lake bed seepage patterns: effects of porous medium and lake properties. *Journal of Hydrology*, Vol. 241, 286-303.
- Harte, P. T., 1997. Preliminary assessment of the lithologic and hydraulic properties of the glacial drift and shallow bedrock in the Mirror Lake area, Grafton County, New Hampshire. Open-File Report, U.S. Geological Survey, Pembroke, NH, 1-42.
- Hayashi, M., and Rosenberry, D. R., 2002. Effects of groundwater exchange on the hydrology and ecology of surface water. *Groundwater*, Vol. 40, Issue 3, 309-316.
- Heaney, M. J., 2007. Marine resistivity as a tool for characterizing groundwater discharge zones at Lake Lacawac, PA. M.S. thesis, Temple University, Philadelphia, PA, 1 – 108.
- Heaney, M. J., Nyquist, J.E., Toran, L.E., 2006. Marine resistivity as a tool for characterizing zones of seepage at Lake Lacawac, PA. In *Abstracts with Programs - Geological Society of America*, October, 2006. Vol. 38, Issue 7, p. 42.
- Johnson, C. D., 1999. Effects of lithology and fracture characteristics on hydraulic properties in crystalline rocks; Mirror Lake research site, Grafton County, New Hampshire. *Water Resource Investigations*, U.S. Geological Survey, 795-802.
- Kalbus, E., Reinstorf, F., and M. Schirmer, 2006. Measuring methods for groundwater-surface water interactions: a review. *Hydrol. Earth Syst. Sci.*, Vol. 10, 873-887.
- Krabbenhoft, D.P. and Anderson, M.P., 1986. Use of a numerical ground-water flow model for hypothesis testing. *Groundwater*, Vol. 24, No. 1, 49-55.
- Lee, D. R., 1977. A Device For Measuring Seepage Flux in lakes and Estuaries. *Limnology and Oceanography*, Vol. 22, No. 1, 140-147.
- Likens, G. E. ed., 1984. *An Ecosystem Approach to Aquatic Ecology: Mirror Lake and its environment*. Springer-Verlag, New York, 1- 324.
- Manheim, F. T., Krantz, D.E., Bratton, J. F., 2004. Studying groundwater under Delmarva coastal bays using electrical resistivity. *Groundwater*, Vol. 42, No. 7, 1052-1068.
- Marescot, L., and M.H. Loke, 2003. Using the depth of investigation index method in 2D resistivity imaging for civil engineering surveys. *Proceedings of the 2004 Symposium on the Application of Geophysics to Engineering and Environmental Problems (SAGEEP)*, Environmental and Engineering Geophysical Society, February 10-14, Las Vegas, Nevada, Paper 13 GSL, 540-547.
- McBride, M. S. and H.O. Pfannkuch, 1975. The distribution of seepage within lakebeds. *Journal of Research*, U.S. Geological Survey., Vol. 3, No. 5, Sept.-Oct., 1975, 505-512.
- Mikochik, J., 2008. Using groundwater modeling to understand the factors controlling lake seepage patterns. M.S. thesis, Temple University, Philadelphia, PA, 1 – 96.

- Moeller, R. E., 1975. Hydrophyte biomass and community structure in a small, oligotrophic New Hampshire lake. *Verh. Internat. Verein. Limnol.*, Vol. 19, 1004–1012.
- National Agriculture Imagery Program, 2003. 15-Minute Quad series, Plymouth-Grafton counties, New Hampshire. From University of New Hampshire GIS Clearinghouse, [www.granit.unh.edu](http://www.granit.unh.edu), accessed 6/08.
- Neal, A., 2004. Ground-penetrating radar and its use in sedimentology: principles, problem and progress. *Earth-Science Reviews*, Vol. 66, 261-330.
- Oldenburg D.W. and Y. Li, 1999. Estimating depth of investigation in DC resistivity and IP surveys. *Geophysics*, Vol. 64, 403-416.
- Paillet, F. L., 1988. Characterizing the circulation of groundwater through fractures at Mirror Lake, New Hampshire. *Abstracts with Programs, Geological Society of America*, 1988, Vol. 20, Issue 7, p. 311.
- Panthulu, R.V., Krishnaiah, C., and Shirke, J.M., 2001. Detection of seepage paths in earthen dams using self-potential and electrical resistivity methods. *Engineering Geology*, 59, pp. 281-295.
- Peake, J. A., 2005. Comparison of electrical resistivity techniques to characterize karst geology, Easton, PA. M.S. Thesis, Temple University, Philadelphia, PA, 1 – 119.
- Reeve, R.C., and M.C. Jensen, 1949. Piezometers for groundwater flow studies and measurement of subsoil permeability. *Agric. Eng.*, Vol. 30, 435-438.
- Reynolds, J. M., 1997. *An Introduction to Applied and Environmental Geophysics*. John Wiley & Sons, NY, 1997.
- Ritter, D. F., Kochel, R. C., and J. R. Miller, 1995. *Process Geomorphology*. Wm. C. Brown Publishers, Dubuque, IA, 334-352.
- Rosenberry, D.O. and Winter, T.C., 1993. The significance of fracture flow to the water balance of a lake in fractured crystalline rock terrain. *Memoires of the 24<sup>th</sup> congress of International Association of Hydrologists*, Oslo, 967 -977.
- Rosenberry, D. O., Bukaveckas, P.A., Buso, D.C., Likens, G.E., Shapiro, A.M. and Winter, T.C., 1999. Movement of road salt to a small New Hampshire lake. *Water, Air and Soil Pollution*, Vol. 109, Issue 1-4, 179-206.
- Rosenberry, D.O., 2005. Integrating seepage heterogeneity with the use of ganged seepage meters. *Limnology and Oceanography: Methods*. Vol. 3, 131-142.
- Scheutz, J.W., 2002. Numerical modeling of seasonal variability in groundwater flow near Mirror Lake, Grafton county, NH. M.A. Thesis, Department of Geology, SUNY Buffalo, 1 – 120.
- Schneider, R. L., 2005. Factors influencing groundwater seepage in a large, mesotrophic lake in New York. *Journal of Hydrology*, August 01, 2005, Vol. 310, Issue 1-4, 1-16.

- Sebestyen, S. D., and R. L. Schneider, 2001. Dynamic temporal patterns of nearshore seepage flux in a headwater Adirondack lake. *Journal of Hydrology*, Vol. 247, 137-150.
- Shaban, A., Mohamad K., Chadi A., and G. Faour, 2005. Geologic controls of submarine groundwater discharge: application of remote sensing to north Lebanon. *Environmental Geology*, Vol. 47, 512-522.
- Snyder, D. D. and A. Wightman, 2002. Application of continuous resistivity profiling to aquifer characterization. *Proceedings of the 2002 Symposium on the Application of Geophysics to Engineering and Environmental Problems (SAGEEP)*, Environmental and Engineering Geophysical Society, February 10-14, Las Vegas, Nevada.
- Sophocleous, M., 2002. Interactions between groundwater and surface water: the state of the science. *Hydrogeology Journal*, Vol. 10, 52-67.
- Taylor, R. W., 1982. The application of combined seismic and underwater resistivity measurements to hydrological studies in Lake Michigan. *Eos, Transactions, American Geophysical Union*, May 04, 1982, Vol. 63, Issue 18, p. 321.
- Taylor, R. W. and D. S. Cherkauer, 1984. The application of combined seismic and electrical measurements to the determination of the hydraulic conductivity of a lake bed. *Groundwater Monitoring Review*, Vol. 4, Issue 4, 78-85.
- Tiedeman, C.R., Goode, D.J., and P.A. Hsieh, 1997. Numerical simulation of groundwater flow through glacial deposits and crystalline bedrock in the Mirror Lake Area, Grafton County, NH. U.S. Geological Survey Professional Paper 1572, 1-50.
- Toran, L.E., Weeks Chair in Environmental Geology, Department of Earth and Environmental Science, Temple University, Philadelphia, PA.
- Wilson, A., 1991. Distribution of hydraulic conductivity in the glacial drift at Hubbard Brook Experimental Forest, West Thornton, New Hampshire. Senior honors thesis, Dartmouth College, Hanover, NH, 1-56.
- Winter, T. C., 1989. Evaluation of inflow to Mirror Lake, New Hampshire. *Water Resources Bulletin*, October, 1989, Vol. 25, Issue 5, 991-1008.
- Winter, T. C., 2000. Geologic controls on the interaction of ground water and surface water. In: *Abstracts with Programs*, Geological Society of America, Vol. 32, Issue 7, p. 58.
- Winter, T. C., 1984. Mirror Lake and Its Watershed: Physiographic Setting and Geologic Origin of Mirror Lake. In: Likens G. E., (Ed), 1985. *An Ecosystem Approach to Aquatic Ecology: Mirror Lake and Its Environment*. Springer-Verlag, New York, NY, 40-83.
- Winter, T.C., 1976. Numerical simulation analysis of the interaction of lakes and groundwater. U.S. Geologic Survey Professional Paper 1001, 1-45.

APPENDIX A  
SOUTHWEST SHORE BATHYMETRY



Southwest Shore Bathymetry, Gathered From Sonar Data.  
Acquisition described in Section 3.10.

## APPENDIX B

### DATA DISCS

#### **DISK 1 - IMAGES.** *Illustrator Original Files, JPGs, Exported Images, and Maps.*

- **Mirror\_Lake\_Maps\_and\_Results**
  - *Mirror\_Lake\_Maps – sedimentation, bathymetry, seepage and other Mirror Lake Maps*
  - *NHMaps – geologic and other maps of NH*
- **Progress\_Report\_Images** – images I used or considered using for my progress report
- **ProposalFigures** – Figures I used in my thesis proposal
- **SAGEEP\_Paper\_Images** – Images from my 2008 SAGEEP paper
  - *AI\_Figure\_Originals* – Original Illustrator Files of the images; “Originla” copies (e.g. “Figure\_1\_Mirror\_Lake\_Basic\_Original” are earlier versions of the final figures, with features not included on later versions)
  - *Exported\_BMP\_Figures* – BMP versions of AI originals
  - *JPGs* – JPGs, BMPs and etc. used in AI figures
  - *Maps* – Maps used in AI figures
  - *Photos*
- **SAGEEP\_Talk\_Images** – Images used for SAGEEP Talk.
- **Thesis\_Images** – A collection of all images used in thesis, organized by section. (Intro & Background, Methods, and Results). Organized within section folders in the same manner as SAGEEP Paper Images (i.e. AI\_Intro\_Originals, Exported BMPs, JPGs and BMPs, and, in addition, Word Versions of Images which have captions)

**DISK 2 – GIS DATA AND PHOTOS.** *A collection of photos and GIS data from Mirror Lake*

**DISK 3 – DATA, DOCUMENTS, REFERENCES.**

- **NM\_Documents** – A collection of all documents I created during thesis work.
- **Radar Data** – GPR data from Mirror Lake, organized by download date.
  - *July26\_2007 - has all perpendicular lines from the SW shore*
  - *July23\_2007 - the "MALAGS" folder has all perpendicular-to-shore radar lines, (all "Dat" files are perpendicular-to-shore surveys at 50 m intervals around the lake)*
- **References** : a somewhat arbitrary collection of papers and other sorts of references. Only a few academic papers I had were in electronic form – most I simply printed and are in binders. If you ask me I can lend you those binders.
  - *SAGEEP Papers, 2002-2007*
  - *A few GPR papers I collected in electronic form, as a favor to the friend of a friend*
  - *A paper on heat as a groundwater tracer*
  - *A master list of references: papers referenced in my thesis are listed here, as well as a few which may not have been.*
  - *A MALA paper on using GPR to map Lake sediments*
  - *Manuals for EarthImager and Sting*
  - *Temperature Data : Includes Lake Lacawac temperature sensor data from '06 and '07, collected by MJH and LT. Data were collected with idea that GW seepage to Lake would be different temperature than lake water, and vice versa. Some possible relationship seen, but very hard to tease out. If I recall properly, we weren't sure how well the temperature sensors were seated in the sediment, so we weren't all that confident in our data.*
  - *Original data is in "Original MJH and LT" folder. May be least confusing to simply look at this data*

- *“Temperature\_Sensor\_Data” includes Matlab scripts we created to help process the data. Matlab sripts are organized by research period, and also Excel files into which some of that processed data was loaded. Graphs are in the sub-folder “Figures”*
  - *“ProcessedData” contains Excel files with the data, and with thinned (“slimmed”) versions of the data which are more manageable in Excel.*
- **SeepageData – seepage data from Mirror Lake and Lacawac. A variety of versions in Excel format, among others, are present.**
    - *Text files include lat/long position for GIS import.*
    - *“Seepage\_compare” is a comparison of Asbury and Temple Seepage measurements.*
    - *“Mirror\_Lake\_Sed\_Summary” is a summary of studies of hydraulic conductivities at Mirror Lake.*
    - *“Seepage\_Spline” is a summary of seepage measurements along the SW shore of Mirror Lake.*
  - **Sting\_Data – Just what it sounds like.**
    - **Calculation\_Experiments –**
      - XYZ\_Format\_files – Inverted Sting files, both real data and synthetic, in XYZ format for use in Sensitivity Analyses
      - Comparison\_of\_V\_over\_I – comparison of values from towed- and stationary-cable surveys conducted over similar terrain
      - Porosity\_vs\_Resistivity - models of the effects of variations in Archie’s law variables on bulk resistivity
    - **LacawacStingData\_07 – data from “test run” at Lake Lacawac in the Spring of 2007**
    - **Mirror\_Lake\_Stationary\_Cable\_Images – JPGs and BMPs of inverted stationary cable surveys at Mirror Lake.**
    - **Mirror\_Lake\_Sting\_Data – original Sting Data from Mirror Lake**
      - Backup – backups of original data, organized by download date
      - BottomLines – Stationary-Cable surveys

➤ *Parallel\_Lines*

*Unmerged\_Long\_Lines* – Individual Sting surveys which were later merged to form Long Line and the parallel-to-shore surveys at 4, 6 and 8-m from shore. Includes graphic summary of location of each of those individual locations.

*Parallel\_Line\_Images* – JPGs and BMPs of inverted sections.

*LL\_merged\_Standard* – final version of 9 separate merged Long Line surveys

*LL\_merged\_8m* – merged parallel-to-shore surveys at 8m from shore

*LL\_merged\_6m* – merged parallel-to-shore surveys at 6m from shore

*LL\_merged\_4m* – merged parallel-to-shore surveys at 4m from shore

*LL\_merged\_2m* – merged parallel-to-shore surveys at 2m from shore

*LL\_Inversion\_Comparisons* – inversions of individual LL components, in high res BMPs

*Chloride\_Search* – Surveys from the Northeast inlet area.

➤ *Perpendicular\_Lines*

*Downloaded\_Data* – original Data

*Eastern\_Shore* – data from the Eastern Shore of Mirror Lake. Includes sub-folder "Sharp\_Terrain" with data from the very sharp dropoff there.

*Northeast\_Inlet\_Area* – data from the northeast inlet area, namely perpendicular line from slightly north of the inlet area

*Perpendicular\_Line\_Images* - BMPs and JPGs of inverted Sting Files

*S5* – SE shore – single line from SE shore.

*Southwest shore* – data from the SW shore of Mirror Lake.

*Map\_of\_Perpendicular\_Res\_Lines* – map which shows location of all of these lines.

TestBoxData – results of resistivity testbox work on sediment samples collected at Mirror Lake

TowedSurveys – Towed-cable surveys from Mirror Lake

- *Extracted Sections – Extracted Sections from a variety of locations around the lake*
- *MIRROR5 – towed-cable survey with 2-m spacing conducted nearest possible to shore*
- *MIRROR6 – towed-cable survey with 2-m spacing conducted slightly further from shore*
- *MIRROR7 – towed-cable survey with 4-m spacing conducted nearest-possible to shore*
- *MIRROR8 – towed-cable survey with 4-m spacing conducted slightly further from shore.*
- *Miscellaneous – aborted or otherwise tainted surveys or survey portions you probably will never need but are there just in case. Complete explanations can be found in field notebooks*